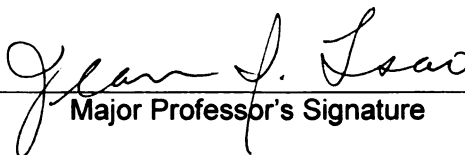This is to certify that the
thesis entitled

QUANTIFYING AGGREGATION OF THE PARASITES OF
THE LYME DISEASE SYSTEM IN MENOMINEE COUNTY,
MICHIGAN

presented by

PAMELA L. ROY

has been accepted towards fulfillment
of the requirements for the

_____M.S._____ degree in _____Fisheries and Wildlife_____

_____
Major Professor's Signature

_____July 10, 2008_____

Date

PLACE IN RETURN BOX to remove this checkout from your record.
TO AVOID FINES return on or before date due.
MAY BE RECALLED with earlier due date if requested.

DATE DUE	DATE DUE	DATE DUE

QUANTIFYING AGGREGATION OF THE PARASITES OF THE LYME DISEASE
SYSTEM IN MENOMINEE COUNTY, MICHIGAN

By

Pamela L. Roy

A THESIS

Submitted to
Michigan State University
in partial fulfillment of the requirements
for the degree of

MASTER OF SCIENCE

Department of Fisheries and Wildlife

2008

ABSTRACT

QUANTIFYING AGGREGATION OF THE PARASITES OF THE LYME DISEASE SYSTEM IN MENOMINEE COUNTY, MICHIGAN

By

Pamela L. Roy

Parasite aggregation is a phenomenon observed in nature across multiple systems and refers to the tendency of most parasites to gather in or on a small number of hosts. An aggregated parasite distribution may help a system maintain itself, and such may be the case for Lyme disease transmission dynamics, establishment and maintenance. Surveys of vegetation, questing ticks, and *Peromyscus spp.* mice in Menominee County, Michigan were conducted over the summer transmission period. Investigations for parasite aggregation in *Borrelia burgdorferi* in tick and mammal hosts and vector ticks (*Ixodes scapularis*) on small mammal hosts revealed aggregation for all populations. Vegetation was compared with the spatial distribution of the pathogen, vector and mammal host. Presence of coniferous trees was spatially correlated with questing larvae, all questing nymphs, all mice and total ticks on mice. Implications of this aggregation and spatial correlation on the Lyme disease cycle are discussed.

.

To overcoming imposter syndrome

ACKNOWLEDGEMENTS

TABLE OF CONTENTS

LIST OF TABLES

LIST OF FIGURES

CHAPTER 1

INTRODUCTION

Parasite aggregation

The theory of parasite aggregation

This study's theory of interest, aggregated distributions of parasite populations among hosts, has a great mass of supporting ecological evidence from across diverse systems (Shaw and Dobson 1995). Ecologists have long observed that parasites are aggregated, rather than randomly distributed, among hosts (Crofton 1971, Anderson and May 1978). Furthermore, there is evidence of a consistent finding that 20% of hosts harbor 80% of the parasites (Woolhouse et al. 1997), and in some human/helminth systems, that only 15% of available hosts feed 80% of parasites (Gregory and Woolhouse 1993). This aggregated distribution may have important implications for host-parasite dynamics and thus for control and management of such systems.

Parasitism is an ecological association between species in which a parasite lives in or on the body of a host (Anderson and May 1978). A more rigorous definition of parasitism is where the parasite gains a benefit to the detriment of the host. Parasites distributed across a host population can be measured by prevalence, or the number of hosts infected, and by load, the number of parasites per host. Parasite aggregation is a phenomenon often observed in nature, among both macro- (e.g. -ticks, lice) and micro- (e.g.- bacteria, protozoa) parasites (Anderson and May 1978, May and Anderson 1978, Shaw and Dobson 1995, Woolhouse et al. 1997). Aggregation refers to the tendency of parasites to group among hosts in an uneven manner, where some hosts will have much

larger burdens of parasites than others, and the variance to mean ratio of these parasite burdens is much greater than one. In aggregated systems, the prevalence may also be low because many of the hosts will have zero parasites.

If aggregation did not occur, one would assume that a host population infected with a particular parasite would have a parasite burden that follows a random distribution. If parasites were distributed among hosts due only to random chance, we would assume the Poisson distribution, where variance is equal to the mean. In nature, it is likely that some potential hosts never encounter a particular parasite; some will encounter them over and over again or may encounter many at once. Most will fall somewhere between those extremes. This is considered the statistical distribution that serves as a null hypothesis to the aggregation hypothesis. Any distribution that follows along a Poisson has a variance to mean ratio of one; when that ratio rises above one, distribution is considered to be greater than random and hence referred to as over-dispersed or aggregated (Shaw and Dobson 1995, Elston et al. 2001).

Multiple studies have documented the phenomenon seen in host-parasite systems where the 20% of hosts with the highest parasite loads account for 80% of the parasites. It should be noted that this finding is species-specific and thus refers to single-species populations.

There has been at least one study documenting the difference in aggregation among endemic foci, where it is demonstrated that there is a direct relationship between pathogen prevalence and intensity of aggregation (Guyatt et al. 1994). The study found that an increase in prevalence of parasite infections was related to an increase in intensity of infections (prevalence of heavy infections). Thus, there can be heterogeneity in

aggregation patterns within an endemic area. The authors hypothesize that this difference may be due to past geographic variation in transmission patterns, such as the age of the endemic foci. Newly infected regions showed a pattern of more extreme aggregation. This difference is hypothesized to be due to the lack of a 'leveling' effect that a population with more infection experience and thus, increased immunity might have (Guyatt et al. 1994).

Examples from the literature span many systems, and include helminthes (Pal and Lewis 2004, Cattdori et al. 2004, Duerr et al. 2004, Churcher 2005), ticks (Randolph et al. 1999a), bacteria (Randolph et al. 1996, Wang et al. 2003), schistosomes (Guyatt et al. 1994, Woolhouse et al. 1998), trypanosomes (Lord et al. 1999) and viruses (Randolph et al. 1996). A range of hosts for these aggregated organisms has also been studied, including humans (Duerr et al. 2004), rodents (Randolph et al. 1999b) and birds (Elston et al. 2001, Kirby et al. 2004). These are in addition to the numerous systems reviewed by Crofton (1971) and Shaw and Dobson (1995).

The seminal texts on parasite aggregation are attributed to Crofton (1971) and Anderson and May (1978). One of the central assumptions in Anderson and May's host-parasite models (1978) is that each parasite increases the probability of host mortality. In order to classify a species as a parasite, there are three conditions that these authors require: use of the host as habitat, nutritional dependence on the host, and causing harm to the host. This harm is often referred to as 'mortality' in the paper, but harm may be described as any decrease in fitness, such as decrease in fecundity or immune function. Many organisms such as mites, fleas and ticks, appear to do little harm to their hosts unless present in great numbers. Parasites range in the amount of harm they cause; some

very nearly kill their hosts and are parasitoid-like, while others act more like symbionts. According to Anderson and May, all of these are considered parasites.

Anderson and May couch their descriptions of parasite-host interactions in a predator-prey framework, a theory familiar to ecologists. In this light, the host is 'prey' to the parasite's 'predator'. It is often difficult to detect the detrimental effect that the predator exerts on the prey since these effects may be subtle or often unobservable. Sometimes the size of parasite and host populations is reliant on their interactions and mimics the classic density-dependent sigmoid functions of predator-prey population curves, and sometimes not. Although the phenomenon of parasite aggregation has been well-documented and described, its mechanisms have not.

Parasite aggregation and tick-borne disease

Ticks are parasites. Laid in a clutch of hundreds or thousands, they begin life aggregated. Once they emerge, they lay in wait for a host to walk by and hitch a ride, since they cannot move very far on their own. They rely on vertebrate hosts for the multiple bloodmeals they will take in their lives. They also rely on their hosts not detecting and grooming them off for the duration of their meal. Once they have fed to repletion, they drop off the host, wherever the host happens to be at the time. Since they can walk no more than a few feet on their own (Daniels and Fish 1990), their distribution is determined by host factors, which can include the host's home range and availability of good habitat for that host (Madhav et al. 2004).

In order for a microorganism to exploit a tick vector for transmission between hosts, it is imperative that it be able to survive between life stages. That is, when a tick

molts to its next instar, a parasitic microorganism must be maintained through these development processes. Further, in order for it to be sustained in susceptible vertebrate populations, it must find a host in which it will survive until the next stage of the vector will again become active. For tick-borne pathogens, a multi-layered aggregation with aggregation occurring at the vertebrate host level (ticks and microorganisms) and the tick level (microorganisms).

Aggregation has been demonstrated for both ticks on rodent hosts as well as for spirochetal bacteria among host-seeking ticks. For both parasites, a similar level of aggregation has been found: 20% of the hosts harbor 80% of the parasites (Wang et al. 2003). Randolph et al. (1999b) shows that 80% of the ticks are found on only 20% of the hosts. This pattern of 80/20 aggregation is the phenomenon of interest.

As numbers of available hosts increase, so do the numbers of parasitic ticks found on those species. For example, Kirby et al. (2004) found that as numbers of red deer, the favored host of the hard tick *Ixodes ricinus*, increase, the tick also flourishes. Specifically, its infestations of red grouse chicks have increased in both prevalence (number of chicks infested) and intensity (number of ticks per infested chick).

There are some disease systems for which aggregation is shown to have an extremely beneficial, and sometimes necessary, effect for parasite maintenance in the system. As reviewed by Randolph et al. (1996), in certain pathogen-tick-host systems, the aggregation of feeding ticks on a host is a necessary means of propagating the spread of the infection. These virus systems include Crimean-Congo hemorrhagic fever, Kyansur forest disease, Louping illness, Thogoto, and tick-borne encephalitis (TBE). Ixodid (hard) ticks are responsible for two of these: Louping illness and TBE. Birds and

mammals can pose as the non-viremic hosts, showing infection only in the tissues where the ticks are feeding, and not systemically (Randolph et al. 1996). Indeed, this clustering of ticks allows for efficient transmission of the pathogen from infected tick to non-systemically infected host to naïve tick.

Potential mechanisms of aggregated parasite distributions

In the 30 years since Anderson and May (1978), the phenomenon of parasite aggregation has been well-documented (Dye 1992, Shaw and Dobson 1995, Woolhouse et al. 1997, Pugliese et al. 1998, , Lord et al. 1999, Elston et al. 2001, Duerr et al. 2003). Known well to exist, the causal mechanisms of this observable fact are less understood.

There are several causes that have been hypothesized to contribute to parasite aggregation. Heterogeneity in dispersal of parasites among hosts may be due to genetic, physiological or behavioral differences in the hosts and may also vary in time and in space (Shaw and Dobson 1995). Even small differences in susceptibility between hosts can produce non-random, aggregated distributions of parasites (Anderson and May 1978). Other of these factors which might influence whether parasites become aggregated on hosts include quality of host habitat, transmission process (for microparasites which live inside the host) or the host's migratory behavior (Shaw and Dobson 1995).

Factors to be taken into account when considering pathogen transmission and potential aggregation by a vector include vector competence, abundance and distribution, as well as host choice, incubation period of the pathogen, and probability of transmitting an infection (Dye 1992). Here, infection is defined as the colonization of a host organism

by a foreign species where the infecting organism, or pathogen, may interfere with the normal functioning of the host. Transmission itself is also influenced by outside factors. For example, in the Lyme disease system, density of feeding *Ixodes scapularis* larval ticks on hosts influences transmission of *Borrelia burgdorferi*, the Lyme disease pathogen. As density of the feeding larvae increases, the transmission efficacy of *B. burgdorferi* increases as well, possibly because of immunosuppressive factors in the tick's saliva, allowing for unrestrained growth of *B. burgdorferi* spirochetes (Levin et al. 1997). However, higher densities of feeding larvae decrease chances of larval survival and a smaller percentage of those ticks will survive to become nymphs, possibly because not all ticks are able to feed to repletion, which may be due to grooming by the host (Levin and Fish 1998).

Additional sources of aggregation may include seasonality of hosts or parasites, aggregation of parasitic life stages, or host effects which may include behavior, physiology or immunology (Shaw et al. 1998). It is clear to see how many of these factors could heavily influence LD dynamics, with its strong patterns of seasonality, and aggregation of the different life stages of its vector (Piesman and Spielman 1979, Wilson and Spielman 1983, Levine et al. 1985).

One factor that may contribute to the abundance of the tick that vectors the Lyme disease pathogen, *I. scapularis*, and hence, its aggregation, is drought (Schauber et al. 2005). Drought increases favorability of habitat for ticks, possibly by suppressing growth of entomopathogenic soil fungus. In wet years, fewer *I. scapularis* survive and LD incidence is lower the following year. Due to their lack of mobility, larval ticks will not travel far from where they were hatched (Daniels and Fish 1990). In a year where more

of them survive, we might expect to see increased aggregation because of their higher numbers at the larval stage. However, this may not necessarily be the case for other life stages, which are more highly dispersed (Madhav 2004).

There may be some evidence of an age-intensity curve in regards to parasite distribution among hosts. In some systems, it may be that peak intensity of infection occurs towards the end of an organism's life (Duerr et al. 2003, Cattadori 2005). Duerr et al. (2003) have identified six factors which may contribute to this age-intensity phenomenon- i) age-dependent exposure, ii) parasite-induced host mortality, iii) heterogeneity within the host population, iv) clumped infection, v) density-dependent parasite mortality and vi) density-dependent parasite establishment.

Several studies have documented the differences in infestation by parasites between sexes. Hypothesized to be a result of immune differences, males of some taxa, especially mammals, tend to carry the higher parasite load (in Hudson, 2002).

Once a system's hosts and parasites have been described and characterized, age and sex of host may give clues as to the parasite burden of an individual. If age and sex distributions of parasites have been well-characterized, falling into certain categories of those characteristics may indicate likelihood of a higher or lower parasite burden. Having such a metric may be epidemiologically useful for targeting interventions that would prevent spread or maintenance of a disease.

The study system: Lyme disease

Lyme disease (LD) is tick-borne, spirochetal disease endemic to much of the United States, Europe and even parts of Asia (Kurtenbach et al. 2006). In the US, Lyme disease is caused by *Borrelia burgdorferi* and transmitted by *Ixodes scapularis*; it is characterized in humans by a distinctive erythema migrans (EM) skin lesion and systemic symptoms. LD is classified as a zoonotic vector-borne disease, and as such, utilizes wildlife reservoirs in addition to susceptible human and canine hosts. In 2003, LD affected approximately 21,000 people in the US, (CDC 2005) and is the most prevalent vector-borne disease in the US. Though not a fatal disease, it usually manifests with an erythema migrans (bulls' eye) rash at the site of the bite or disseminated, arthritic joints, flu-like symptoms, and rarely, neurological symptoms such as Bell's palsy or 2nd or 3rd degree heart block.

Additionally, the tick and vertebrate reservoir species have distinct roles in propagating the disease. *B. burgdorferi* persists in ecosystems by alternating between the midguts of ticks and the tissues of wildlife reservoirs. Because *B. burgdorferi* is not spread person-to-person, it is a disease that relies on ecosystems to flourish by a year-round maintenance in wildlife reservoirs and the vector tick. The pathogen is maintained in the bloodstreams of mammals for 10 to 14 days (Hanincová et al. 2008), and thereafter found only in skin and internal organs. *Peromyscus leucopus*, the major reservoir for *B. burgdorferi*, are thought to be infected for life (Hanincová et al. 2008). The pathogen is also maintained in infected ticks for their entire lifespan (VanBuskirk and Ostfeld 1995), provided that they do not feed on a host with bactericidal properties, such as the

western fence lizard (*Sceloporus occidentalis*) (Lane 1989) or the white-tailed deer (*Odocoileus virginianus*) (Telford, Mather et al. 1988).

I. scapularis is a generalist parasite with three post-egg life stages, and a lifespan of two years in the northern U.S. Ticks start out as uninfected larvae (Patrican 1997), which typically feed on birds and small mammals in the northern U.S. Newly emerged larvae have the opportunity to pick up the spirochete in their first bloodmeal from an infected host. They then molt into nymphs, and seek their second bloodmeal. It is at this life stage, because of their small size and potential for infectivity, nymphal ticks pose the greatest threat for infection to humans (Falco 1988). This is also the first life stage capable of transmitting the pathogen back to the wildlife population and completing the transmission cycle. After nymphs obtain their blood meal and molt into adults, they parasitize a large mammalian host, often a white-tailed deer, to feed and mate, dropping off to lay eggs in the leaf litter of the forest (Figure 1.1).

This thesis explores whether pathogen distribution among the vector and host populations of the LD system is aggregated, considering infection prevalence (proportion of ticks and mice infected with *B. burgdorferi*) and vector load (number of ticks on mice). This project is conducted in a Lyme disease endemic area of Michigan. It measures the degree of aggregation among the hosts, vectors and pathogens in the system, and the degree to which this aggregation is influenced by ecological factors. The ecology of the system is considered and examined together with each step of the vector life cycle (Figure 1.2) in order to form a more complete picture of the ecology of the Lyme disease system of Menominee County.

10
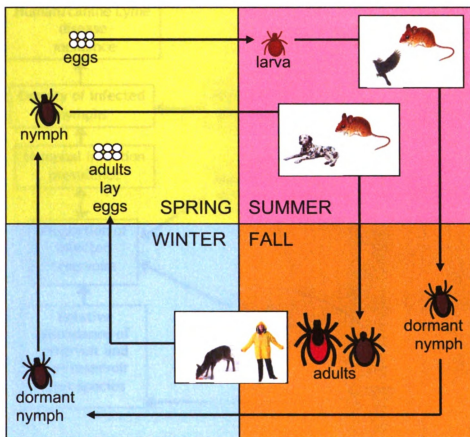
Figure 1.1. The two-year life cycle of *Ixodes scapularis*. Ticks start out as eggs in the spring, and take two bloodmeals (males) or three bloodmeals (females) from different hosts in their lifetimes. Figure modified from one produced by the American Lyme Disease Foundation.
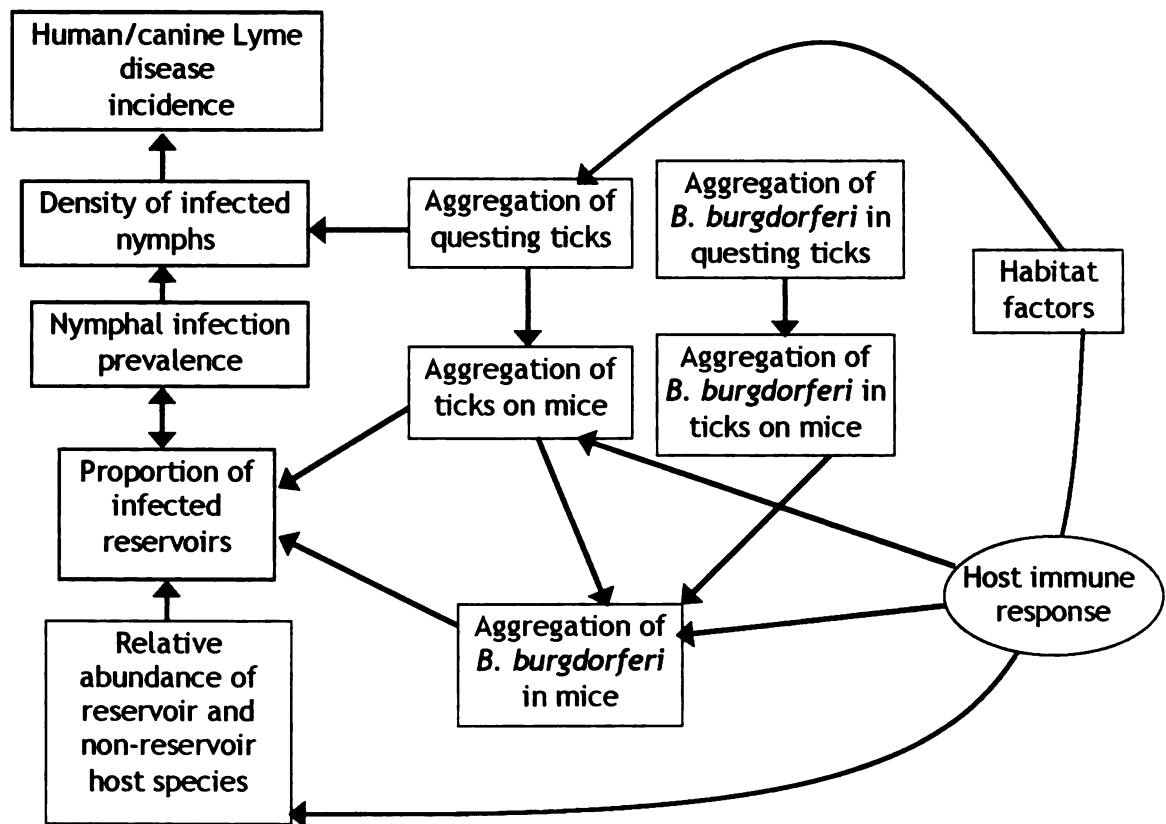
Figure 1.2. Schematic model of LD transmission dynamics.

The study of the LD system in Michigan is a subset of the national disease system; the study of this subset may bring to the surface implications of importance for the system in other geographic locations. In order to investigate the system as it operates in an endemic area, sampling took place in Menominee Township in Menominee County, Michigan (Figure 1.3).
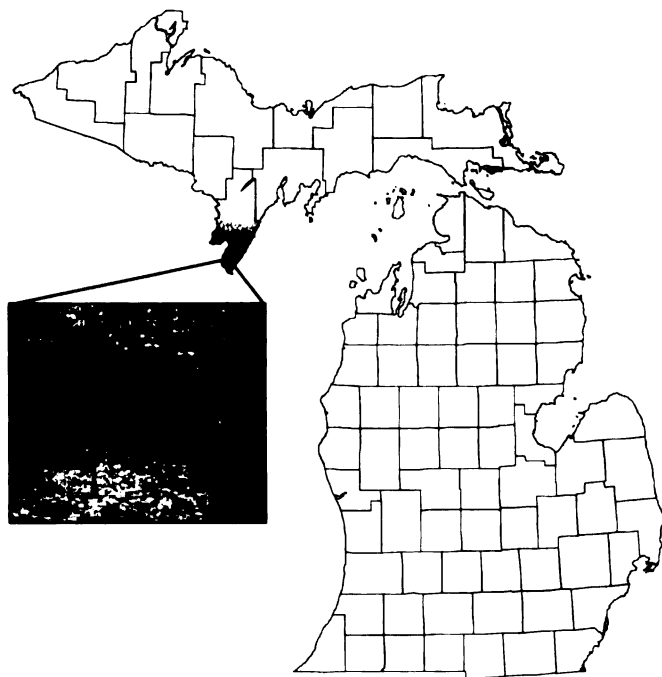
Figure 1.3. County map of the state of Michigan, including both the Upper and Lower Peninsulas. Shading indicates Menominee County. Inset shows the study site (N 45°9'46.2", W 87°42' 48.0"). Images in this thesis are presented in color.

Michigan's history of Borrelia burgdorferi *and* Ixodes scapularis

It has been over 30 years since LD was first discovered in Connecticut; now

people get ill with LD in many states across the country, although there still appears to be

just two major foci for the disease, one in New England and one in the Upper Midwest

(CDC 2008). The spatial and temporal trends of disease distribution in the US has

generally been a radial spread from the sites where it was first recognized, provided there

was no geographic barrier to the movement and establishment of *I. scapularis* and its

hosts, such as a coastline (Steere et al. 2004).

The history of Lyme disease in Michigan begins with a paper published in the

Vector Control Bulletin of the North Central States (Strand et al. 1992) documenting the

presence of *B. burgdorferi*-infected *I. dammini* (now *I. scapularis*) in Menominee

County. The Midwest's first report of *I. scapularis* and erythema chronicum migrans

rash in a human associated with the bite of that tick came from Wisconsin in 1970

(Jackson and DeFoliart 1970, Scrimenti 1970). Since then, additional populations of

I. scapularis infected with *Borrelia burgdorferi* have been found in Wisconsin (Anderson

et al. 1987), Minnesota (Drew 1988) and Indiana (Pinger et al. 1996). Menominee

County was the first county in Michigan to report an established population of

I. scapularis (Strand et al. 1992) and *B. burgdorferi* (Walker et al. 1994).

Thus, Menominee County was the first county in the state of Michigan to be

declared endemic, and several studies have found *B. burgdorferi*-positive *I. scapularis*

there since (Walker et al. 1994, Walker et al. 1998, Friedrich 2003, Foster 2004, Hamer

et al. 2007). Situated along a border with Wisconsin to the west, and with the shore of

Lake Michigan to its south, it may be that the geography of the county is such that the

populations of *I. scapularis* and *B. burgdorferi* have not had an opportunity to spread radially. Large numbers of birds migrate along the flyway over the area, a peninsula located between two Great Lakes. As such, the area may be used as a rest area for many birds (Diehl et al. 2003) and it is possible that the ticks may have arrived as passengers of these birds from the southern US.

More recently, unpublished work done by researchers at Michigan State University has shown the development of a new endemic focus in Michigan. A population of infected *I. scapularis* has been found in southwestern Michigan and appears to be spreading north along the lakeshore (Foster 2004, Hamer et al. 2007, Hamer 2008 (in progress)). A landscape model for Michigan (Foster 2004) based on data from Wisconsin and Minnesota (Guerra et al. 2002) shows that much of Michigan is suitable for both the tick and the pathogen to flourish (Figure 1.4). There is evidence of established populations of *I. scapularis*, *B. burgdorferi* and human cases of disease in the southwest portion of the state, and north along the Lake Michigan coast (Figure 1.4) (Foster 2004, Hamer et al. 2007, Hamer 2008 (in progress)).

It is important to note that Menominee County is still the only county in Michigan considered 'endemic' for LD. Lack of data from southwestern Michigan may be due to constraints of legislature, physician willingness and Michigan Department of Community Health (MDCH) resources. In order for MDCH to officially declare a county 'endemic', multiple, culture-confirmed (typically from EM skin biopsy) cases of LD must be reported. This requires physicians to biopsy patients and understandably, most physicians are more interested in treating patients than aiding in the collection of this

data, which is not necessary for diagnosis. To our knowledge, no cases have been culture-confirmed from this area (MDCH, personal communication).
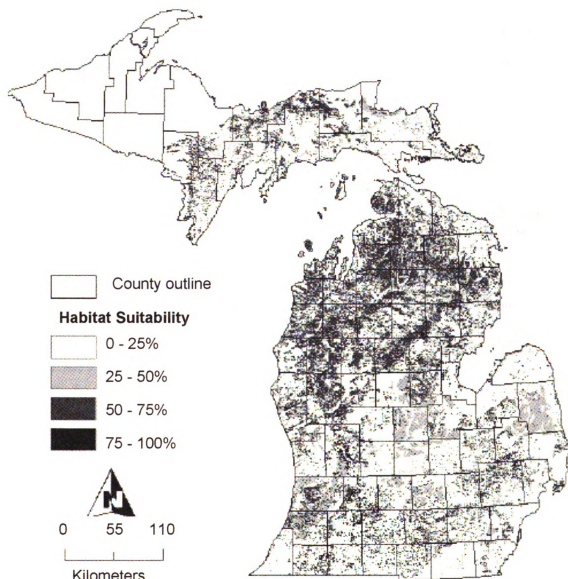
Figure 1.4. A model of habitat suitability for *I. scapularis* establishment (Guerra et al. 2002) applied to Michigan predicts the potential future distribution of the tick, with the darkest areas indicating highest risk for establishment upon introduction. Courtesy Erik Foster, 2004, in thesis.

In 1990, Lyme disease became a reportable disease in Michigan. Reliable human case data is available electronically from the Michigan Department of Community Health from 1992 to the present. Human case incidence from a 9-county region in the Upper Peninsula, surrounding Menominee County summed over the 16-year period from 1992 to 2007 is approximately 67.3 cases per 100,000 population. Human case incidence from the same period for a 6-county region of southwestern Michigan is just 5.1 cases per 100,000 population. The case rate for all the remaining counties combined is only 1.4 per 100,000 population for the same time frame (Table 1.1, Figure 1.5).

Table 1.1. Counties in regions of the state of Michigan with elevated case rates (cases per 100,000 population) over a cumulative, 16-year period from 1992 to 2007. Data courtesy Michigan Department of Community Health. See Figure 1.5 for map.

Region	Case rate	Counties
Upper Peninsula	67.3	Alger, Baraga, Delta, Dickinson, Gogebic, Iron, Marquette, Menominee, Ontonagon
Southwest	5.1	Allegan, Berrien, Kalamazoo, Muskegon, Ottawa, Van Buren

Case rates per 100,000 population 1992-2007
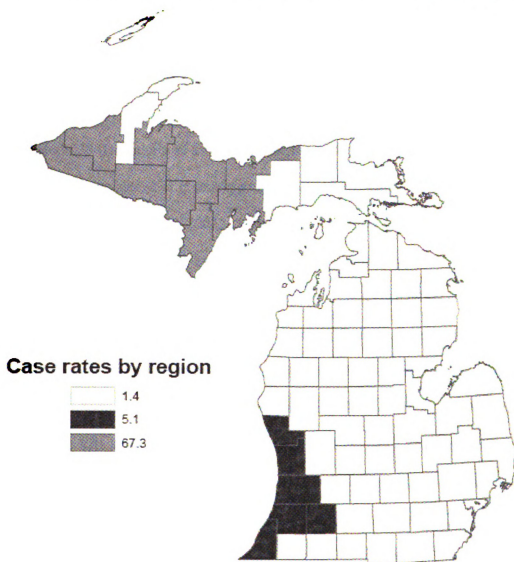
Figure 1.5. A map displaying the differences in infection prevalence of human Lyme disease cases in Michigan. Case rates per 100,000 population are additive over a 16-year period. See Table 1.1 for names of counties included in shaded regions. Data courtesy Michigan Department of Community Health.

In Menominee County, there exist two sympatric mouse species- *Peromyscus maniculatus gracilis* (deer mouse) and *Peromyscus leucopus* (white-footed mouse) (Strand et al. 1992, Friedrich 2003). The existence of these sympatric species most likely has some impact on the disease system dynamics there. These species probably act together as the most reservoir competent species; much like *P. leucopus* alone does in the Northeastern US (LoGiudice et al. 2003). One researcher found no significant difference in the infection prevalence of *P. leucopus* (34.2%) and *P. maniculatus gracilis* (27.7%) in Menominee County (Friedrich 2003). Thus, for the purposes of my analysis, these two species will be lumped together and referred to as *Peromyscus spp.*

There is some preliminary evidence to support the theory of aggregation of *I. scapularis* among *P. leucopus* in Michigan (Table 1.2). Data for sites in Lower Michigan demonstrate aggregation and, without detailed statistical analysis, appear to fit the negative binomial distribution. At Van Buren State Park, in 2004, of 67 white-footed mice trapped, 10% had no *I. scapularis* infestation, but the range of infestation included up to 52 ticks on one individual (Figure 1.6). However, at Duck Lake that same year, there were 178 *P. leucopus* trapped, with over 80% free of *I. scapularis*, and the upper limit of tick load only 4 ticks (Hamer, 2006). The data show that that the populations with more individuals infested also show a higher upper limit for tick burden (Table 1.2), perhaps indicating a positive relationship between infection prevalence and intensity.

Table 1.2. *I. scapularis* burdens on *P. leucopus* collected in 2004 and 2005 in southwestern Michigan. These data are supportive of the aggregation theory of ticks on small mammal hosts. Unpublished data courtesy Sarah Hamer, 2006.

Site	Year	# *P. leucopus*	% unparasitized	Upper limit of tick burden
Van Buren	2004	67	10%	52
Van Buren	2005	15	27%	20
Duck Lake	2004	178	>80%	4
Duck Lake	2005	88	>80%	6
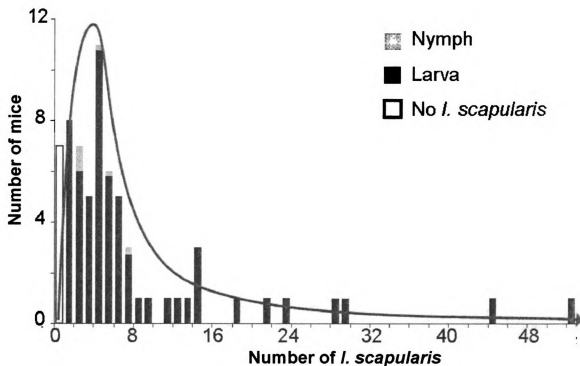
Figure 1.6. *Ixodes scapularis* on *Peromyscus leucopus* trapped at Van Buren State Park, 2004. Solid line shows the curve approximating the NBD. Unpublished data courtesy Sarah Hamer, 2006.

Aggregation & Lyme disease

There are several levels on which aggregation may occur in the LD system. First, there is the distribution of ticks on small mammal (mouse) hosts. Second, the distribution of *B. burgdorferi* in *I. scapularis* hosts. Third is the grouping of *B. burgdorferi* in the mouse host (Figure 1.7).
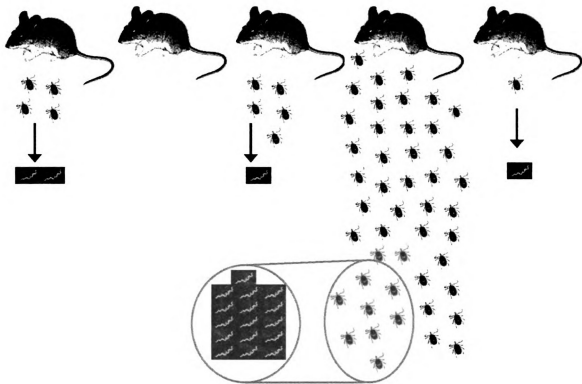
Figure 1.7. A visual representation of aggregation on multiple levels. In a host population (mice, level 1), aggregation of ectoparasites (ticks, level 2), occurs. Further, aggregation of endoparasites (spirochetes, level 3) occurs within the tick population.

There are several ecological aspects of the LD system that may affect the spread of the pathogen. The aspects of the disease system that this inquiry focuses on are the distribution of pathogen load in the *I. scapularis* nymphs and adults, the distribution of pathogen load in and *I. scapularis* ticks on *Peromyscus spp*. The maintenance cycle, and by extension, the gradual spread of LD, requires that infected nymphs transmit the pathogen to reservoir hosts and larval ticks to become infected from reservoir hosts.

The probability of a host becoming infected is a positive function of the proportion of ticks that are infectious. Aggregation of the pathogen in hosts may influence the proportion of ticks that are infectious by infecting many of the naïve larval ticks that feed on them, which then molt into infected nymphs. The highly infected ticks are able to deliver a high dose of pathogen to their next host. In this way, the cycle of the pathogen moving from host to tick and to a new host is the basis for the spread of the LD pathogen, and aggregation may play a role in this spread.

There is a high degree of aggregation of *B. burgdorferi* load among field collected host-seeking nymphs in LD endemic woods of the Northeastern US (Wang et al. 2003), and additional laboratory studies (Levin and Fish 2000) have demonstrated that the lower 20% of ticks positive for *B. burgdorferi* may not be capable of transmitting the disease because their spirochete loads are too low to transmit an infectious dose. At a field site in southern Connecticut, where the nymphal infection prevalence is ~ 32% and nymphal densities are high, nearly 100% of mice become infected by summer's end (Bunikis et al. 2004). There, pathogen aggregation in nymphs may not have a large ecological impact on host infection dynamics, unless high pathogen loads in hosts allow for a more efficient transmission back to ticks. If almost all the mouse hosts are infected, a tick's chances of

becoming infected by feeding on any individual mouse in that population is high. However, recent figures from Menominee County indicated infection prevalence for *Peromyscus spp.* from 28-34% (Friedrich 2003).

It should be noted that in the Lyme disease system, ticks play multiple roles, acting as a parasite, host and vector species. In the system in general, *I. scapularis* ticks act as a vector of a parasite (*B. burgdorferi*). It is important to consider that the ticks are simultaneously parasitized by *B. burgdorferi* as they parasitize a host for their blood meal.

Intensity of infection or load of *B. burgdorferi* spirochetes in both the tick (Wang et al. 2003) and host (Tsao, unpublished data, personal communication) has been previously considered. The force of infection from tick to mammal and back most likely plays an important role in this infection intensity, where force of infection is defined as the number of new infections per number of susceptible hosts exposed per unit time.

For an endemic parasite, the force of infection can be calculated using age-prevalence data (Anderson and May 1991). In some systems, it may be that peak intensity of infection occurs towards the end of an organism's life (Duerr et al. 2003, Cattadori 2005). I hypothesize that it might be the case in the Lyme disease system that mouse host populations demonstrate higher infection intensities later in life, because they have had more opportunities to become infected, or their immune systems begin to fail as they age.

Further, there may be evidence that multiple pathogen strains may aggregate in hosts (Lord et al. 1999). For LD in particular, there is some evidence that there will be more strains present in an endemic area, and fewer in a newly invaded area, such as

Lower Michigan. There is evidence that genotypic variation has some impact on the pathogenesis of disease (Wang et al. 2001) and hence, its impact on humans.

It has been shown in a laboratory experiment that approximately 20% of infected nymphs are not transmitting *B. burgdorferi* to hosts (Levin and Fish 2000). I hypothesize that this could be a parasite factor; there could be a threshold number of parasites in a host that signals the parasite to move out of that host. It is possible that this 20% has spirochete burdens too low to have successful colonization and therefore transmission.

Combining Woolhouse et al.'s hypothesis (1997) that only 20% of the hosts are responsible for 80% of the infections with the estimated transmission data from the aforementioned laboratory experiment (Levin and Fish 2000), it is possible that of the infected ticks, the lower 20% are not contributing to LD spread, the middle 60% are responsible for 20% of the incidence, and the remaining 20% of ticks with the highest parasite load are contributing to 80% of the LD incident infections (Figure 1.8). Thus, the proportion of ticks that are infectious is a subset of all infected ticks. The probability of a host becoming infected may be a positive function of the number of parasitizing ticks.

The intensity of infection, or the degree to which an organism is infected, is the aspect of interest in regard to the ticks' infection with *B. burgdorferi*. Intensity of infection refers to the number of pathogenic organisms found inside a host. Force of infection refers to the rate at which susceptible individuals become infected by a pathogen, and can be used to compare the rate of transmission between different groups of the population for the same disease, or even between different diseases. The force of infection from tick to mammal species and then back to tick may also play an important
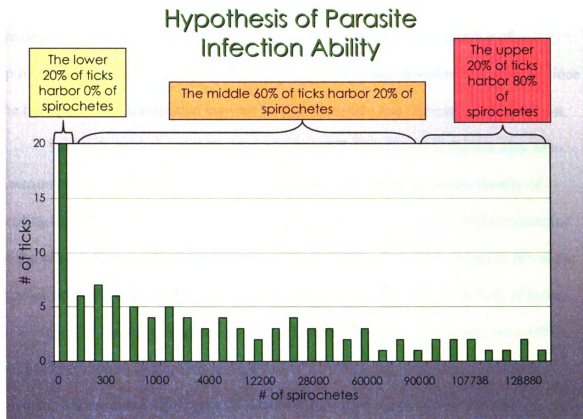
Figure 1.8. A visual representation of the hypothesis that the upper 20% of parasite loaded ticks harbor 80% of the spirochetes (false data set). Images in this thesis are presented in color.

role in regards to infection intensity. The intensity of the infection can affect transmission efficiency in both directions. If a tick or host has a low number of spirochetes, (and thus intensity of infection is low) transmission will not be efficient since the few spirochetes transmitted may not be able to survive and replicate in the new host.

Studies have shown that the transmission of *B. burgdorferi* to the tick may be a function of the density of feeding ticks on the host. In a laboratory study, density of feeding larvae on infected mouse hosts was compared with the success of the acquisition of the spirochete in the feeding larvae (Levin et al. 1997). At low densities (25 larvae per mouse), up to 90% (23 ticks per mouse) of larvae successfully fed and molted; of those, an average of 17% were infected. At high densities (250 larvae per mouse), only 16% (40 ticks per mouse) of ticks successfully fed and molted, but on average, 32% were infected. On the hosts with higher densities of feeding larvae, although a lower percentage of ticks successfully molted, raw numbers of survivors were still higher, and percentage of infected ticks was double that seen in the larvae fed at low densities.

When ticks are aggregated on hosts, their survivorship may be reduced, but the overall number of infected ticks is still higher than if the ticks were spread out on hosts at low densities. Thus, aggregation may help play a role in the maintenance of the LD cycle. Another study that also demonstrated lower feeding success by *I. scapularis* with increased densities of feeding larvae also showed that aggregation of the hosts reduced density of feeding ticks since grooming behaviors increased when mice went from solitary to co-nesting (Levin and Fish 1998). Although survivorship for *I. scapularis* is less favorable under crowded conditions, it is more favorable for *B. burgdorferi*, since co-feeding increases the chances of spirochete transmission to other vectors.

Describing Aggregation

How I. scapularis *ticks become infected and* B. burgdorferi *are maintained among ticks*

In the two year life cycle of *I. scapularis*, the tick will take three bloodmeals. The first occurs in the summer of first year of life, as a larva, during which it can acquire the *B. burgdorferi* pathogen, and after which, it molts into a nymph and over winters until the following spring. That spring, it takes its nymphal bloodmeal, which is another opportunity for it to acquire *B. burgdorferi*, and then molts into an adult, at which time the females take their final bloodmeal that fall or winter. The way the tick finds its host is slightly different each time.

As a larva, the tick seeks a host from the spot it hatched out of its egg (where its egg and all its siblings' eggs were laid), and usually seeks a small rodent or bird host to feed on. However, I. scapularis are generalist feeders, and will opportunistically feed on whatever host it can.

As a nymph, the tick is questing close to the spot where it had dropped off its first host as an engorged larvae. It is also looking for a small-sized host to feed on. Finally, as an adult, it seeks out its bloodmeal from the spot it dropped off its nymphal meal host, but this time, often ends up on a large mammal (deer, bear, human, dog) to feed. Even though it is possible that the tick might not become infected until its adult stage, at that point, it is a dead-end host since it takes no further blood meals. It is also important to note that transovarial transmission is low and therefore the amount of infected larvae is negligible (Patrican 1997).

Although the tick has two chances to become infected and then pass on that infection, there are still many ticks that do not acquire the *B. burgdorferi* spirochete in

27

either of their first two bloodmeals. Because there are so many uninfecteds, or ticks with

a zero spirochete burden, there are specific distributions that are used to describe the

distribution of spirochetes across tick or host populations.

Another way to think about this is the probability that a host becomes infected

with *B. burgdorferi*. That probability is a function of the probability of contact with a

tick, times the prevalence of infection (estimated as prevalence of *B. burgdorferi* in the

tick population), times the probability to transmit the parasite, which itself is a function of

spirochete load.

The negative binomial

The negative binomial distribution (NBD) has been in use for some time as a

descriptor of biological data (Bliss and Fisher 1953). In a review of 49 published

wildlife/parasite systems, Shaw et al. (1998) demonstrated that 48 of these 49 systems are

well-described by the NBD. Since then, more host/parasite systems that display strong

aggregation employ the NBD in order to statistically describe the system (Rosa and

Pugliese 2002, Wang et al. 2003). The NBD is a discrete probability distribution and

generalization of the Poisson that describes greater variance (Elliott 1977, in Guyatt et al.

1994).

The NBD of a population is described by the 'k' parameter, which can be

approximated by the formula $k\text{-hat} = x^2 / (s^2 - x)$, where x is the sample mean and s^2 is

the sample variance. *k* is a value between 0 and infinity, and the smaller *k* gets, the more

highly aggregated the population. In a completely aggregated system, *k* = 0, and all the

parasites are on one host. Generally, when $k \leq 5$, the distribution is best approximated by

the NBD (Anderson and May 1978, Hudson et al. 2002). The 'k' parameter describes the number of failures encountered before finding a success. When an outcome for the NBD is termed a failure, it refers to it as a '0'- since the possibilities of outcomes in the binomial distribution are limited to '0' or '1'. Using the NBD to describe infection in these host/parasite systems, the infected hosts are scored a '1', ascribed the characteristic 'success', and the uninfected hosts scored '0', or 'failures'.

In these host/parasite systems, the 'successes' and 'failures' or 'infecteds' and 'uninfecteds', will lie on either side of some determined cut point. The cut point it determined as a parasite burden above which an infection may be successfully transmitted, and below which it cannot. Hosts with a number of parasites below that cut point have an intensity of infection too low to transmit the pathogen successfully, and therefore, those hosts are considered uninfected.

This distribution is useful when there are binomial outcomes, and the probability of success can be described as a proportion, π. The 'k' parameter is used to describe the degree of dispersion, with an inverse relationship to degree of aggregation (Paterson and Lello 2003, Pal and Lewis 2004). As the parameter 'k' decreases, it indicates a higher degree of aggregation (Hudson 2002). However, as the 'k' parameter approaches infinity, the negative binomial converges with the Poisson (Elliott 1977, in Guyatt et al. 1994, Hudson et al.). Rosa and Pugliese (2002) point out that k is not a parameter corresponding to a particular biological process, but instead, a population statistic.

Variance to mean ratio

Variance to mean ratios can be used to determine if aggregation occurs, where values greater than one indicate aggregation (Lord et al. 1999, Elston et al. 2001). Variance is generally assumed to be greater between groups than within groups (Elston et al. 2001). However, when population sizes are small, the mean tends to be underestimated. This is likely due to incomplete sampling of the population and thus missing the individuals with the highest parasite loads (Gregory and Woolhouse 1993). When the variance is equal to the mean, the distribution fits the random, or Poisson distribution.

Mixed models

The generalized linear model (GLM) is also useful for describing distributions found in nature. This is because mixed models incorporate an error term into the GLM to account for random effects (Paterson and Lello 2003). The general model form is: $y_i = X_i\beta + \varepsilon_i$, where there is a slope parameter (β) and an error term (ε). The standard GLM will have variance equal to the mean, with Poisson distributed errors.

Here, the mixed models will be referred to as GLMM (generalized linear mixed model). The GLMM can be used to analyze parasitological data that does not conform to a normal distribution, and also controls for correlations between data points that arise from grouped observations. A GLMM regression equation takes on this general form: $y_i = X_i\beta + Z_i b_i + e_i$, where the newly introduced term, Z, is the random component of the model. The properties of this model are as follows: $\mathrm{var}(y_i) = E(\mu_i) + \mathrm{var}(\mu_i)$. Here the

30

variance is far greater than the mean (Paterson and Lello 2003). The analogous GLMM with Poisson-distributed errors is described by $var(y_i)=E(\mu_i)$.

These GLMM have commonly been used when describing macroparasite distributions among hosts, and employ a restricted maximum likelihood (REML) method of analysis (Kirby et al. 2004). Wilson et al. (1996) argue that the negative binomial and the GLM may not be sufficient and that using log-transformed data for aggregation analysis may sometimes be the better option. This is because the aggregation data often have a large number of zeroes, and log-transforming changes the zero values.

Lloyd's mean crowding index

Lloyd's mean crowding (LMC) index is the variance to mean ratio expressed from the point of view of the parasite. The general form of the index is:

$$m^* = m + (s^2/m - 1),$$ where m^* is the index parameter, m is the sample mean, and s^2 is

the sample variance (Lloyd 1967). If the distribution of parasites among hosts is normal, the variance to mean ratio equals 1, and the index (m^*) will be equal to the mean, indicating that on average, as many parasitic organisms are experiencing crowding as those not experiencing crowding. If the distribution is over-dispersed, then the variance to mean ratio will be greater than 1, and hence, the crowding index will be greater than 1, indicating that more parasitic organisms than not are experiencing crowding.

LMC measures the number of other parasites experienced by the average parasite in the sample population. When aggregation occurs, and most of the parasites are crowded in or on only a few hosts and only a few parasites are not crowded in or on their

host. The number of the index cannot be directly translated into an interpretation of the number of other parasites a parasite is experiencing.

Statistically modeled systems

Statistical models provide powerful tools for describing how and why biological processes influence parasite infection and aggregation, including exposure of hosts, and virulence and movement of parasites. A deterministic model proposed by Crofton (1971) does not take into account stochastic variables inherent in the study system. One basic characteristic of these deterministically modeled systems is the assumption that the parasite reproduces at a much higher rate than the host (Crofton 1971).

According to Paterson and Lello (2003), the problem with some statistical parasitological models is pseudoreplication, whereupon spatial or temporal correlations make observations non-independent. That is an issue for this study in this system, where repeated sampling of the same mammals caught at different times forgoes assumptions of independent capture events. Rosa and Pugliese (2002) argue that models that address aggregation have thus far only focused on parasite abundance, but that focus should perhaps shift to include factors affecting parasite dynamics and evolution. This study attempts to address some of these concerns by taking into account host spatial structure and immune response.

Other researchers have already attempted to model the Lyme disease system in a process-based, rather than statistical way (VanBuskirk and Ostfeld 1998). Some of these models even take into account the that there is not a constant species-specific rate of infectivity, recently the issue of reservoir competence, or the degree to which a host is

32

capable of harboring and propagating infection in its body and is subsequently able to infect a feeding vector has been introduced (Schauber and Ostfeld 2002). The specific infectivity of a host can be represented by multiplying the proportion infected (I) by the reservoir competence of that species (Mather 1993, Schauber and Ostfeld 2002). Certainly, in a disease system involving *B. burgdorferi*, we do not see any self-cure immunity in any of the species considered reservoir hosts or disease-susceptible hosts.

Studies have documented the transmission dynamics for other disease systems (Woolhouse et al. 1998, Randolph 1999a), or to create a predictive model of disease transmission or disease risk, such as that for *Babesia microti* (Mather et al. 1996). A study by Pugliese et al. (1998) developed a mechanistic epidemiological model for macroparasite aggregation.

Research Questions

Through the study of the ecology of many vector-borne and zoonotic disease systems, the scientific community has illuminated some of the events contributing to the spread of these diseases. For instance, disease ecologists have linked the spread of West Nile virus across the US to bird migration patterns (Reed et al. 2003, Owen et al. 2006).

By understanding the mechanisms for the transmission and maintenance of vector-borne and zoonotic diseases, we have the opportunity to develop preventive measures against these diseases. For example, if it is known that bird migration is contributing to virus transmission to local birds, humans or horses via mosquitoes, then it

is prudent to control mosquito populations is high risk areas during high risk times of the year.

My overall hypothesis is that the infected *I. scapularis* questing nymphs in Menominee, Michigan have over-dispersed loads of *B. burgdorferi*. Further, adult life stages of ticks will show the greatest spirochete loads, and adult reservoir-competent hosts will show higher spirochete and tick loads than juveniles. The LD transmission cycle in Menominee County may be influenced by changes in infection prevalence of hosts, spirochete load, spirochete distribution in *I. scapularis* ticks and small mammal hosts, and that the age-structure of those tick and reservoir host populations impact spirochete loads and distributions in these same populations.

The null hypothesis is that a host population demonstrates a random distribution of parasite burden. An even distribution would not be a realistic model for parasite distribution, as it would assume that every host in the system has the same number of parasites. Realistically, we know that some hosts will never become infected, and that '0' burden cannot be accounted for in an even distribution, unless all hosts had '0' parasite burden, which would nullify the disease system. Characteristics that distinguish an aggregated distribution from a random one include a variance to mean ratio greater than 1, the estimate of the NBD parameter k that is low, prevalence of infection and mean parasite burden, dispersion pattern of parasites among hosts, as well as patterns in aggregation, as defined by Shaw and Dobson (1995).

Through this research I have posed the following overall questions:

- Is aggregation occurring in the parasite populations of Menominee County's endemic Lyme disease system?

- If so, do habitat factors contribute to this aggregation?

- Are any of these factors spatially correlated, and what are the possible explanations for this spatial correlation?

These broader questions can be broken down into more focused, specific questions that ask about the nature of aggregation in the system, and then the contributing factors.

Description of aggregation in the system

- Does aggregation of parasites occur in this system and to what degree?

- Does aggregation occur at the pathogen level, the tick level, or both?

- Is there aggregation of ticks that are off-host?

- Is there aggregation of ticks that are on-host?

- Is there aggregation of hosts?

- Are aggregation patterns different among different life stages of ticks?

Processes that contribute to aggregation in the system

- What measured factors might have led to aggregation on any level?

- What possible influence might these factors have?

I addressed these questions by performing, at three trapping grids, three times each over the summer transmission period, a vegetation survey, a survey of questing ticks, and a survey of *Peromyscus spp* mice. This study quantifies the distribution of *B. burgdorferi* in larval, nymphal and adult *I. scapularis* ticks and mammal hosts as well as the distribution of ticks on their small mammal hosts. The study determines the proportion of ticks and hosts are carrying spirochetes and what proportion of hosts are carrying ticks. Distributions of the spirochete, tick and host populations were examined on the landscape. Implications of aggregation on the LD cycle are discussed.

35

CHAPTER 2

METHODS

Field methods

Study site, sampling design and field schedule

The study site is in southwestern Menominee County, in Michigan's Upper Peninsula. In this area, abundant *Borrelia burgdorferi*-infected tick populations exist (Strand et al., 1992). Menominee County was chosen as the study area for this reason; the particular site (N 45°9'46.2", W 87°42' 48.0") was chosen based on the oak-dominated forest and sandy soil, *I. scapularis'* preferred habitat (Guerra et al., Figure 1.4). Figure 1.6 shows the study area where three, 1.15 ha grids were sampled for mammal, tick and *B. burgdorferi* populations.

The three grids were situated 12 m apart. Three grids were chosen in order to have replication for the area. The grids were placed according to where they would fit on the chosen piece of private property. The grids were set up with an 8 by 10 array of trap points spaced 12 m apart with an overall trapping area of 1.15 ha (Figure 2.1). The grids were set to be this size to maximize mouse capture by using all available traps. Each point had two Sherman traps spaced approximately 0.5 m apart. The traps were placed as close to the trap point as possible while keeping them in areas where small mammals were likely to be (i.e. – not on bare, uncanopied ground).
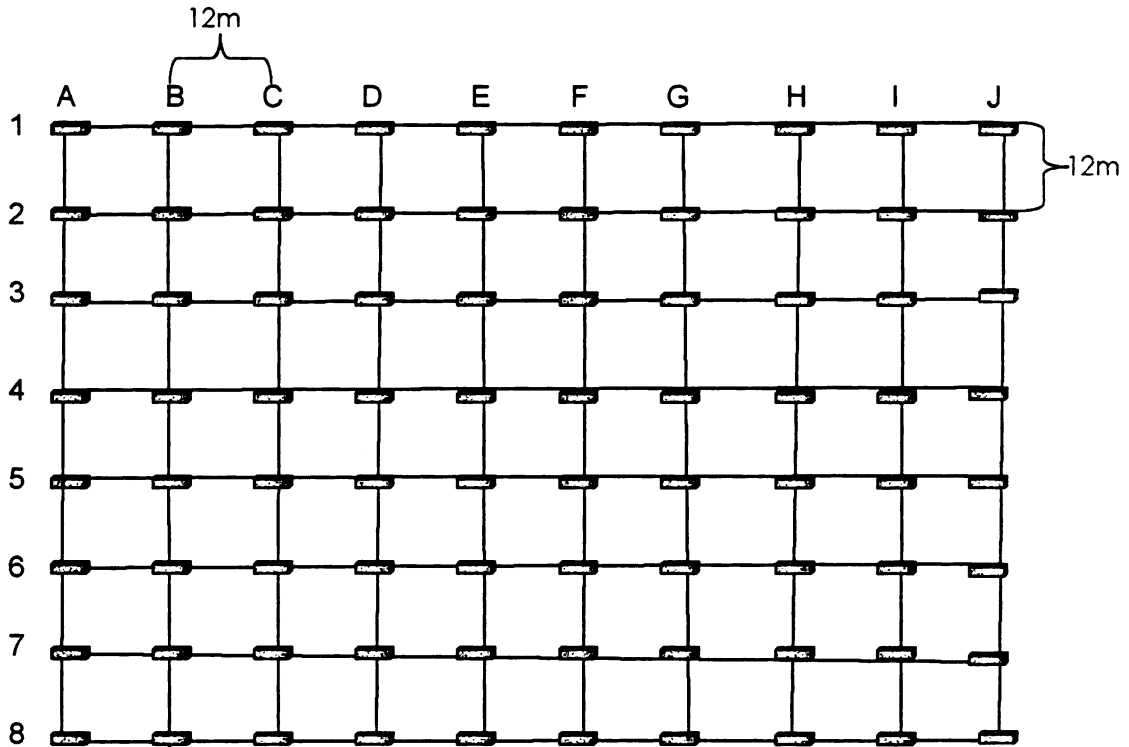
Figure 2.1. Eight by ten trapping grid with 12 m between trap lines (total 1.15 ha). Grey rectangles at grid vertices each represent 2 Sherman long-folding traps used to minimize the effect of trap saturation.

The fieldwork took place from the end of May to mid-August 2006 because this is

thought to be the time of year when both the ticks and their hosts are most active in this

area of Northern Michigan (Walker et al. 1994, Friedrich 2003). During this time, small

mammal traps were employed to trap rodents, questing ticks were collected by dragging,

and vegetation at each trap point was characterized. The procedure for each grid

(replicated per each of three grids, for three 12-night cycles) was as follows, with each of

the following tasks accomplished. The 160 traps were set and checked for 4 continuous

nights, for a total of 5760 trap nights. Whole grid dragging and fine-scale dragging

occurred on one dry day per trap period so as to maximize ability to capture questing

ticks. Vegetation sampling occurred once per grid for the whole season. Daily tasks are

outlined in detail in Table 2.1. Details for each of these tasks are explained below.

Table 2.1. Daily field tasks representing one grid's schedule. This cycle of tasks occurred once per trapping grid for three grids. The entire cycle of three grids was conducted four times over the course of the season.

	Task 1	Task 2	Task 3	Task 4
Day 1	Set up flags and two Sherman traps at each trap point	Drag for ticks	Sample vegetation	Set traps open in the evening
Day 2	Traps checked	Process animals	Finish vegetation sample/ tick drag	Set traps open in the evening
Day 3	Traps checked	Process animals	Finish vegetation sample/ tick drag	Set traps open in the evening
Day 4	Traps checked	Process animals	Finish vegetation sample/ tick drag	Set traps open in the evening
Day 5	Traps checked	Process animals	Remove traps from grid	Begin Day 1, task 1 on new grid

Vegetation sampling

Vegetation was surveyed on each grid because it is thought that habitat has an

influence on where organisms move and prefer to live, and vegetation is an important

part of habitat. In this case, we sampled both understory and trees since those can both

influence animals' habits. Vegetation sampling occurred only once at each of the grids.

Vegetation data were collected at each of the 80 locations corresponding to the trap

points. Northing and the Easting for each trap point were recorded. Understory was

characterized for the 12 m square (24 m^2) surrounding each trap (Figure 2.2), and

recorded as per the code in Table 2.2. Understory was considered to be any non-tree

vegetation, such as shrubs and herbaceous growth. From the flag, the genera of the three

closest mature trees were recorded, defined as having at least a 10" diameter at breast height.
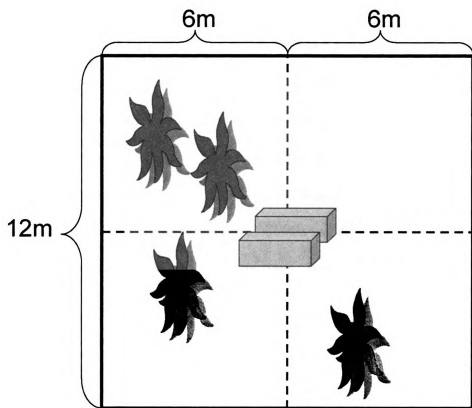
Figure 2.2. Scheme for vegetation sampling. The grey boxes represent the Sherman traps present at each point where Easting and Northing coordinates were taken. The $12m^2$ box around it represents the area around each point considered for vegetation sampling. Dotted lines represent the trap lines on the grid. Images in this thesis are presented in color.

Table 2.2. Categories used for understory classification. Any non-tree vegetation was considered understory.

Code	Description
0	No understory; bare ground.
1	Light cover, up to 33% covered in understory vegetation.
2	Moderate cover, 34% to 66% covered in understory vegetation.
3	Heavy cover, 67% to 100% covered in understory vegetation.

Questing tick collection

Questing ticks were collected using a standard 1 m^2 white corduroy cloth dragged over the forest floor (Falco and Fish 1992), along predetermined transects (Figure 2.3). These transects ran between the trap lines which had been previously set. We sampled for questing ticks using two dragging schemes - 'whole grid' and 'intensive sampling'. We did this to later calculate if any ticks were missed with the coarser-scale sweep of the area. Stops were made every 24 m for whole-grid transect dragging, and every 8 m for intensive-sample dragging (see below for more details). A common distance to drag between stops is 20 m (Diuk-Wasser et al. 2006), but we used 24 m since it lent itself to easy counting with the 12 m spacing of traps. At each stop, if ticks were observed on the cloth, they were removed and placed in labeled vials containing 70% ethanol. These were stored at room temperature until identification could take place. Ticks of all life stages were collected.

Dragging was completed following the arrows in Figure 2.3. For 'whole grid' sample, dragging began 6m before the first flag, and ended 6 m past the last flag indicated in Figure 2.3, and thus the total length of the transect was 120 m. The drag cloth was checked at the place indicated in the figure by a flag, i.e., every 24 m. The dragging transects ran between the trap transects.

At each grid, one of the little squares was randomly chosen for the 'intensive-sample during each rotation (Figure 2.4). These intensive sample surveys were conducted before the whole grid survey. For this survey, the cloth was checked every 8 m. In cases where there were large numbers of larvae on the cloth, they were lifted off

the cloth with clear packing tape and the tape was subsequently stuck to an acetate

transparency for later identification.
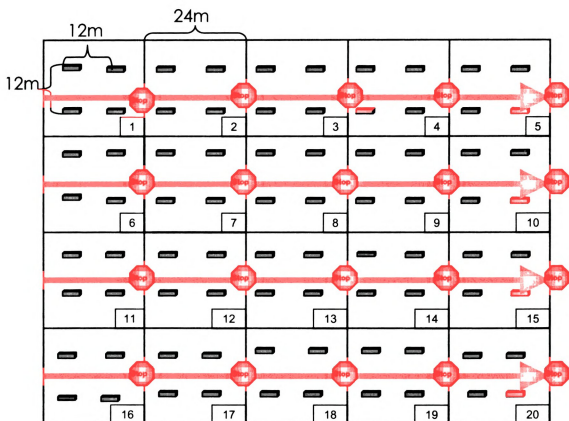
Figure 2.3. Scheme for drag-collecting ticks from grids. As indicated, dragging transects were conducted between trapping lines. At each stop point, indicated by the stop signs every 24 meters, drag cloths were lifted and checked on both sides for ticks. Images in this thesis presented in color.
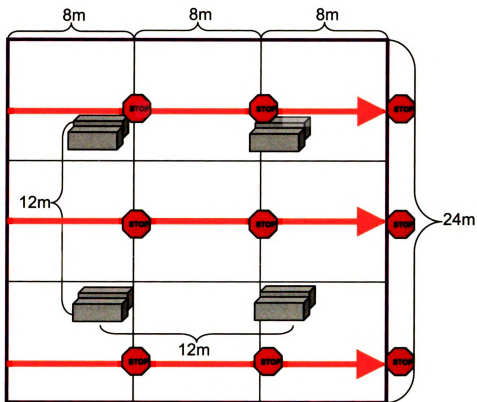
Figure 2.4. Intensive drag-sampling scheme for questing ticks, for one of the 20 above-labeled 24 m^2 grids (Fig. 2.3), chosen at random for each grid, at each time step. Arrows indicate transects dragged between trapping lines and stop signs indicate where drag cloths were checked for ticks. Images in this thesis presented in color.

Due to the nature of this preservation, these ticks could not be assayed for the presence of *B. burgdorferi*. However, questing larvae are not likely to be infected since transovarial transmission is highly inefficient (Piesman et al. 1986, Patrican 1997).

For the purpose of comparing tick densities across habitat types, I also sampled another study site in the county for host-seeking ticks. This site is found in the Escanaba River State Forest is on the eastern side of Menominee County. This habitat was characterized by cedar swamp and a high water table. Dragging for ticks at this site

occurred once every two weeks during the season. 500 m were dragged each time and used for comparison with the southwestern Menominee County site.

Small mammal trapping and processing

Trapping effort was limited to one grid per day; traps were set between 17:00 and 19:00 in the evening and checked each day at 7:00. Traps were baited with a mixture of crimped oats and raw peanuts. Upon checking, if a trap was found to have an animal, it was brought back to the processing station. Empty traps were closed at that time. Processing was done while the animal was alert and not sedated. Data were collected as follows: trap number and location of capture, recapture status, mass, age, sex, reproductive status, species, ear length measurement (for *Peromyscus spp.* only) and number of larval and nymphal ticks feeding. Ticks were removed and placed in labeled vials containing 70% ethanol. Approximately 2 mm punch biopsy of ear skin was taken and similarly preserved. Each animal was given a uniquely numbered ear tag (Monel 1005-1, National Band and Tag, Newport, KY). To obtain a blood sample, each mouse was placed head first in a 50 ml conical tube with breathing holes drilled into it. Blood was obtained by cutting off the tip of the tail with a sterile scalpel. Blood was collected in Microvette tubes (Sarstedt, Nümbrecht Rommelsdorf, Germany) and preserved on ice until they could be centrifuged to separate serum from cells that afternoon. The bleeding was stopped by the use of styptic powder and application of pressure.

After blood collection, mice were observed for 10-15 minutes. If the mice were alert and healthy, they were released at the site of capture. Mice that appeared cold or were still bleeding were treated by being placed on an activated charcoal hand warmer or

had more styptic powder applied to their tails, respectively. Mammal mortality due to handling was low, for a total of three deaths of the 757 captures (0.4%).

Animals were treated in accordance with the approved Michigan State University All University Committee on Animal Use and Care protocol (12/03-152-00). All workers in the field were outfitted with the proper personal protective equipment. These items consisted of a white cotton tick suit, latex gloves and a respirator for small mammal handling. All workers were certified by the Michigan State University Office of Radiation, Chemical and Biological Safety on their N95 respirators prior to animal handling.

Laboratory methods

Tick identification

All ticks collected from the vegetation (questing) and off hosts (feeding) were identified by life stage and species. To identify, ticks were placed in individual small Petri dish under a dissection scope, and using a dichotomous key (Sonenshine 1979), were determined to be larva, nymph, adult female or adult male. Upon identification, nymphal and adult ticks were individually placed into new, DNAse/RNAse-free 1.5 ml microcentrifuge tubes for storage at -80°C until DNA extraction could be completed. Larvae were pooled by host or by drag location and date, due to their small size and low probability of carrying the *B. burgdorferi* spirochete. Each pool contained between 1 and 100 larvae.

Each new tube was given a unique identifier, a number followed by a letter to indicate species and life stage. 'A' coded for *I. scapularis* larvae, 'B' for *I. scapularis* nymphs, 'C' for *I. scapularis* adult females and 'D' for *I. scapularis* adult males. For example, 45B indicated the 45th tick identified in the series, and that it was an *I. scapularis* nymph. A master spreadsheet correlated each tick back to the individual mammal off of which it had been collected and capture date.

DNA extraction

DNA was extracted using DNeasy kits (Qiagen, Valencia, CA). Preparation of the samples involved removing each tick from its tube, placing it on a Kimwipe (Kimberly-Clark, Neenah, WI) inside a fume hood and allowing the ethanol to evaporate. Ticks were then placed individually in a new, DNAse/RNAse-free 1.5 ml

microcentrifuge tubes, frozen in liquid nitrogen, and crushed with a sterile pestle in order

to crush the exoskeleton and allow the contents of the midgut to be exposed to the first

buffer solution in the kit.

The following modifications were made to the Qiagen protocol: ticks were lysed

overnight in lysis buffer, AE (elution) buffer was heated to 70°C before adding to the spin

column for final elution and each sample was eluted into a 50 µl final volume. Samples

were stored at -80°C until PCR could be performed. Each batch was extracted with both

a positive (*B. burgdorferi* culture) (Table 2.3) and negative (sterile water) control.

Table 2.3. Table of sources of the cultures used to create the standard curves for qPCR.
The standard curves were used to determine the number of organisms present in a
sample. All cultures were grown from adult *I. scapularis* collected from the field in April
2006. Listed is the location where that tick was collected, its assigned code, the resulting
standard curves, the number of spirochetes at each point in the curve and the strain of
each culture. All cultures grown and standardized by Sarah Hamer.

Location collected	Code	Curves created	Number of spirochetes	Strain
Castle Rock State Park, IL	c131	A, B, C	$2.27 * 10^4, 10^3, 10^2, 10^1, 10^0, 10^{-1}$	CS8
Tippecanoe State Park, IN	c017	D, E, F	$2.82 * 10^4, 10^3, 10^2, 10^1, 10^0, 10^{-1}$	297
Governor Dodge State Park, WI	c336	G, H, I	$2.79 * 10^4, 10^3, 10^2, 10^1, 10^0, 10^{-1}$	156b

Checking positive controls for DNA and quantitative reliability

Each tick sample was to be assayed for *B. burgdorferi* using a quantitative PCR.

For each run of this assay, standard curves of known quantities of *B. burgdorferi*

spirochetes were needed. To generate these standard curves, *B. burgdorferi* spirochetes

were first cultured and counted using a Petrof-Hauser chamber, by S. Hamer (Table 2.3).

Nine 5-point dilution series were created, each containing between 2 and 3 organisms times the following orders of magnitude: 10^4, 10^3, 10^2, 10^1 and 10^0. These cultures were then extracted using the aforementioned Qiagen DNeasy kit and modifications. These nine series were then tested for reproducibility using the qPCR protocol and found to perform reliably (Figure 2.5).
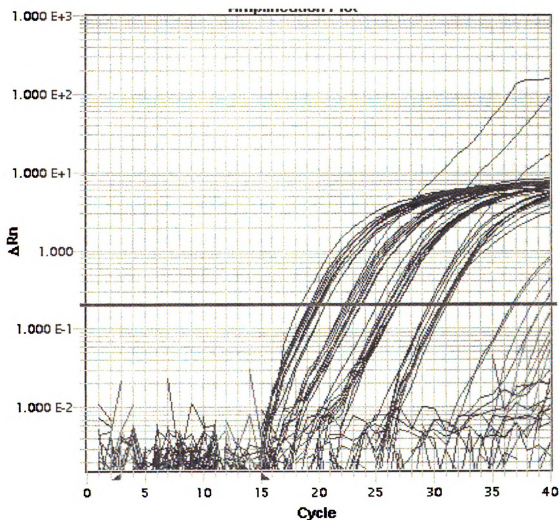
Figure 2.5. The amplification plot for the standard curve trial for *B. burgdorferi* for five dilutions ranging from 10^{-1} to 10^3. (SDS 2.3). Nine samples for each dilution had been prepared, and the points for each order of magnitude clump together on the graph, showing their close Ct values and thus tight reproducibility. Ct value refers to the cycle number at which the PCR product with the labeled probe was detectable above a preset threshold.

Quantitative (qPCR) on extracted tick DNA for B. burgdorferi

Quantitative PCR (qPCR) is a method for detecting the exact number of copies of a piece of DNA in a sample. By amplifying a portion of the genome for which there is only one copy, the resultant copy number can reveal the number of *B. burgdorferi* organisms in the sample (Wang et al. 2003). The amount in the sample can then be extrapolated to the whole sample (tissue, tick) by multiplying that number by the volume of the whole DNA extraction. For example, if one used 1 µl of a 50 µl sample, you would multiply the final number by 50 to estimate the number of copies of the DNA in the entire sample.

There are several other less-precise methods which can detect the spirochete's DNA, although not the copy number; those published in the literature, such as molecular typing of *B. burgdorferi* PCR-RFLP (polymerase chain reaction restriction fragment length polymorphism) analysis (Liveris et al. 1995). These methods also used a standard dilution; the products were run out on a gel, and then the samples were compared to that dilution series by comparing band intensity by eye. These methods do not have the power to provide an estimate for the spirochete load in the sample with the same precision as qPCR.

DNA from ticks was checked for the presence of the 16s intergenic spacer region in *B. burgdorferi*, of which there is only one copy, via quantitative real-time PCR at Michigan State University's Research Technology Support Facility's Genomics Core. The primer used was chosen from Tsao et al. 2004 (16s forward, 23 bases: 5'-GCT GTA AAC GAT GCA CAC TTG GT- 3' and 16s reverse, 22 bases: 5' –GGC GGC ACA CTT AAC ACG TTA G -3'). The process used a TaqMan major groove binding (MGB)

protein and the 6FAM fluorescent label, known as the probe (22 bases: 5'- 6FAM TTC GGT ACT AAC TTT TAG TTA A MGB- 3'). This probe is employed in order to quantify the PCR product without gel electrophoresis (Morrison et al. 1999).

All reactions were run on the Applied Biosystems (ABI) 7900. Master mix for 15 μl reaction was as follows: 7.5 μl 2x ABI TaqMan PCR master mix, 1 μl probe at 200 nm/L, 1 μl each forward and reverse 16s primers at 900 nm/L, 1.5 μl PCR-grade water, and 3μl template DNA. Reactions were run in 96-well PCR plates. Each sample was run in triplicate, along with a serial dilution of 10^0 - 10^5 B. *burgdorferi* spirochetes to create a standard curve, positive and negative extraction controls and positive and negative PCR controls (Table 2.3). Only one positive control (serial dilution) and set of three negative controls (water substituted for DNA) were run per day for all the plates. The number of plates run per day varied from one to four.

Each run was recorded on ABI's software (SDS 2.3). The data were derived as a Ct value, or the cycle number at which the amplicon crosses the threshold of detectibility. This value was used to determine the number of spirochetes per sample. The three points of each sample were averaged and that value was placed on a standard curve created from the serial dilutions (Figure 2.6). The number of spirochetes in the sample was derived from that particular day's standard curves. That number was multiplied by 50 to calculate the number of spirochetes in the tick, because only 1 μl of the 50 μl of extracted DNA were used.

If the numbers for the replicates were not close in value (meaning there was a difference of more than ± 1.0) or if one or two of the values were recorded by the robot as undetermined, the plot of the amplification curve was examined to determine if the value

49

was real or an artifact. Real amplification manifests as a smooth exponential curve, whereas contamination and other interference will result in broken, jagged, or straight lines. Samples determined to not show real amplification were recorded as zero spirochetes. Samples where all three points came up as undetermined were also determined to contain zero spirochetes. Undetermined samples were those that the machine was not able to assess a Ct value on. If there appeared to be a discrepancy in the data, and one of the replicates appeared to amplify and the other two did not, that sample was re-run. If two of the replicates amplified and one did not, then the two that provided a positive result were averaged for that sample's Ct value.

The plotted regression equation reads $y = 2E+09e^{-0.6374x}$, $R^2 = 0.9985$. The y-axis is "Number of spirochetes in the sample (log scale)" ranging from 0.1 to 100000, and the x-axis is "Ct value" ranging from 15 to 35.
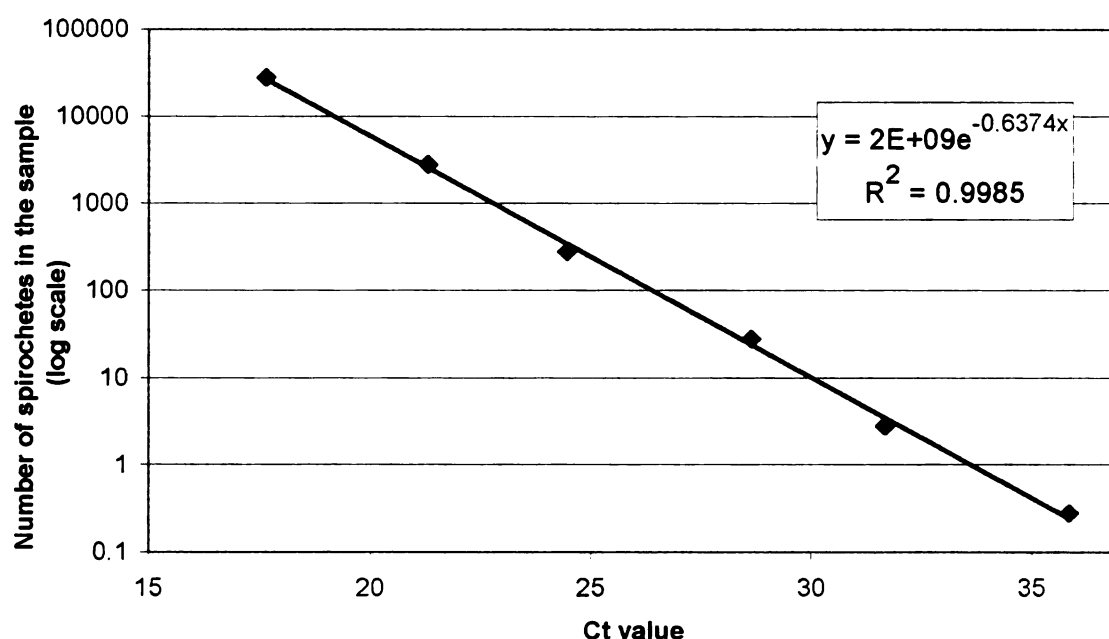
Figure 2.6. An example of a standard curve used to determine numbers of spirochetes in tick and tissue biopsy samples. Ct value refers to the cycle number at which the PCR product with the labeled probe was detectable above a preset threshold. The regression equation calculated by Microsoft Excel was used to determine the number of spirochetes present in the sample. The Ct value of the sample was substituted for x, and y, or the number of spirochetes was obtained algebraically.

50

Mammal tissue DNA extraction and optimization

Ear tissue biopsy punches from all mammals captured underwent DNA extraction using DNeasy kits (Qiagen, Valencia CA). Samples were prepared for extraction by removing them from their original ethanol-filled tube to a Kimwipe to dry under the hood before getting placed into a new, clean microcentrifuge tube. Modifications made to the Qiagen protocol were the same as for the tick extractions. Ear punch DNA was stored at 4°C until the desalting procedure could be performed shortly thereafter. In order to ensure that the amount of mammalian DNA in the ear punch biopsy extractions would not overwhelm the primers for *B. burgdorferi*, an optimization trial to determine DNA sample concentration was performed; additionally we tested whether desalting the extracted DNA would be needed. The total eluted 50 μl volume of the DNA was first divided into two 25 μl aliquots. One was used for desalting. Desalting the samples required the use of flow-through columns to remove impurities (Pure Biotech LLC, Middlesex, NJ). The sample was placed on hydrated gel matrix inside a spin column and spun in the microcentrifuge. The spinning allowed the eluted DNA to flow through, and trapped any interfering salts in the gel. The remaining volume was smaller in all cases, and varied from approximately 10 μl to 24 μl.

The desalted and virgin aliquots of each sample were then further divided by removing 5 μl of the volume of DNA, adding it to a new tube, and diluting 1:10 by the addition of 45 μl of sterile PCR-grade water. Thus, in total, four subsamples (Figure 2.7) of the original elution were made (i.e., salted 1X, desalted 1X, salted 0.1X, and desalted 0.1X), and the PCR trials could begin in order to find the optimal combination of DNA techniques.

51

A non-random sample (n = 10) of mammal DNA was chosen to undergo the trial

to determine the optimal treatment of DNA for detection of *B. burgdorferi*. The samples

were chosen because of the likelihood that the animal had been bitten by an infected tick.

Therefore, the samples were from older mice from which we had pulled an engorged tick

which tested positive for *B. burgdorferi* using qPCR.
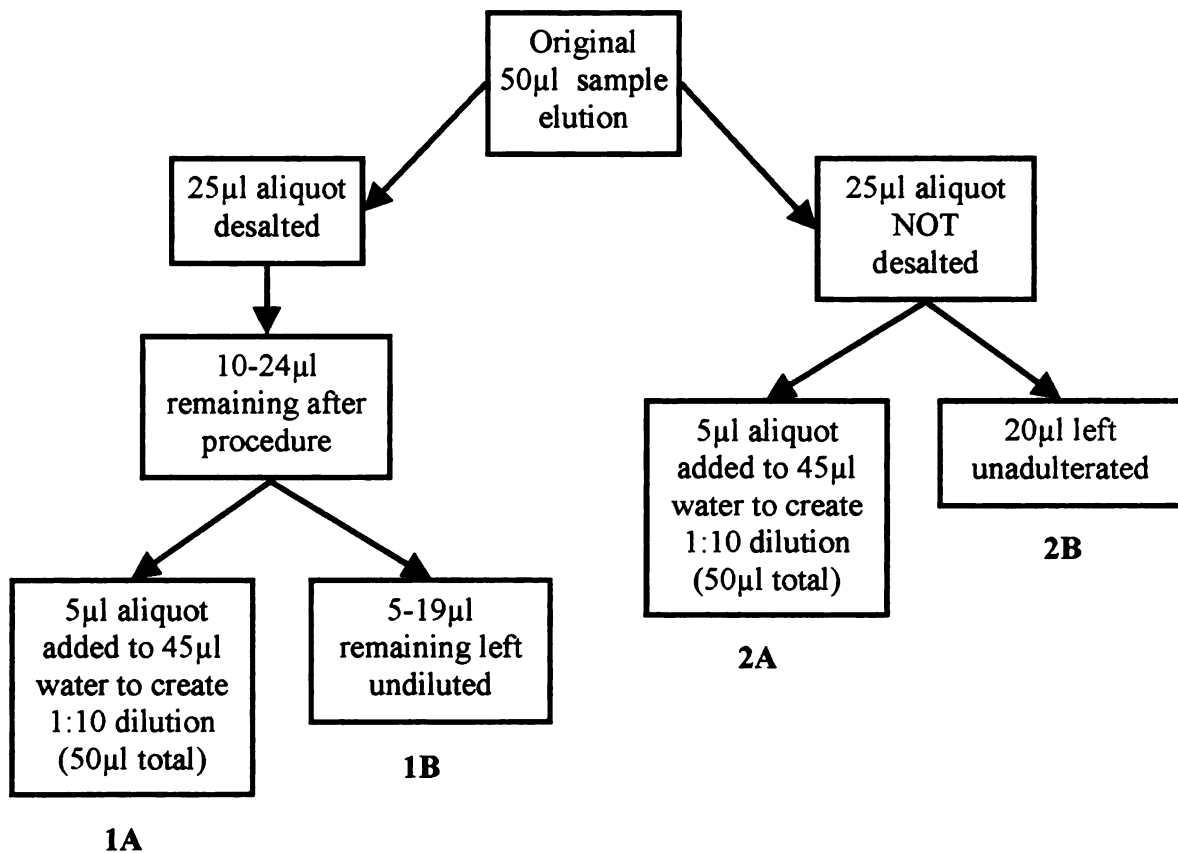
**Figure 2.7. Creating mammal DNA samples to optimize detection of *B. burgdorferi*
by PCR.** Flowchart detailing the steps to create the 4 subsamples from each original
50μl elution of DNA from mammal ear biopsy punches. The 10 samples used for
optimization trials were those from older mice infested with ticks that had tested positive
for *B. burgdorferi*.

The PCR trial conducted was a nested reaction for amplification of the intergenic spacer region (IGS) between 16s (rrs) and a 23s (rrlA) rRNA genes in *B. burgdorferi*, (Bunikis et al. 2004b). PCR with gel electrophoresis was used for this trial so that the product could be visualized.

The outer reaction was run in an Applied Biosystems GeneAmp 9700 96-well thermocycler in a 50 µl reaction volume. Each well contained 43 µl PCR Supermix (Invitrogen), 1 µl each outer-forward (IGS F: 5'GTA TGT TTA GTG AGG GGG GTG3') and outer-reverse (IGS R: 5'GGA TCA TAG CTC AGG TGG TTA G3') primers (0.16pmoles) and 5µl template DNA. The positive control was extraction from culture c017-p8 (courtesy S. Hamer), and the negative control was water. Reaction times were as follows. The initial denature ran for 1 min at 80°C and then 3 minutes at 94°C, followed by 35 cycles (30 seconds at 94°C, 30 seconds at 56°C, 60 seconds at 74°C). The final extension ran for 7 minutes at 72°C. Samples were stored at 4°C until inner reaction could be completed.

The inner PCR followed the same protocol for mastermix preparation detailed for the outer PCR reaction, but instead used the inner forward (IGS Fn: 5'AGG GGG TGA AGT CGT AAC AAG3') and inner reverse (IGS Rn: 5'GTC TGA TAA ACC TGA GGT CGG A3') primers. The template DNA used was 5uL of the product from the previous PCR. The inner program was the same as above but with the following modifications: the initial denature ran for 1 min at 80°C and 90 sec at 94°C, followed by 40 cycles of the previous denature-anneal-extend cycle. Samples were stored at 4°C until gel electrophoresis in 2% agarose gel.

Assaying mammal tissue biopsies for Borrelia burgdorferi

Quantitative PCR for biopsies was conducted as per the tick samples. The primer targets the 16s intergenic spacer region (Bunikis et al. 2004b). The product is detected using the TaqMan MGB (major groove binding) protein and the 6FAM fluorescent labeled probe. Primer sequence: 5'6FAM-TTC-GGT-ACT-AAC-TTT-TAG-TTA-A-MGB (Applied Biosystems). All reactions were run on the Applied Biosystems (ABI) 7900, at the Research and Technology Support Facility on site at Michigan State University. Master mix for 15ul reaction: 7.5 µl 2x ABI TaqMan PCR master mix, 1 µl probe at 200 nm/L, 1µl each forward and reverse 16s primers at 900nm/L, 1.5 µl PCR-grade water, and 3 µl template DNA. Each sample was run in triplicate, along with a serial dilution of spirochetes to create a standard curve, and positive and negative extraction controls and positive and negative PCR controls.

Data were derived in the same manner as the tick qPCR assays, although the number of spirochetes was calculated by multiplying the standard curve-derived value by 500 (times 10 for the 1:10 dilution, times 50 for the entire 50 µl elution). Rules for re-testing and determination of real or artificial amplification were followed as described for ticks.

Enzyme-linked immunosorbent assay (ELISA) of Peromyscus spp. *serum samples*

Serum samples from *Peromyscus spp.* were tested for the presence of antibodies to a *B. burgdorferi* antigen. Of the 238 small mammals captured during the field season, 167 were *Peromyscus spp.*, and of those, 150 (90% of the total *Peromyscus spp.* captured) were tested with ELISA. It was this study's intent to look at *Peromyscus spp.*

only in order to control for confounding factors such as species differences. Furthermore, because this test requires the use of a species-specific anti-conjugant, only *Peromyscus spp.* could be tested. Sera from field-collected *Peromyscus leucopus* from Lyme endemic site in Connecticut were used as positive and negative controls (Tsao 2004 and Bunikis 2004).

Medium binding 96-well plates were used for this assay. Plates were first blocked with 50μl 1% milk-PBS overnight at room temperature (22°C). 1% milk-PBS made with dried milk powder. The following day, after rinsing wells twice with PBS-Tween 20, serum samples were diluted 1:100 in 1% milk-PBS and added to the wells. Samples were run in duplicate. The plates were then incubated at room temperature for one hour, and washed six times with PBS-Tween 20. The diluted (1:1000) goat anti-*Peromyscus leucopus* IgG horseradish peroxidase conjugated antiserum (60 μl) (Kirkegaard & Perry, Gaithersburg, Maryland) was added to the wells in bright light and incubated one hour at room temperature. Following that, plates were washed eight times with PBS-Tween 20. 100 μl 3.3', 5.5'-tetramethylbenzidine (TMB) substrate was then added, and after three minutes at room temperature, the reaction was stopped with 50 μl 1N HCl .

Immediately after reaction termination, samples were read in a Molecular Devices Kinetic Microplate Reader (Sunnyvale, CA). Samples with optical density (OD) readings > 3 standard deviations above the negative value mean were considered positive. All OD values were normalized by subtracting the empty well average (see plate map, Figure 2.8). Samples that yielded a positive result were subsequently run in an endpoint titer assay to determine the dilution at which the sample would remain positive, in order to assess the relative strength of antibody response.

The endpoint titer assay was performed using the same ELISA protocol as for the screening assay, but the samples tested were run at three dilutions: 1:200, 1:400 and 1:800. The endpoint titer for a specific sample was determined to be the last dilution at which the OD reading was still > 3 times above the negative value mean.

PLATE MAP											
				Peromyscus spp. samples A							
	1	2	3	4	5	6	7	8	9	10	11	12
A	6	6	7	7	10	10	12	12	15	15	16	16
B	18	18	19	19	20	20	21	21	22	22	5	5
C	24	24	27	27	28	28	29	29	30	30	31	31
D	32	32	43	43	42	42	44	44	45	45	46	46
E	47	47	48	48	49	49	36	36	37	37	34	34
F	35	35	40	40	41	41	38	38	39	39	54	54
G	51	51	52	52	218	218	101	101	55	55	56	56
H	57	57	E	E	470++	470++	449+	449+	298-	298-	E	E

Figure 2.8. Generalized plate map for the ELISA assay. Several of the wells were left empty in order to later calculate an average baseline (wells labeled 'E'). The positive controls (denoted ++ and +), negative control (denoted -) and samples (all other numbers) were arranged in the remaining well according to the diagram.

Statistical analyses

All data analysis was carried out using SAS (SAS Institute, Cary, NC) and ArcGIS (ESRI, Redlands, CA).

For measurements of variance to mean ratios, LMC index and k values, basic algebra was employed to obtain these numbers for the populations. The variance to mean ratios were compared against the null hypothesis that the populations followed a random distribution, and therefore were compared to Chi-square values accordingly. This

method, derived from Elliot (1977) is called the Index of Dispersion (I_D), and uses the following formula:

$$I_D = (s^2/x) * (n - 1)$$

where s^2 is the sample variance, x is the sample mean and n is the sample size. This Index is then compared to the Chi-square value for the appropriate $(n - 1)$ degrees of freedom. A value greater than that Chi-square value indicates that the population deviates from the random distribution.

It has been shown that as sample size decreases, values of sample mean parasite burden, variance, and level of aggregation are underestimated because there is low power for detection of the few hosts with large parasite burdens (Gregory and Woolhouse 1993). The sample mean will underestimate the true mean as sample size decreases and/or aggregation increases (Pacala and Dobson 1988). Therefore, if host sample sizes are unequal in regard to age classes, there may also be an artifact of significant patterns in age classes where sample sizes are smaller and aggregation more severe, such as in the oldest age classes (Gregory and Woolhouse 1993).

Age classes matter for both ticks and mice; the numbers of adults will invariably differ from the numbers of juveniles or nymphs based on factors such as mortality rates, behavior, and seasonality. Thus, sample size for statistical power was considered for this study so as to avoid this potential problem. When considering groupings for statistical analysis of measures of aggregation, as often as possible, the data were broken down by trap period and by grid. When sample sizes were low, like for nymphal ticks picked up on the drag, they were grouped by trap period and not by grid, since activity of these ticks

is seasonal and their activity is more likely to vary by season than by place in the same region.

Maps displaying kernel density were compiled for comparison of clustering patterns for nymphs off mice of all species and nymphs off mice that were just *I. scapularis*. Similar maps for larvae were constructed as well. Data tables with latitude and longitude coordinates were entered into ArcMap. Clusters were examined visually on the maps.

Questing ticks were not sampled at the trap points. In order to derive the numbers for the questing ticks at each trap point, the data were plotted in ArcMap (ESRI, Redlands, CA) and interpolated by ordinary kriging, using default parameters. This created a continuous surface over the grid. The trap points were overlaid with this surface (Figure 2.9) and the value of the rasterized surface was extracted at each trap point to get an approximate value for each. That value is the estimated number of ticks for that point that would have been collected by dragging over that point.
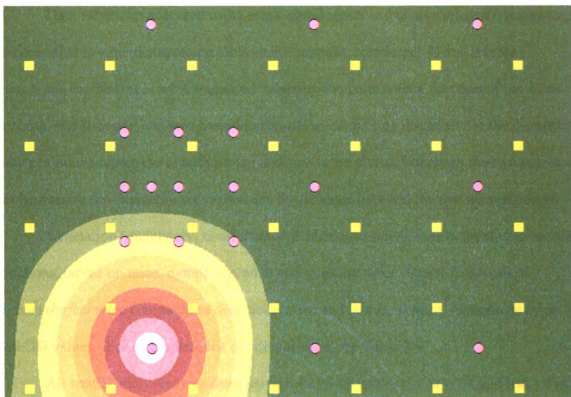
Figure 2.9. Example of overlaying the rasterized surface (calculated from the drag sample points, pink circles) with the trap points (yellow squares) from one grid. The concentric colored circles in the bottom left are radiating from one point with a high number of total ticks collected from dragging. The solid green around the rest of the figure indicates zero values at the remaining trap points. Figures in this thesis presented in color.

Further, the data used for the mouse captures was the first capture of that individual in the trapping period only. In order to avoid the problems associated with repeat captures and lack of independence, only these captures were used in the spatial analysis. In certain cases, this made the sample size for a grid at a particular time period very small, and the analysis reflects this lack of power, since the grids were lumped by trap period for all other analyses.

Data were then analyzed using cross-correlogram and cross-variogram techniques to determine at what distances variables were spatially correlated. Using a cross variogram, lag distances were measured, whereby the units were a function of the 12 m spacing, and thus one unit was considered equal to 12 m. Lag distances are the distance between points where the maximum lag distance is the distance between the two points farthest apart; the minimum lag distance is the distance between the two closest points.

Vegetation (understory, coniferous and deciduous trees) were compared to mouse locations, larvae on mice, nymphs on mice and questing ticks. Quantified loads of *B. burgdorferi* were compared to drag ticks, mice and larvae on mice, nymphs on mice and OD values. For a complete list of comparisons, see Table 2.4.

All spatial analyses were done using SAS (SAS Institute, Cary, NC). First, all of the variable comparisons listed in Table 2.4 were examined using regression and a cross-correlogram of the residuals at each of three trap periods, for a total of three analyses per comparison. Data sets were examined individually and heavily skewed sets were log-transformed. Since captures and ticks picked up on dragging were low at some of these 'snapshots', grids were combined at each time period and examined by time period, because sample sizes were too low to show significant correlograms.

Table 2.4. Variables compared using regression and a cross-correlogram. Vegetation actually refers to three variables: understory, deciduous trees and coniferous trees, and three separate analyses were run. Values of the coefficient of correlation, r, and the distance at which the association was still significant are listed. Comparisons in bold were significant for at least one of the runs. See Table 3.7 and 3.8 for results.

Factor 1	Factor 2
Vegetation	number of mice
Vegetation	number of infected mice
Vegetation	total ticks on mice
Vegetation	questing larvae
Vegetation	questing nymphs
Vegetation	infected questing larvae
Vegetation	infected questing nymphs
Questing larvae	number of infected mice
Questing nymphs	number of infected mice
Total questing ticks	number of infected mice
Questing larvae	total ticks on mice
Questing nymphs	total ticks on mice
Total questing ticks	total ticks on mice
Infected questing larvae	infected larvae on mice
Infected questing nymphs	infected nymphs on mice
Spirochetes in questing nymphs	infected larvae on mice
Spirochetes in questing larvae	infected nymphs on mice

Significance was determined by calculating r, the coefficient of correlation and determining the distance at which the two were still related. If the significant cutoff distance, determined by r, was smaller than one unit (the minimum lag distance possible, or the distance between 2 trap points, in meters or in decimal degrees) then the association was not considered significant. Values of r for each comparison are listed in Table 2.4.

The value of r was calculated using the formula:

$$t = r * \left(\sqrt{n-2}\right) / \left(\sqrt{1 - r^2}\right)$$

61

where *t* is looked up in a t distribution table by significance value and sample size, and then *r* is solved algebraically. For these comparisons, 0.05 was chosen as the level of significance. Sample sizes for all comparisons were based on 240 observations. Thus, the significant *r* value used for a cutoff was 0.1069.

Since distances at which the variables are spatially correlated are given in decimal degrees, these distances must be converted to meters in order to understand them in terms of real distances. This was done using the conversion factor that one degree of latitude at 45° N is equal to 111.113 km, or 111,113 m.

Associations that were significant by this process and made sense biologically were then examined by spatial regression in order to make predictions about one variable based on another. These statistical models will be based on the formula:

$$Y = \beta_0 + \beta_1 X(s_i)$$

where *Y* is the dependent variable, β_0 is the intercept, $\beta_1 X$ is the independent variable and s_i is the residual, or error term.

Datasets were examined at each time period with a semi-variogram. These variograms can be found in the Appendix, Figure A.1 to Figure A.19.

CHAPTER 3

RESULTS

Descriptive statistics

Vegetation sampling

All three grids were sampled for vegetation at each of 80 trap points on the grid.

Each point was assessed for amount of understory; a categorical descriptor was assigned

(see Table 2.2 for description). Understory coverage was compared using chi-square test.

Grids were found to have significant differences in understory composition ($\chi 2$ statistic

682.4, df = 24, p-value < 0.0001). These differences were further investigated using the

chi-square test to do pair-wise comparisons. Grids III and IV were found to have

significantly different understory composition ($\chi 2$ statistic 468.0, df = 21, p-value <

0.0001). Grids III and V were found to have significantly different understory

composition ($\chi 2$ statistic 468.0, df = 15, p-value < 0.0001). Grids IV and V were found

to have significantly different understory composition ($\chi 2$ statistic 450.2, df = 18, p-value

< 0.0001). In sum, all three grids were significantly different from one another in

understory coverage. When taken together, grid III had the greatest amount of

understory, an average category classification of 1.84 at each trap point, followed by grid

V, with 1.83 at each point, and then grid IV, with 0.99 at each point.

Plots were also sampled by recording the genera of the three closest mature trees

to each trap point and compared using the chi square test. Overall, there were 14 genera

of trees present at the grids. Grids were found to be significantly different in tree

composition ($\chi 2$ statistic 5167.1, df = 228, p-value < 0.0001). Table 3.1 shows a list of

trees and their numbers at each grid. Overall, grid III has about twice as many oaks as

the other grids. Grid IV has more than twice as many hemlocks than the other grids, and grid V has twelve times more aspens than the others.

Table 3.1. Genera of trees at each grid. A total of 240 data points was taken at each grid.

Tree (genus)	Grid III	Grid IV	Grid V
Oak	75	38	28
Maple	82	75	82
Hemlock	15	54	21
Basswood	0	2	1
Ash	12	31	36
Pine	25	14	12
Aspen	3	0	36
Cedar	4	14	18
Birch	13	8	4
Filbert	0	1	0
Spruce	1	0	0
Elm	1	0	0
No tree	9	3	2
Total	240	240	240

These differences were further investigated using the chi-square test to do pairwise comparisons. Grids III and IV were found to be significantly different from each other ($\chi 2$ statistic 3953.2, df = 180, p-value < 0.0001). Grids III and V were found to be significantly different from each other ($\chi 2$ statistic 3680.5, df = 154, p-value < 0.0001). Grids IV and V were found to be significantly different from each other ($\chi 2$ statistic 3620.8, df = 150, p-value < 0.0001). Kriged surfaces of all three vegetation samples for all three grids are shown in Figure 3.0A, Figure 3.0B and Figure 3.0C.
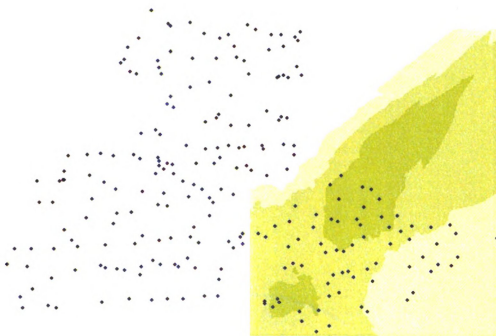
Figure 3.0A. Kriged surface of understory vegetation layer. Data were interpolated using ordinary kriging between 12 data points. Darker colors indicate heavier understory cover. Dots represent trap points. Figures in this thesis presented in color.
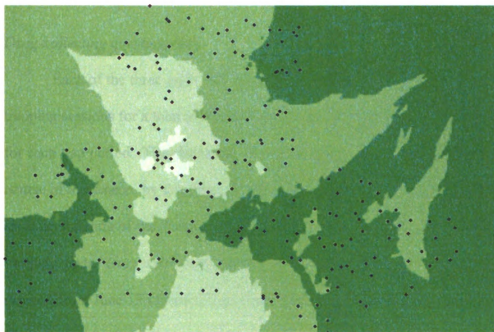
Figure 3.0B. Kriged surface of deciduous tree layer. Data were interpolated using ordinary kriging between 12 data points. Darker colors indicate heavier deciduous tree cover. Dots represent trap points. Figures in this thesis presented in color.
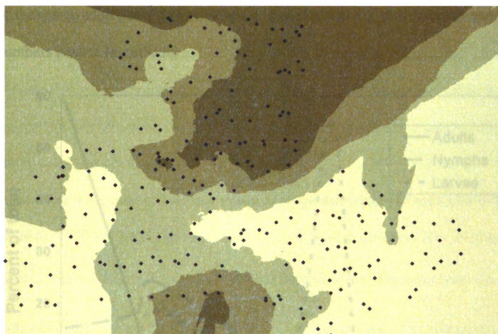
Figure 3.0C. Kriged surface of coniferous tree layer. Data were interpolated using ordinary kriging between 12 data points. Darker colors indicate heavier coniferous tree cover. Dots represent trap points. Figures in this thesis presented in color.

Drag-collecting questing ticks

Each of the three grids was dragged for questing ticks during each of the three

trapping sessions for a total of 9 collections. The three grids were chosen as replicates

for each trap period. The phenology for the *Ixodes scapularis* ticks collected over the

course of the season, by life stage, is shown in Figure 3.1. For this graph, in order to get

an understanding of the change in activity over time, data are pooled from all three

trapping grids. Drag collections began on June 13 and ended August 5, with period 1

running from June 13 to June 25, period 2 from July 7 to July 19, and period 3 from July

23 to August 5. Collections are represented as proportions of the total collected (per

stage) on that date rather than raw numbers. Sampling appears to have begun at the end

of the spring adult peak, no obvious peak nymphal activity was detected, and larval

numbers peaked in mid-July.
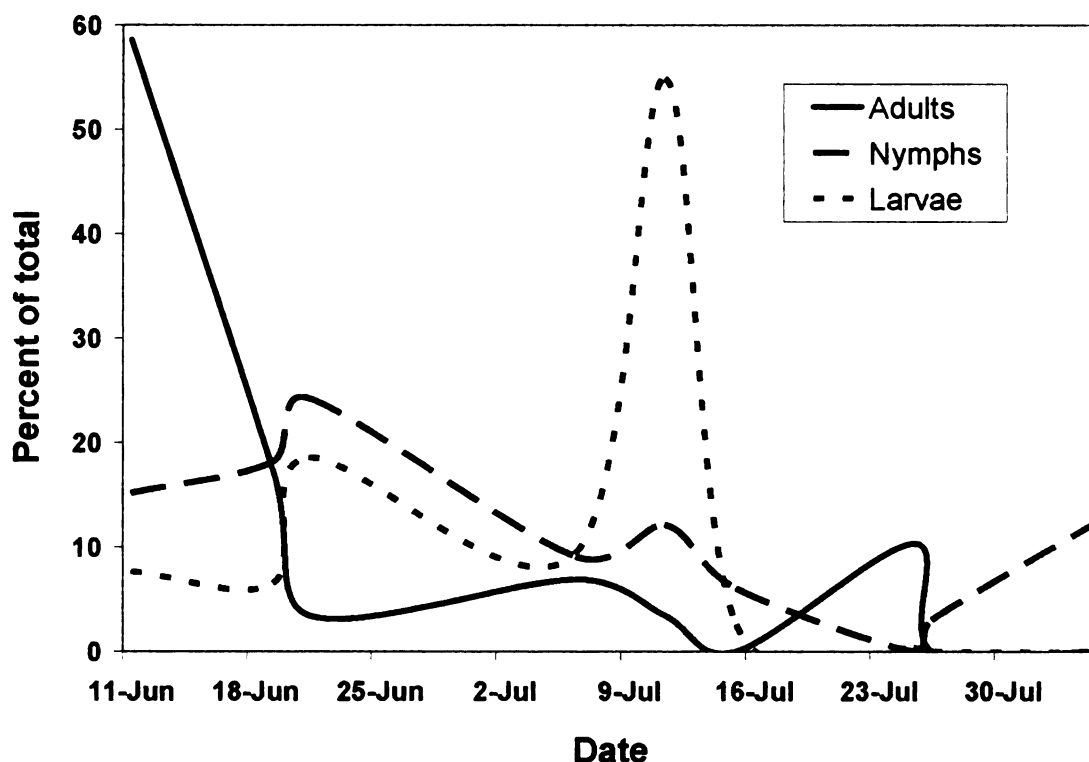
Figure 3.1. Questing *Ixodes scapularis* ticks collected over time at the study site (Menominee County) in 2006. Data are pooled from all three trapping grids. Collections are represented as proportions of the total collected (per stage) on that date rather than raw numbers. Sampling appears to have begun at the end of the spring adult peak. No obvious peak nymphal activity was detected. Larvae numbers peaked in mid-July.

The drag collected questing *I. scapularis* ticks were sampled two ways, in order to

get a relative measure of how sensitive the sampling methods were. Drag-collecting can

be a sensitive method to detect questing ticks in the environment (Fish 1995), but there is

a need to balance covering a large area with the frequency of stops. If one is stopping

frequently, there is more time and effort being spent, but stops farther apart may allow for

ticks to fall off the cloth again before they can be seen. In part, this whole grid/subset

comparison was done to get a feel for the balance between effort and detection ability. If we find that our large-scale effort is missing some ticks, we can note that in our analysis, and use this information to inform our next study. If we find that the detection methods were equal, then we can be satisfied with the amount of effort put into the drag-sampling scheme.

The ticks were collected first on one small sub-square of each grid (Figure 2.3), equal to $1/20^{th}$, or 5% of the total area and stops were made every 8 m, over a total of 72 m^2, to check the cloth for ticks. Second, sampling over the entire grid was conducted, with stops every 24 m, over a total of 480 m^2. Although the small subsquare itself represents 5% of the total area, the amount dragged, 72 m^2, is actually 15% of 480 m^2.

However, in order to accurately compare them, we need to take into account the entire sampled area. If the entire area is considered the whole-grid drag plus the subsquare, (480 m^2 + 72 m^2), the whole-grid drag accounts for 87%, and the subsquare is 13% of that total. Therefore, we would expect the whole-grid collected ticks to account for 87% of the total ticks recovered, and the subset of ticks to account for 13%. Of course, this assumes spatial homogeneity of ticks over the landscape.

Specifically, the percent of *I. scapularis* larvae detected overall in the intensive sample was 9.1% of the total, instead of the 13% that we would expect. Of all ticks recovered, 8.4% of larvae, 32% of nymphs and 11.6% of adults were recovered from these intensive samples. The results are mixed- for total ticks and larvae, the intensive sample underestimated. The estimation for the adult ticks was about right, and the

nymphal ticks were overestimated. These results do not strongly indicate that many ticks, besides nymphs, were missed on the large-scale dragging effort.

On average for the whole season, drag collection yielded about 8 *I. scapularis* nymphs per 1000 m^2. At the peak of their activity, that number was 17 per 1000 m^2. For all *I. scapularis* lifestages, there was an average of 78 per 1000 m^2, but that number varied from 2 to 89 at each of the sampling times. Variation through time is shown in Figure 3.1.

Mammals

Most of the small mammals captured at the site were *Peromyscus spp.*, accounting for 68.3% of the 230 total individual animals captured. Since there were so few *Peromyscus maniculatus gracilis* caught, they were added to the numbers of the *Peromyscus leucopus* since they essentially function as a single species in this system (Friedrich 2003). Because of the number of mice caught and their role in the Lyme disease system as a highly reservoir-competent host, these mouse species are considered the main study population. Other small mammals caught, with their relative percentages of the total number of captures, are listed in Table 3.2.

Table 3.2. Percent of total small mammal captures among all three grids by species at the field site in Menominee County, June-August 2006. A total of 230 individuals were captured.

Species	Common name	# caught	% of total
Peromyscus leucopus	White-footed mouse	151	65.7
Peromyscus maniculatus gracilis	Deer mouse	6	2.6
Tamias striatus	Eastern chipmunk	32	13.9
Clethrionomus gapperi	Southern red-backed vole	29	12.6
Blarina brevicauda	Short-tailed shrew	5	2.2
Glaucomys sabrinus	Northern flying squirrel	4	1.7
Dedelphis virginiana (juvenile)	Opossum	2	0.9
Napeozapus insignis	Woodland jumping mouse	1	0.4

Traps were set for a total of 5,760 trap nights. The 705 individual captures of all mammals provide a capture success rate of 12.2%. Of the 705 captures, 579 of those (82.0%) were *Peromyscus spp.*

Population estimates for *Permyscus spp.* at the study site were estimated for each grid at each time period. Population abundances were derived using the interactive software program CAPTURE (United States Geological Survey, Patuxent, Rhode Island). Assumptions of the test for abundance included a closed population. Estimates for each of the nine intervals are listed in Table 3.3. These population estimates are also shown in graphical form in Figure 3.2. Population estimates listed by trap period and by grid yields a range from 19 to 56. Including the 95% confidence intervals in a range estimate expands to between 16 and 77 individuals per grid per trap period. For the graph, error bars were calculated using the average 95% confidence intervals for that grid.

Over time, the population sizes appear to shrink and then grow. Sample sizes for grid IV were more consistent within the grid and did not track with the other grids sample

sizes at time period 3. Sample sizes for grids III and V are consistent throughout the

season. There was no significant difference in numbers among grids. Approximately

34% of mice were captured on more than one grid, suggesting a lack of independence of

grids.

Table 3.3. Population estimates and standard error for each 1.15 ha grid at each time
period. Three grids were sampled three times each over the trapping season from June to
August, 2006, in Menominee County, MI. The three grids were enumerated with Roman
numerals III, IV, and V. Population estimates were derived using Program CAPTURE
(United States Geological Survey, Patuxent, Rhode Island).

Trap Period	Grid	Population estimate	95% confidence interval
1	III	19, se = 3.72	16 - 32
1	IV	27, se = 3.33	25 - 40
1	V	42, se = 5.82	36 - 59
2	III	25, se = 2.34	25 - 41
2	IV	27, se = 3.48	24 - 40
2	V	27, se = 2.62	27 - 41
3	III	56, se = 7.38	47 - 77
3	IV	29, se = 3.13	27 - 41
3	V	51, se = 7.30	42 - 71
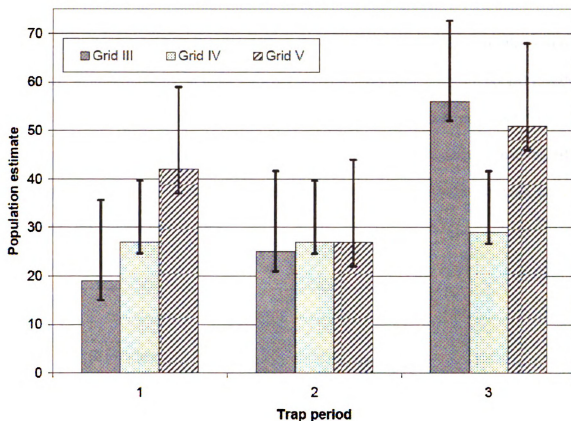
Figure 3.2. Population estimates for mice each trap period, by 1.15 ha grid.
Estimates calculated using program CAPTURE (United States Geological Survey,
Patuxent, Rhode Island). Error bars were calculated using the average 95% confidence
intervals for the grid.

Quantifying spirochete load in ticks

A total of 929 tick samples were assayed using the quantitative PCR method.

These tick samples included flat questing ticks, engorged and partially engorged ticks

removed from hosts, all three lifestages (larvae, nymphs and adults) and both

Dermacentor variabilis and *Ixodes scapularis* species. In total, 30.8% were positive.

This number represents of a mix of species, life stages and on and off host ticks.

The breakdown of percent positive ticks is presented in Figure 3.3A and

Figure 3.3B. In these, *I. scapularis* positives are shown by life stage and location (on or

off host). In these data, larval ticks were not tested individually, but were pooled together

with other larvae from the same animal or same drag transect because most were

expected to be negative. Generally, more of the on-host ticks were positive than the off-

host ticks. Infection prevalence of questing *I. scapularis* increases with life stage, and

adults had the highest rate at 57%.
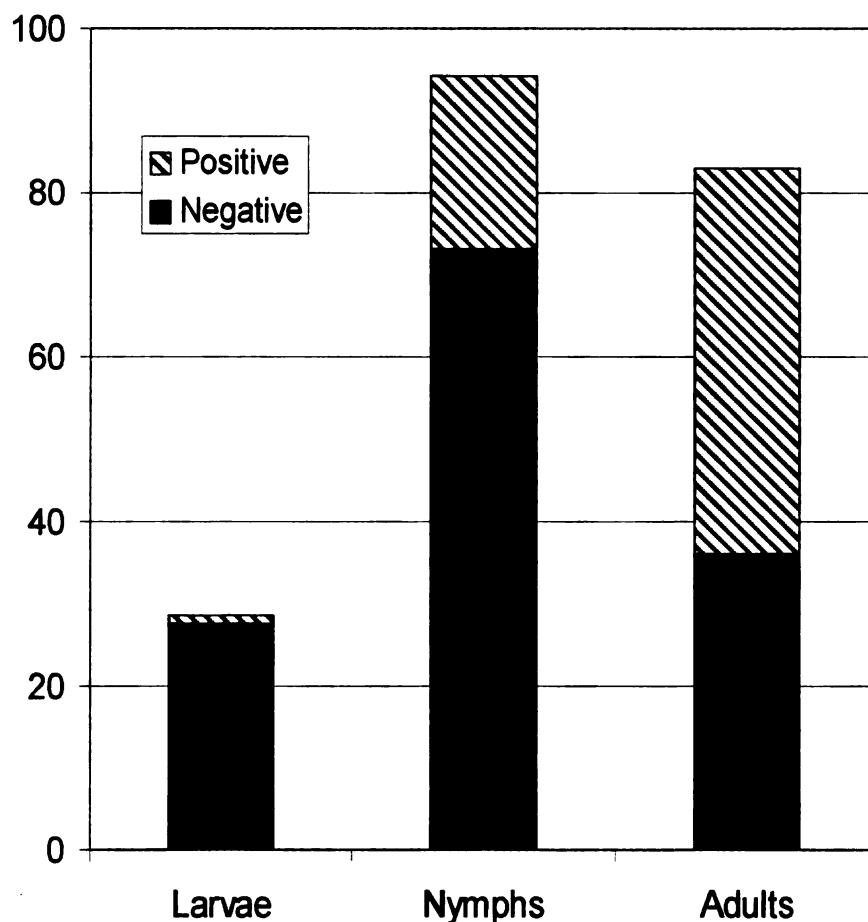
Figure 3.3A. Questing *Ixodes scapularis* ticks testing positive and negative for *Borrelia burgdorferi*. Approximately 3% of larvae, 22% of nymphs and 57% of adults tested positive for *B. burgdorferi*. Larval ticks were not tested individually, but were pooled with other larvae from the same animal or same drag transect.
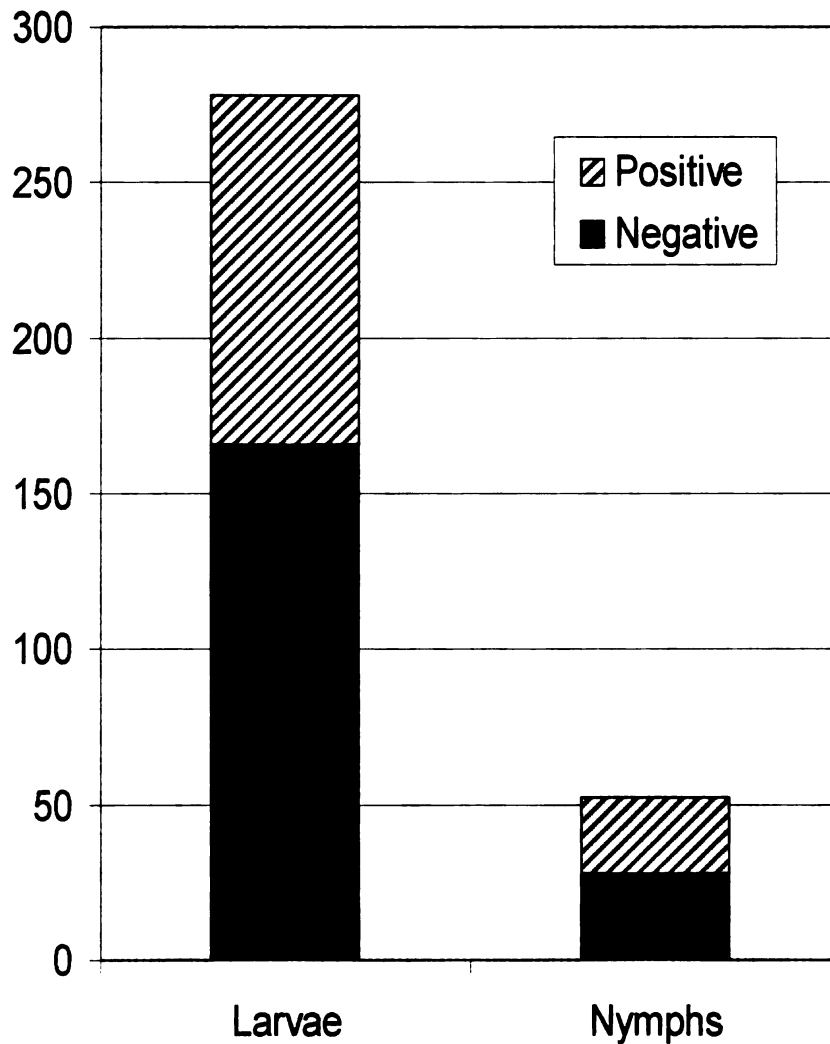
Figure 3.3B. On-host *Ixodes scapularis* ticks testing positive and negative for *Borrelia burgdorferi*. Approximately 40% of larvae and 46% of nymphs tested positive for *B. burgdorferi*. Larval ticks were not tested individually, but were pooled with other larvae from the same animal or same drag transect.

Quantifying spirochete load in mouse tissue

Before PCR of the mouse tissue could begin, the optimal treatment and dilution

for the eluted DNA had to be determined. One trial was conducted using 10 samples.

Using the results of the trial to determine the best dilution for the mammal ear biopsy

DNA (Figure 2.7) by PCR amplification, the desalted 1:10 dilution of the original DNA

was selected. The gel picture shows amplification most clearly in the lanes for this

combination of treatments (Figure 3.4). The samples that had been desalted and diluted

1:10 were selected for use in qPCR. The fragment size expected was a 987 base pair

amplicon. Sample 29, desalted and a 1:10 dilution, and sample 38, both undiluted

desalted and a desalted 1:10 dilution show amplification. The molecular ladder used was

the Invitrogen E-Gel low-range quantitative DNA ladder.

Ear biopsies were taken on mice at their first time of capture during each trap

period and checked for infection by qPCR. Overall infection prevalence for mice at their

first capture was 33%. For trap period 1, 50% of mice trapped first during that trap

period were infected, trap period 2, 26% of mice were infected, and trap period 3, 16% of

mice were infected.

Spirochete burden values were compared for juvenile (young of the year) mice

and adult mice at each trap period, and adult mice were expected to have higher burdens

because of their increases chances of exposure. At trap period 1, spirochete burdens were

found to be significantly different, (Student's t-test, one tailed, unequal variance,

$p = 0.005$, $df = 50$) as adults had a higher spirochete load, with an average of 405

spirochetes and juveniles had an average of just 18. For trap period 2, spirochete burdens

between age classes were also found to be significantly different, (Student's t-test, one

tailed, unequal variance, p = 0.017, df = 45) with adults demonstrating a higher average

burden (110 spirochetes) than juveniles (18 spirochetes). For time 3, the age classes were

still significantly different (Student's t-test, one tailed, unequal variance, p = 0.015,

df = 36). Adults had an average of 2805 spirochetes and juveniles had zero.
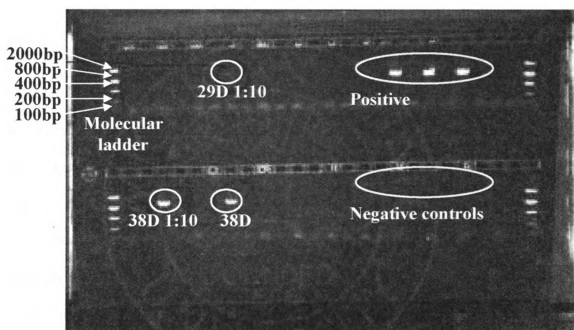
Figure 3.4. Electrophoresis gel result from the ear biopsy DNA treatment trial. The fragment size expected was a 987 bp amplicon of the intergenic spacer region (IGS) between 16s (rrs) and a 23s (rr1A) rRNA genes in *B. burgdorferi*, (Bunikis et al. 2004b). Sample 29, desalted and a 1:10 dilution (faint), and sample 38, both undiluted desalted and a desalted 1:10 dilution show amplification. Standard used Invitrogen E-Gel low-range quantitative DNA ladder.

Ticks on mammals

By individual mouse, 74% (165 of 224) of mice became parasitized over the course of the trap season. If each mouse capture is counted separately, of 705 capture events, 396 were parasitized, so per capture, 56.2% of mice were parasitized. The lower per-capture parasitism rate indicates that at least some mice had tick burdens of zero at some captures and burdens of greater than zero at others. A bar chart showing total tick burdens over the course of the trapping season is displayed in Figure 3.5. Mice were numbered chronologically as they were caught, and so mice caught early on in the season are represented by lower numbers. Mice caught earlier in the season also showed overall higher total tick burdens as compared to those caught later on. This difference is due to the seasonal activity of the ticks (Figure 3.1) as well as the increased likelihood that a mouse caught early in the season would be caught again and multiple captures added up to larger tick burdens.

Data used for the following analyses including the animal's first capture only during each of the trapping periods. Recapture data were eliminated from the analysis to avoid issues surrounding lack of independence and repeated measures. Since only first captures were used, sample sizes were low at each grid (~15 individuals) and therefore, were lumped together with the other grids' samples from that same trap period in order to increase statistical power.
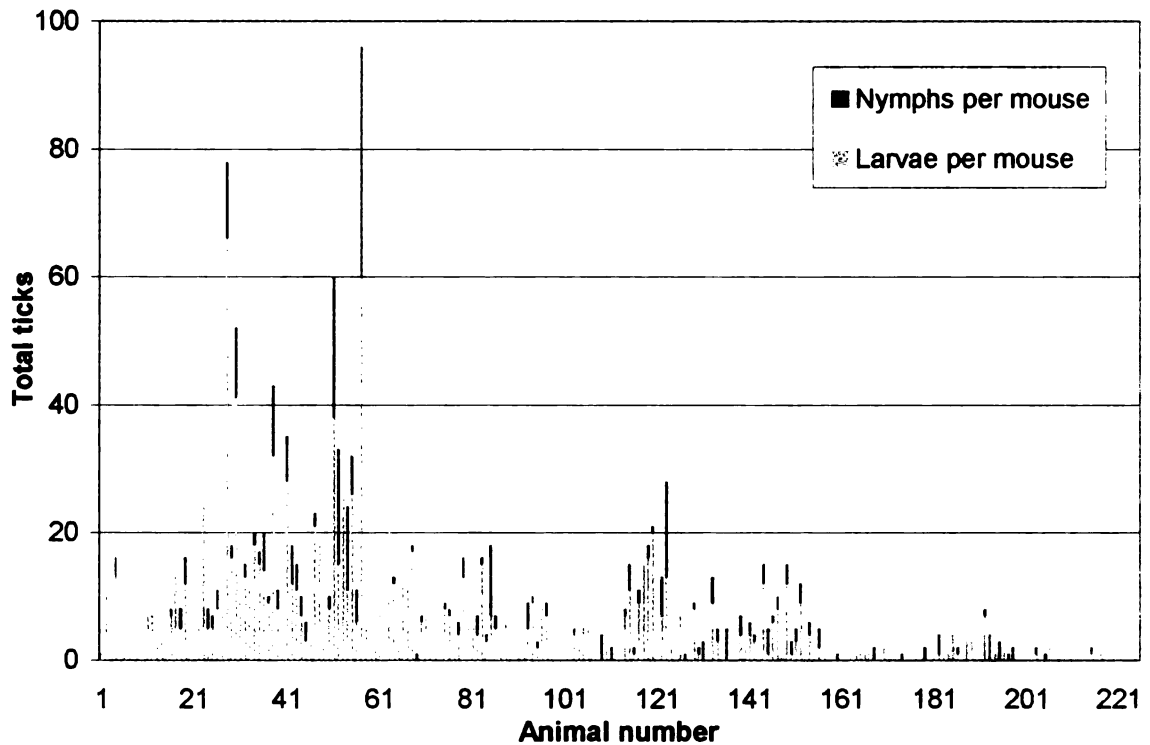
Figure 3.5. Frequency histogram for number of total ticks on mice over the course of the trapping season. Numbers for each mouse are cumulative over the whole season.

Burdens of *I. scapularis* ticks parasitizing mice were compared on mice of

different age classes. Mice in the field were aged by size and stage of pelage (small, all

grey fur = 1, or juvenile, medium, grey to brown fur = 2, or subadult, and large, all brown

fur = 3, or adult). Since all mice categorized 1 and 2 were young of the year, and their

sample sizes were relatively small compared to the adult mice, they were lumped together

in the juvenile category, denoted in some of the figures by the numeral 1. Thus, mice

were divided by age class and categorized as a juvenile or an adult, where the adults

displayed brown pelage and were sexually mature. Comparison of tick burdens by age

class and trap period is shown in Figure 3.6.
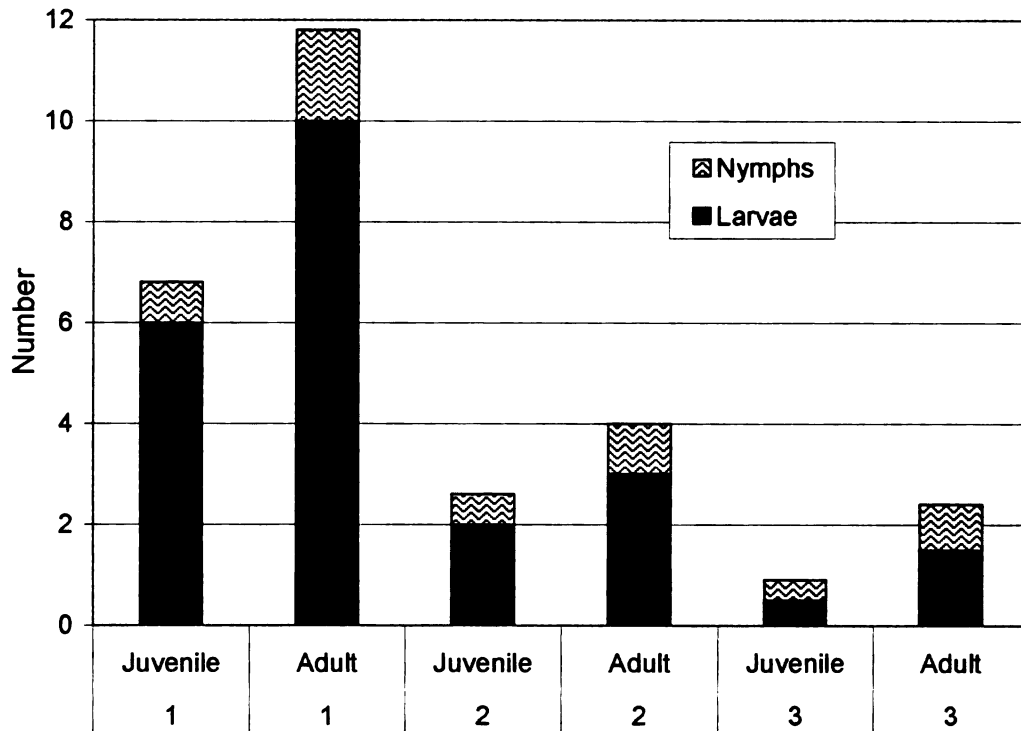
Figure 3.6. Comparison of average tick burdens per mouse by trap period (number) and age class (juvenile or adult).

For the first trap period, larval burdens were found to differ by age (Student's t-test, two tailed, unequal variance, p=0.029, df = 50). However, nymphal burdens were not significantly different based on age (Student's t-test, two tailed, unequal variance, p=0.097, df = 46). Adult mice were likely to feed more nymphal ticks than juvenile mice. On average, adults fed almost 10 larvae and 2 nymphs, and juveniles fed almost 6 larvae and less than one nymph in the first round of captures. Comparison of the total number of larval and nymphal *I. scapularis* ticks is illustrated in Figure 3.7, and shows no significant difference in overall tick burden between age groups. Juveniles had an average of more than 6 ticks per animal and adults a burden of 12 ticks per animal.
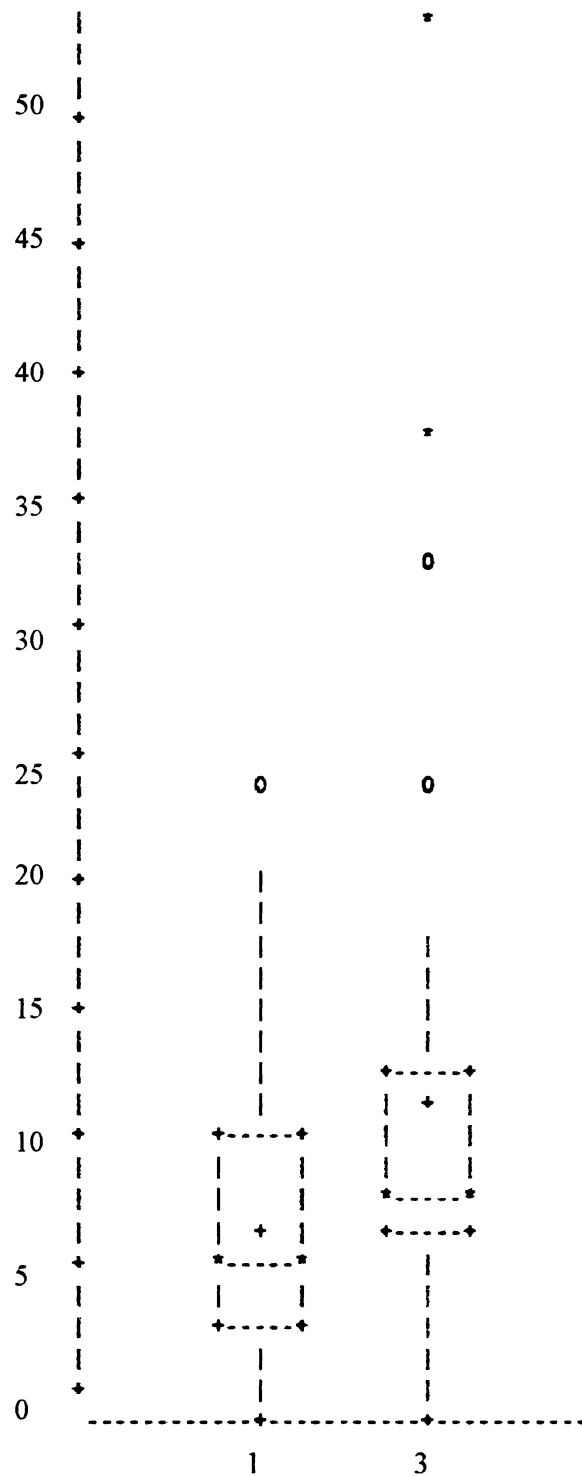
Figure 3.7. Comparison of total *I. scapularis* burdens (larvae and nymphs) between juvenile (age=1) and adult (age=3) age groups for animals captured in trap period 1. Only tick burdens for animals captured the first time are included in this dataset. Repeat captures are omitted to avoid lack of independence and repeated measures issues. Boxplot shows no significant difference between age groups.

80

For the second trap period, larval burdens were found to differ by age (Student's t-test, two tailed, unequal variance, p=0.04, df = 36). Nymphal burdens were also significantly different based on age (Student's t-test, two tailed, unequal variance, p=0.001). Adult mice were likely to feed both more larvae and nymphs than juvenile mice. On average, adults fed more than 3 larvae and 1 nymph, and juveniles fed 2 larvae and less than one nymph. Comparison of the total number of ticks is illustrated in Figure 3.8, and shows no significant difference in overall tick burden between age groups. Juvenile mice fed an average of nearly 3 ticks in total and adults an average of almost 5 ticks in total for the trap period.

For the third trap period, larval burdens were not found to differ by age (Student's t-test, one tailed, unequal variance, p=0.068), nor were nymphal burdens (Student's t-test, two tailed, unequal variance, p=0.256). On average, adults fed 1.5 larvae and less than one nymph, and juveniles fed less than one larva and less than one nymph. Comparison of the total number of ticks is illustrated in Figure 3.9 and shows no significant difference in overall tick burden between age groups. Juvenile mice fed an average of less than 2 ticks per animal, and adults also fed an average of less than 2 ticks.

Since the season changed over the course of the study, the mice that were juveniles in the beginning had matured by the end of the study. All the hosts were aged at each time and differences among age classes compared. However, by the end of the season (the third and last rotation), almost all of the mice were part of the most mature age class, and thus, comparisons between age classes were probably not as meaningful due to lack of sample size of the younger age class.

```
   |
16 +
   |
   |                              0
   |
14 +
   |
   |                              0
12 |
   +                             |
   |                             |
   |                             |
   |                             |
10 +               |             |
   |               |             |
   |               |             |
   |               |             |
8  +               |             |
   |               |             |
   |               |             |
   |               |             |
6  +               |        +-----+
   |               |        |     |
   |               |        |     |
   |               |        |  +  |
4  +       +-----+ |        *-----*
   |       |     | |        |     |
   |       |     | |        |     |
   |       |  +  | |        |     |
2  +       |     | |        +-----+
   |       |     | |             |
   |       *-----* |             |
   |       |     |               |
0  +       +-----+               |
   ----------------+----------------+-----
              1              3
```
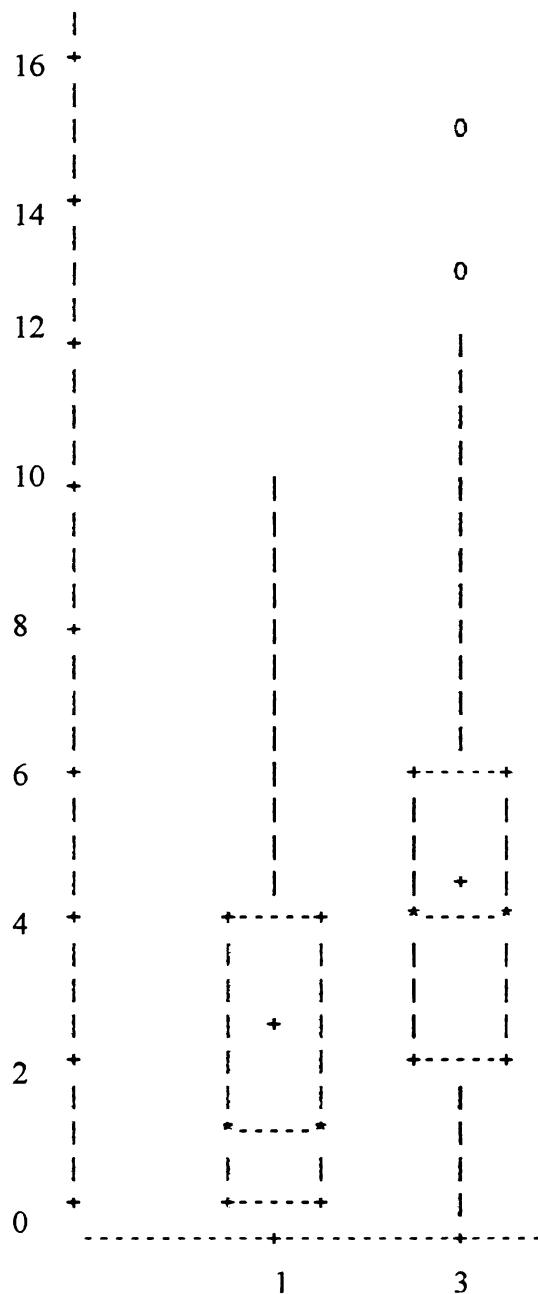
Figure 3.8. Comparison of total *I. scapularis* burdens (larvae and nymphs) between juvenile (age=1) and adult (age=3) age groups for animals captured in trap period 2. Only tick burdens for animals captured the first time are included in this dataset. Repeat captures are omitted to avoid lack of independence and repeated measures issues. Boxplot shows no significant difference between age groups.

82

```
8  +                 0
   |
   |
   |
7  +
   |
   |
   |
6  +
   |
   |
   |
5  +                          0
   |
   |
   |
4  +              |
   |              |
   |              |
   |              |
3  +              |
   |              |
   |              |
   |              |
2  +         +-----+        |
   |         |     |        |
   |         |  +  |   +-----+
   |         |     |   |     |
1  +         *-----*   *--+--*
   |         |     |   |     |
   |         |     |   |     |
   |         |     |   |     |
0  +         +-----+   +-----+
   -----------------+-----------+-----
                    1           3
```
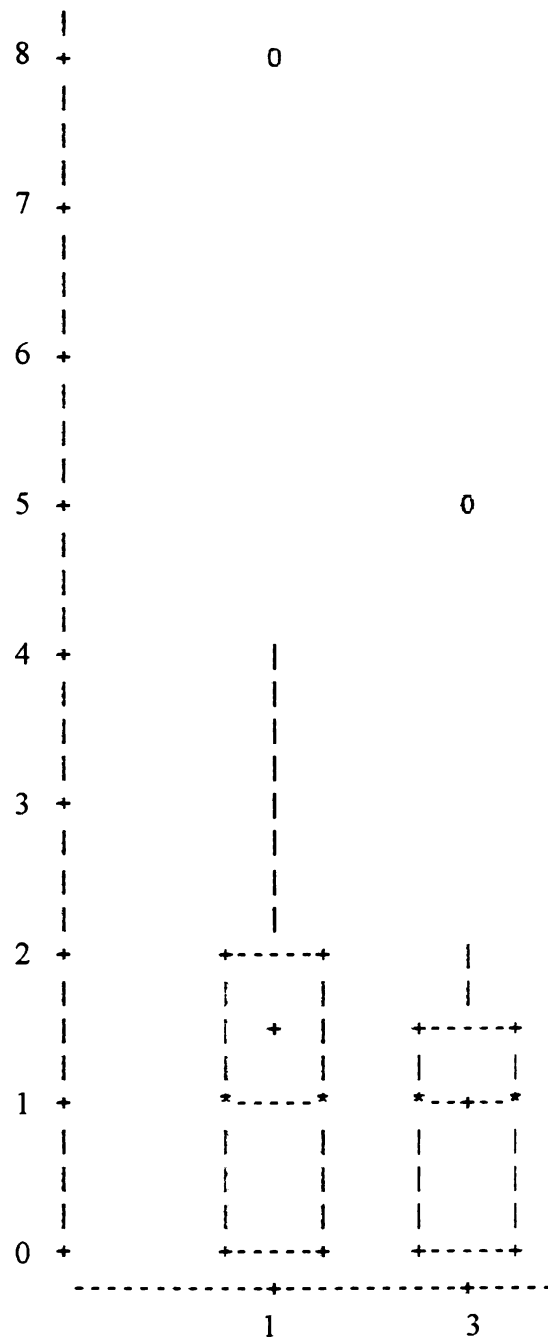
Figure 3.9. Comparison of total *I. scapularis* burdens (larvae and nymphs) between juvenile (age=1) and adult (age=3) age groups for animals captured in trap period 3. Only tick burdens for animals captured the first time are included in this dataset. Repeat captures are omitted to avoid lack of independence and repeated measures issues. Boxplot shows no significant difference between age groups.

Mouse infection status as measured by serology (ELISA)

A one-way ANOVA was conducted to determine effect of plate on sample OD. Using a null hypothesis that there is no effect of plate, analysis determined that there is indeed no effect of plate (F=0.00, F < $_{0.5, 3, 383}$ (critical value = 2.6), p= 0.9996). Since $F_{calculated} < F_{table}$, we fail to reject the null hypothesis and say that there is no detectable difference in the values of the positive and negative controls between plates.

Of the total number (238) of animals caught, 167 were *Peromyscus spp.* Of these, 150 had serum samples suitable for testing. Thus, serology was completed on 90% of the captured mice. For mice tested, 50% were seropositive at the time of testing. Of those, 75 were gave a positive result at the first 1:100 dilution, and 75 gave a negative result. Sera from field-collected *Peromyscus leucopus* from Lyme endemic site in Connecticut were used as positive and negative controls (Tsao 2004 and Bunikis 2004). A cutoff value for negative and positive values was determined by averaging the values from the negative controls in the plates, and adding 3 standard deviations to that number. The resultant value was 0.8784. All samples whose optical density (OD) values fell above that cutoff were considered positive. Two peaks, a negative and a positive peak, can be seen in the frequency histogram of the OD values (Figure 3.10).

Samples that yielded a positive result were then re-tested to determine an endpoint titer for positivity. Each sample that had previously been positive at a dilution of 1:100, were then run at 1:200, 1:400 and 1:800. These results, compared with the original average adjusted OD values, are shown in Figure 3.11. Negative values are not shown on this graph. The graph displays the trend that typically, higher average adjusted OD values correlated with higher endpoint titers.

84
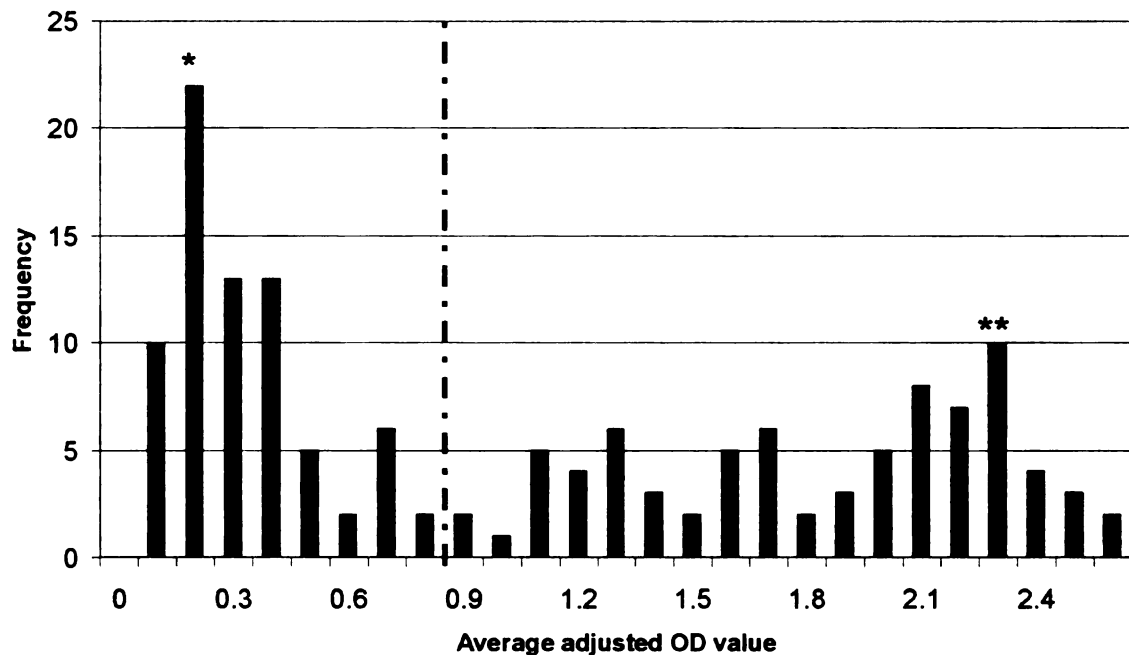
Figure 3.10. Frequency histogram showing the average adjusted optical density (OD) values for the *Peromyscus spp.* serum samples collected in Menominee County from June - August 2006. Two peaks in the data are evident; one in the negative range at 0.2 (*), and the other in the positive range at 2.3(**). The cutoff value of 0.8784 is represented by the dashed line. The cutoff was calculated to be 3 SD above the negative control average. Values above the cutoff were considered positives, or serum samples with antibodies to *Borrelia burgdorferi*, and values less than the value of the line are considered negatives, samples without antibody response.
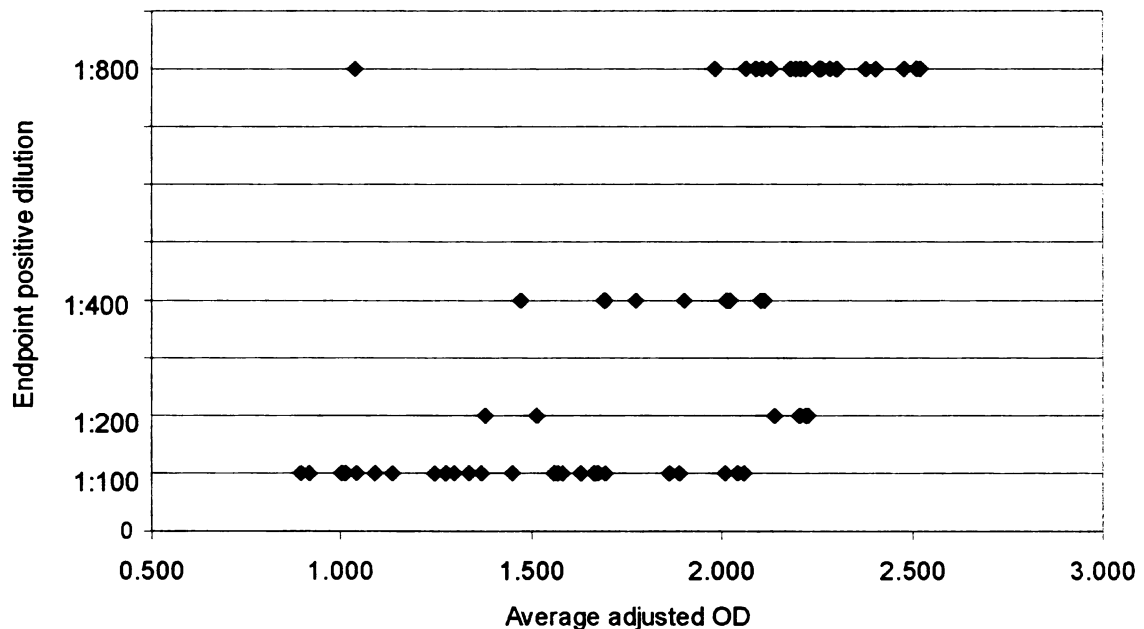
Figure 3.11. Comparison of the average adjusted optical density (OD) values per sample with the endpoint dilution at which the sample was still positive. Graph demonstrates relationship between average adjusted optical density (OD) value for a sample and the final dilution at which it was positive. Negative values are not shown on the graph. The graph displays the trend that typically, higher average adjusted OD values correlated with higher endpoint titers.

There was no clear pattern of OD values over time or by grid. Average adjusted OD values were compared for juvenile (young of the year) mice and adult mice, and were found to be significantly different, (Student's t-test, one tailed, unequal variance, $p<0.0001$) as adults had a higher average OD value of 1.7 and juveniles had an average of just 1.1 (Figure 3.12). Comparison of the relationship between tick burden (log-transformed) and average adjusted OD value between age groups for trap period 1 is shown in a scatterplot in Figure 3.13. The scatterplot for trap period 2 (Figure 3.14) and trap period 3 (Figure 3.15) are also shown. At all three time periods, the adult mice generally had higher OD values and total tick burdens then their juvenile counterparts.
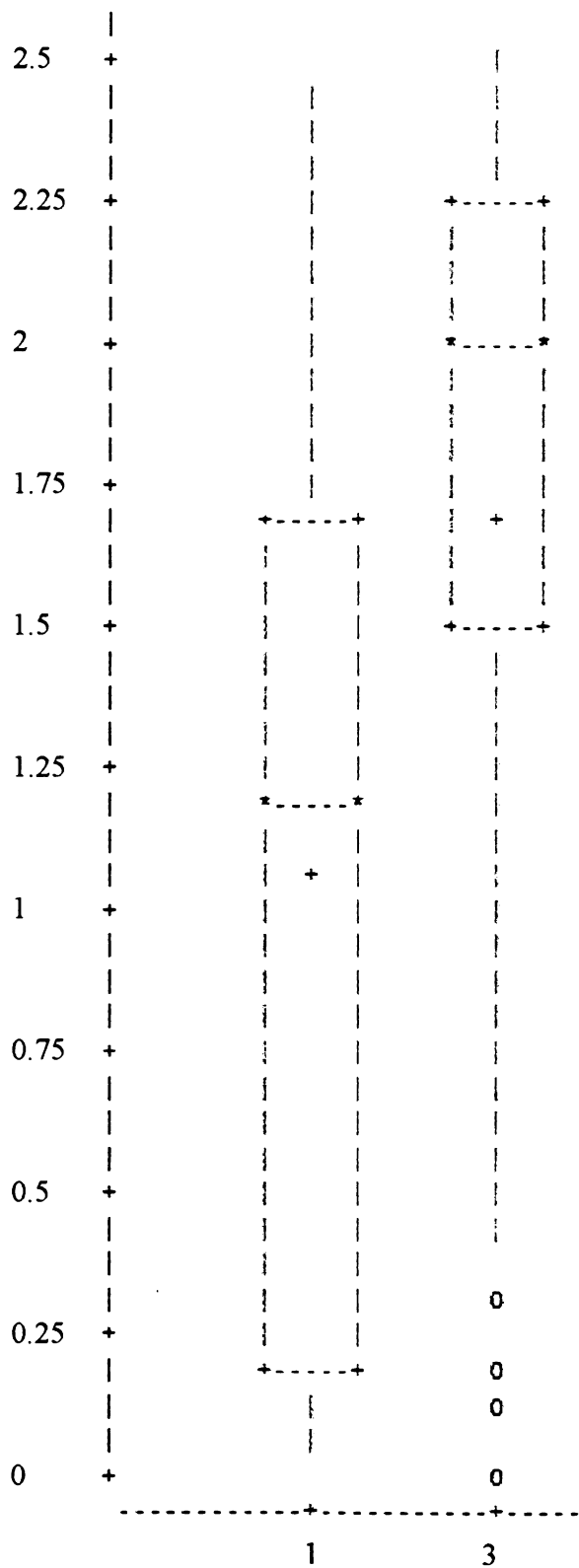
Figure 3.12. Comparison of the average adjusted optical density (OD) values for each population with the age of the population. Graph demonstrates the average OD values of the serum samples of juvenile mice (age category 1) with adult mice (age category 3).

87
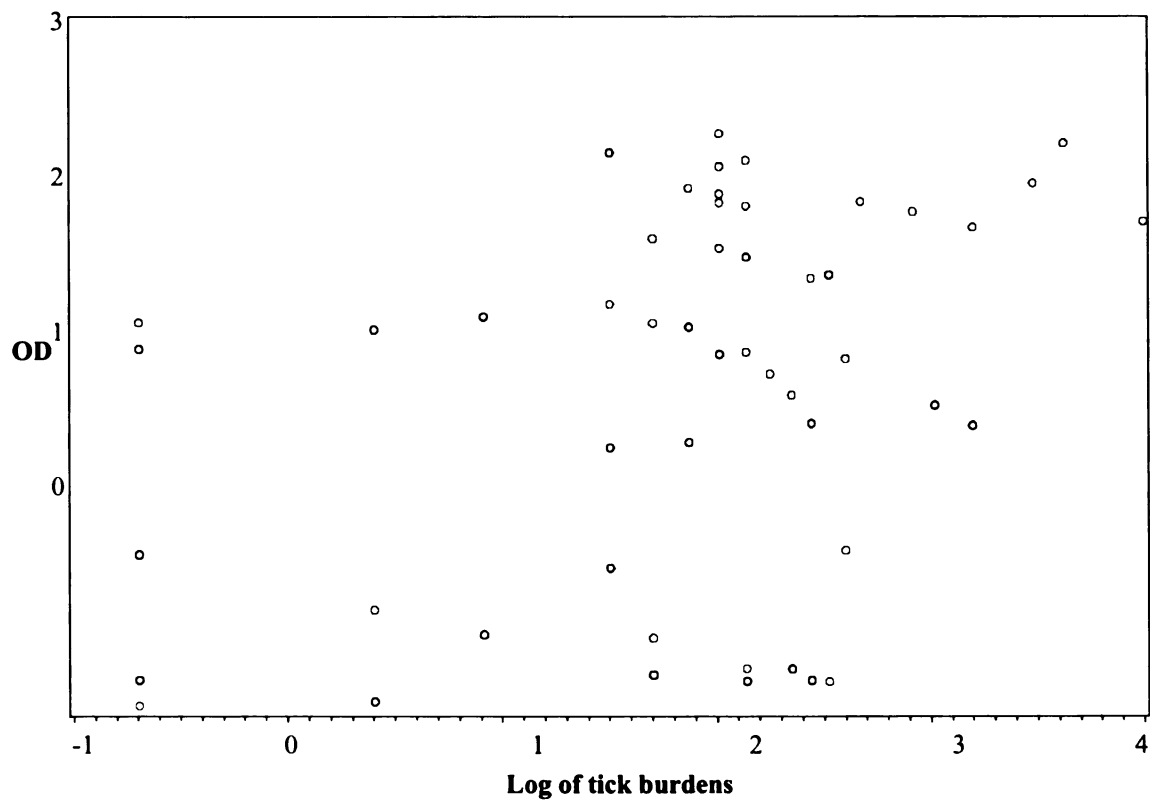
Figure 3.13. Scatterplot comparison of tick burdens (log-transformed, on x-axis) and average OD values (on y-axis) for trap period 1. Juvenile mice (a=1, black circles) and adult mice (a=3, red circles) of the *Peromyscus spp.* were trapped at the field site in Menominee County, 2006. Images in this thesis are presented in color.

3

2

OD 1

0

-1   0   1   2   3
Log of tick burdens
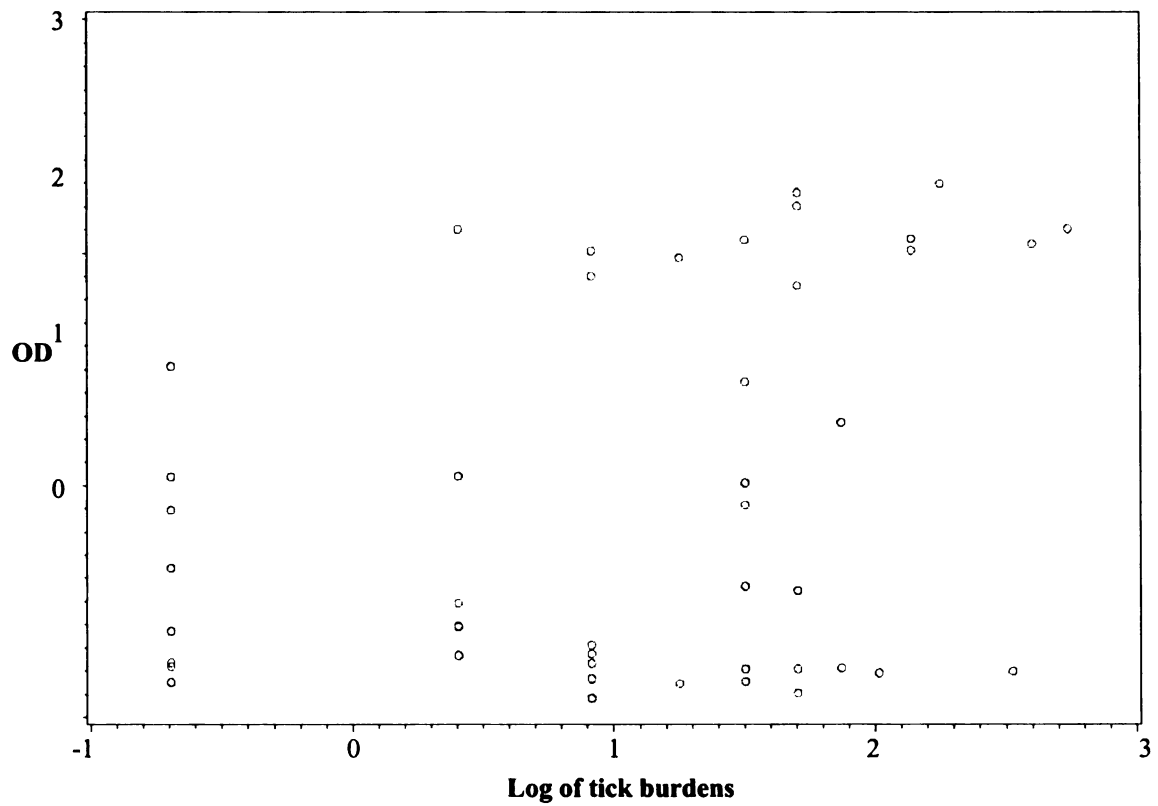
Figure 3.14. Scatterplot comparison of tick burdens (log-transformed, on x-axis) and average OD values (y-axis) for trap period 2. Juvenile mice (a=1, black circles) and adult mice (a=3, red circles) of the *Peromyscus spp.* were trapped at the field site in Menominee County, 2006. Images in this thesis are presented in color.
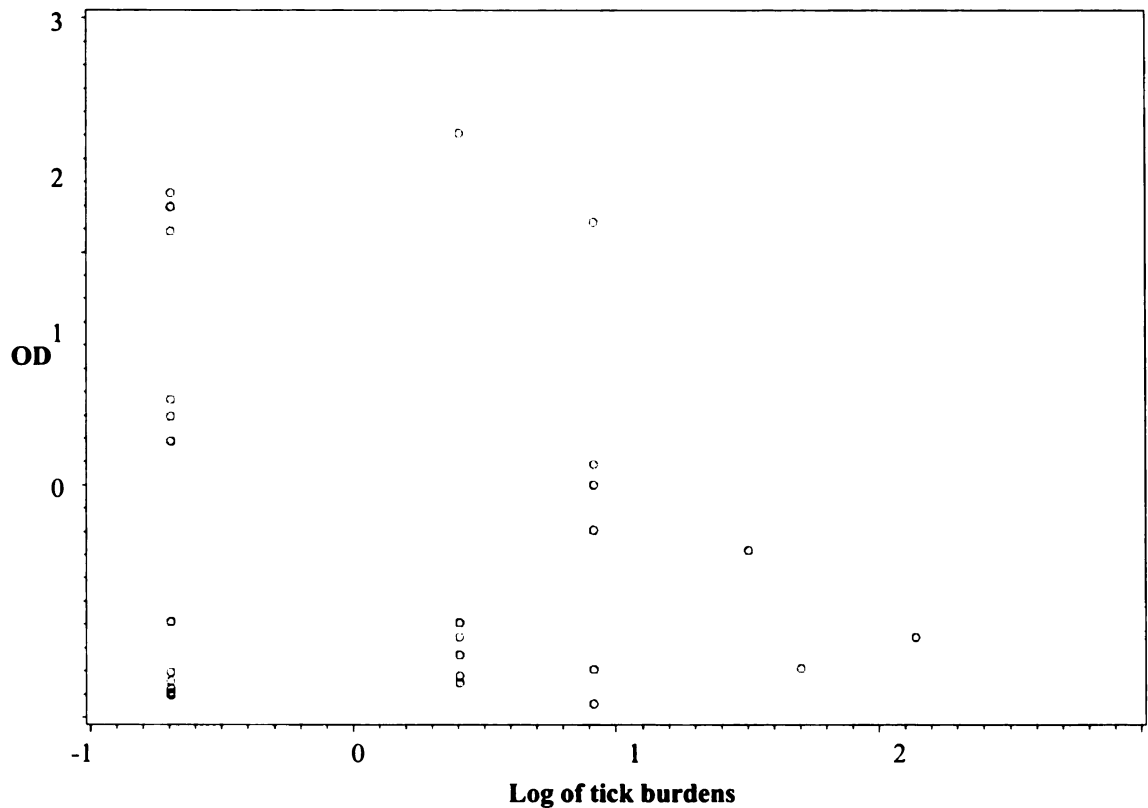
Figure 3.15. Scatterplot comparison of tick burdens (log-transformed, on x-axis) and average OD values (on y-axis) for trap period 3. Juvenile mice (a=1, black circles) and adult mice (a=3, red circles) of the *Peromyscus spp.* were trapped at the field site in Menominee County, 2006. Images in this thesis are presented in color.

For analysis of the relationship between the number of ticks (data for tick burdens on mammals were log-transformed in order to meet normality requirements for data analysis) and the average adjusted optical density (OD) values, it does not matter whether the three times are looked at separately or together. For trap periods 1 and 2, for age 3 the two measures were positively related, and for trap period 3 these factors were not related. At age 1, there is no relationship between tick burden and OD value at any time interval.

Aggregation results

Aggregation was assessed using three measures: the variance to mean ratio, the k statistic of the negative binomial distribution and Lloyd's mean crowding index (LMC). Measures of aggregation were calculated for the following populations: spirochetes in questing ticks, spirochetes in bloodfeeding ticks, spirochetes in mice and bloodfeeding ticks on mice. The ticks were grouped by lifestage. Only larval ticks from animals were separated by trap period and grid. Nymphal ticks from animals were separated by trap period only because sample sizes were small, and questing ticks were not separated by trap period or by grid since sample sizes were too low to have sufficient power.

Spirochetes in questing larvae show very little aggregation because there are so few *B. burgdorferi* organisms in the population, since generally, the ticks hatch uninfected. Loads in the larval ticks that were positive were very low; the one positive pool had a total of 9 spirochetes. The spirochetes from the ticks that had been feeding on mice show a high degree of aggregation, most likely as a reflection of the distribution of the spirochetes among their hosts. In general, measures of aggregation for all examined populations indicated higher degrees of aggregation when grids were lumped by trap period than when examined alone.

Variance to mean ratios

The variance to mean ratio indicates an aggregated population when greater than one. Table 3.4 shows the variance to mean ratios for the listed populations. Variance to mean ratios for populations of *I. scapularis* ticks on mice by lifestage, trap period and grid are presented in Figure 3.16. Overall, the larvae have higher ratios, indicating more

highly aggregated populations. In general, trap period 1 shows the most highly

aggregated populations of ticks on mice. Comparisons of variance to mean ratios and

sample sizes for ticks on mice and spirochetes in mice are shown in Figure 3.17 and

Figure 3.18, respectively.

Table 3.4. Variance to mean ratios, Lloyd's mean crowding (LMC) index and the negative binomial statistic k for number of *B. burgdorferi* organisms in the listed populations of *I. scapularis*. Variance to mean ratios greater than one indicate aggregation. Values of k less than one indicate aggregation. LMC values indicate how many other parasites the average parasite shares a host with. Spirochetes in questing larvae show very little aggregation because there are so few *B. burgdorferi* organisms in the population, since generally, the ticks hatch uninfected. The spirochetes from the ticks that had been feeding on mice show a high degree of aggregation, most likely as a reflection of the distribution of the spirochetes among their hosts.

Population	Variance to mean ratio	k	Lloyd's mean crowding index
All larval ticks on mice	14680	0.0657	15660
Larval ticks, trap period 1, grid III	4970	0.1507	5725
Larval ticks, trap period 1, grid IV	13524	0.1749	15894
Larval ticks, trap period 1, grid V	1152	0.2037	1392
Larval ticks, trap period 2, grid III	4848	0.0640	5174
Larval ticks, trap period 2, grid IV	23252	0.1018	25629
Larval ticks, trap period 2, grid V	7115	0.0881	7753
Larval ticks, trap period 3, grid III	6605	0.0514	6964
Larval ticks, trap period 3, grid IV	16763	0.0356	17387
Larval ticks, trap period 3, grid V	5393	0.0603	5735
All nymphal ticks on mice	22895	0.1313	25908
Nymphal ticks, trap period 1	20720	0.1214	23244
Nymphal ticks, trap period 2	27893	0.2223	34097
Nymphal ticks, trap period 3	2668	0.3261	3541
Questing larvae	8.8	0.0594	-7
Questing nymphs	5984	0.0630	6376
Questing adults	3600	0.3689	4930
Mice, trap period 1, grid III	2731	0.1585	3163
Mice, trap period 1, grid IV	403	0.6924	680
Mice, trap period 1, grid V	119	0.3468	159
Mice, trap period 2, grid III	585	0.1377	664
Mice, trap period 2, grid IV	230	0.2511	286
Mice, trap period 2, grid V	266	0.2753	337
Mice, trap period 3, grid III	53462	0.0775	57605
Mice, trap period 3, grid IV	82	0.1012	89
Mice, trap period 3, grid V	859	0.2511	1073

Figure 3.16. Variance to mean ratios for *I. scapularis* ticks on mice by trap period and grid. The dotted line represents the cutoff for an aggregated population, or a variance to mean ratio of 1. Overall, the larvae have higher ratios, indicating more highly aggregated populations (black symbols). Trap period 1 shows the most highly aggregated populations of ticks on mice.
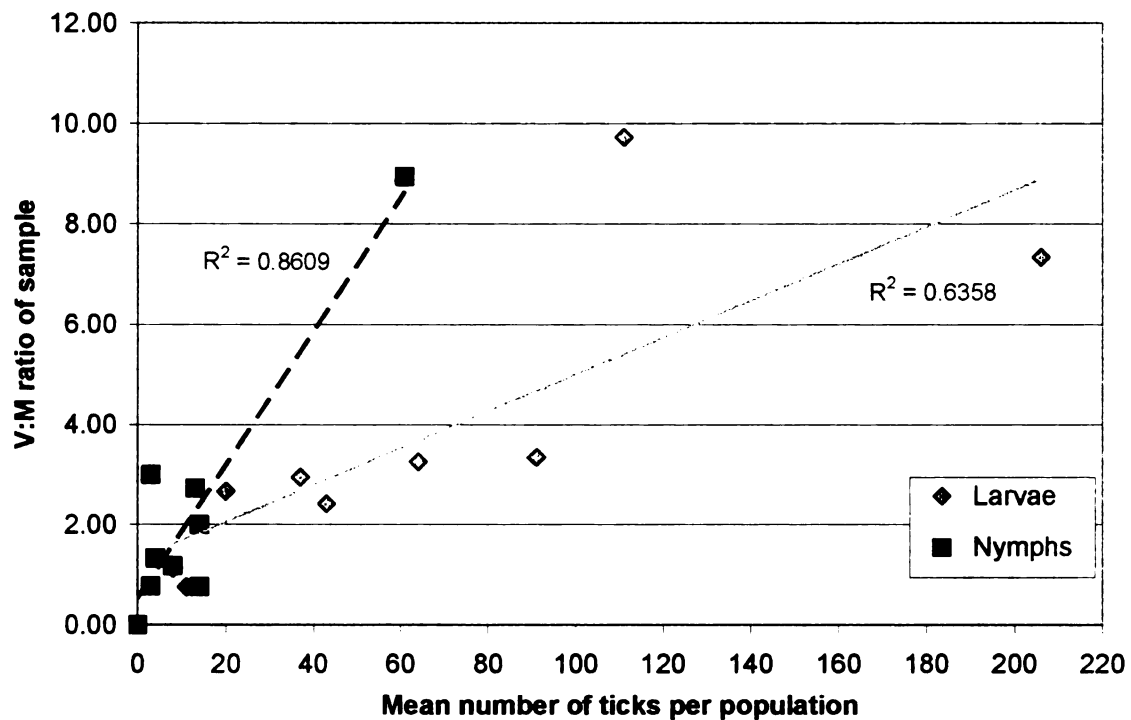
Figure 3.17. Comparison of mean number of ticks found on mice per trap period by grid, to the variance to mean ratio for the same population. Ticks were divided by lifestage. Generally, as the number of ticks in the population increases, so does the variance to mean ratio for that population, indicating that degree of aggregation may partly be a function of n. This graph illustrates how smaller sample sizes may not reflect the true degree of aggregation, since highly parasitized individuals (of which there are few) will be missed.

Figure 3.17 shows the comparison of number of ticks found on mice per trap period by grid to the variance to mean ratio for the same population. In this figure, ticks were divided by lifestage. Generally, as the number of ticks in the population increases, so does the variance to mean ratio for that population, indicating that degree of aggregation may partly be a function of n. This graph illustrates how smaller sample sizes may not reflect the true degree of aggregation, since highly parasitized individuals (of which there are few) will be missed.

94
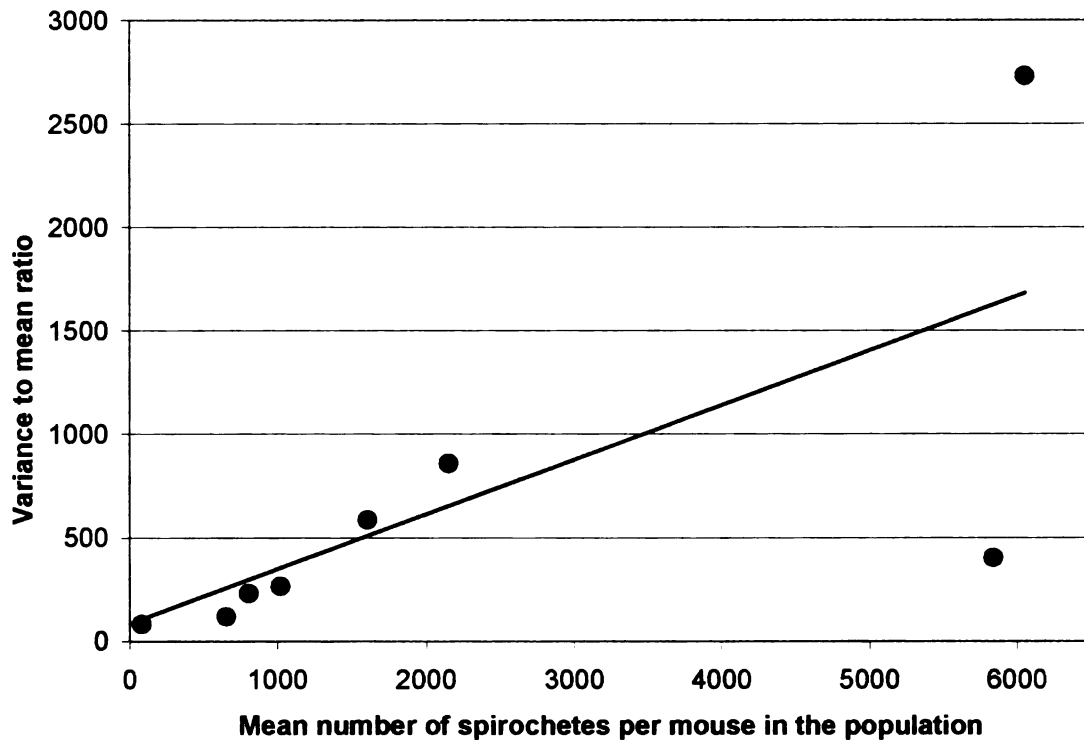
Figure 3.18. Comparison of mean number of spirochetes found in mice per trap period by grid, to the variance to mean ratio for the same population. Generally, as the number of individuals in the population increases, so does the variance to mean ratio for that population, indicating that degree of aggregation may partly be a function of n. This graph illustrates how smaller sample sizes may not reflect the true degree of aggregation, since highly parasitized individuals (of which there are few) will be missed. The lowest point is the data point for grid IV, trap period 3. The highest point is grid IV, trap period 1. There appear to be only 8 points because two of the data points overlap completely.

Figure 3.18 demonstrates comparison of number of spirochetes found in mice per trap period by grid to the variance to mean ratio for the same population. As the number of individuals in the population increases, so does the variance to mean ratio for that population, indicating that degree of aggregation may partly be a function of n. This graph illustrates how smaller sample sizes, especially when loads are lower, may not reflect the true degree of aggregation, since highly parasitized individuals (of which there are few) will be missed.

95

Negative binomial distribution

Values of k, a measure of aggregation, were calculated using the following

approximation of k, from Ludwig and Reynolds (1988), which is as follows:

$k = x^2 / (s^2 - x)$, where x = the sample mean and s = the sample variance. k is a value

between 0 and infinity, and the smaller k gets, (but typically less than 1) the more highly

aggregated the population. Table 3.4 shows the k parameter for the listed populations.

All of the values of k were below 1, indicating a negative binomial distribution.

Lloyd's mean crowding index

The calculation for crowding is a straightforward algebraic equation:

$m^* = x + (s^2/x - 1)$, where m* = the adjusted mean (or LMC index), x = sample mean,

s = the sample variance. Table 3.4 shows the LMC index for the listed populations. The

LMC index is high for all populations, indicating crowded conditions for all.

Spatial clustering of mice

ANCOVA for spatially correlated relationships shows that the Gaussian model

fits the data the best (AIC= 119.8), indicating that mouse captures were spatially

correlated (Figure 3.19). The captures were plotted on the grids at which they were

captured in ArcMap (ESRI, Redlands, CA) and these are presented, by trap period, in

Figure 3.20. Trap period 1 has the most captures, and trap period 3 the least. The very

smallest dots on the maps indicate zeroes.
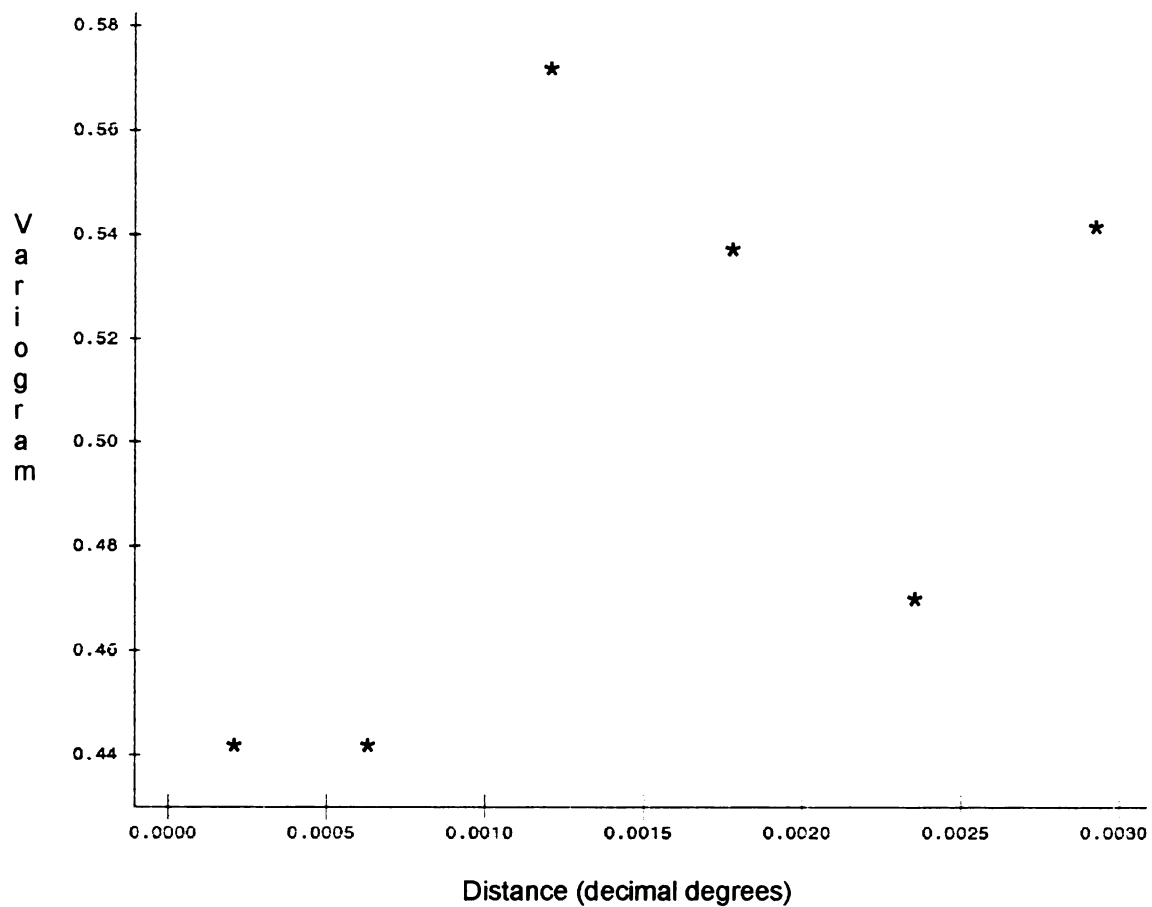
Figure 3.19. Gaussian spatially-correlated mouse chart. Variogram for distance, showing the approximate Gaussian curve for spatial correlation.

Figure 3.20. Maps displaying areas of mouse capture, by trap period (1, 2 and 3). Dots represent each trap point and the size of the dot indicates the 0, 1 or 2 captures for that trap period.

Looking at the all three grids and trap periods together because mouse densities on grids did not differ over time, there was a spatial correlation in average adjusted OD data up to 0.0006 distance units, or 66.7 m. The distance units used were decimal degrees; one degree of latitude at the 45th parallel is equal to 111.133 km. This means that mice up to 66.7 m apart have related values for their average adjusted ODs. The OD value is a measure of the level of antibody response that the mouse has had to *Borrelia burgdorferi*. Therefore, we assume that mice with similar OD values have had similar levels of exposure to *B. burgdorferi*, not taking individual immunological differences into account. Therefore, mice within 66.7 m of each other are likely to have similar exposure levels to *B. burgdorferi*, and at distances greater than that, are not likely to be similar.

Aggregation and spatial clustering of ticks

Aggregation of ticks on mice occurred at our field site. Frequency histograms show aggregated distributions of larvae on mice (Figure 3.21), nymphs on mice (Figure 3.22) and total ticks on mice (Figure 3.23) for first capture of individuals at each time period. For first time captures, Figure 3.24 describes how the same mouse can be simultaneously parasitized by both larvae and nymphs. Overall, mice had higher larval burdens than nymphal burdens. Graph does not differentiate if there was more than one mouse at a data point.

There were two lifestages each of two species of ticks on the mice. Larvae and nymphs of both *I. scapularis* and *Dermacentor variabilis* were present. For all three of the above histograms, the variance to mean ratio and k statistic indicate a high degree of

99

aggregation, and the LMC index indicates that the average parasite endures a high degree
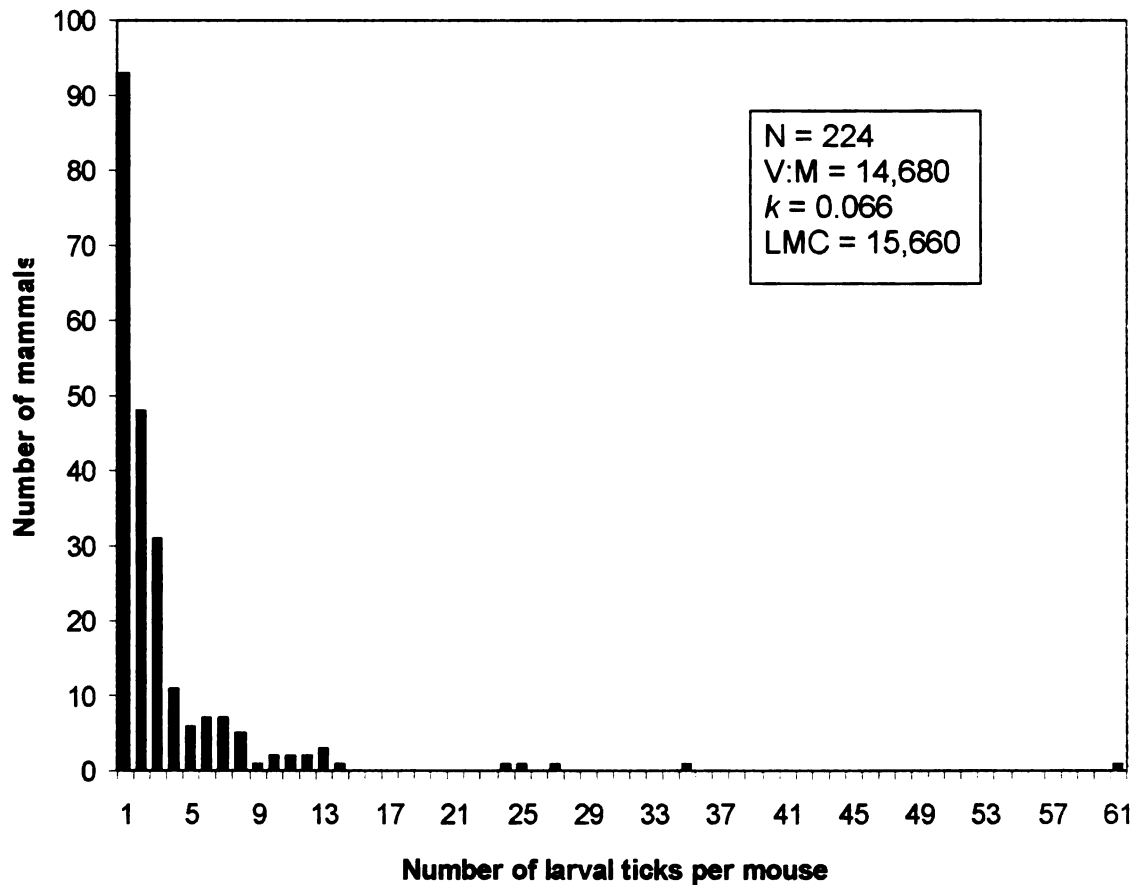
of crowding.

Figure 3.21. Frequency histogram for number of larval ticks on mice at first capture. The v: m ratio and k statistic indicate a high degree of aggregation. The LMC index indicates that the average parasite endures a high degree of crowding.
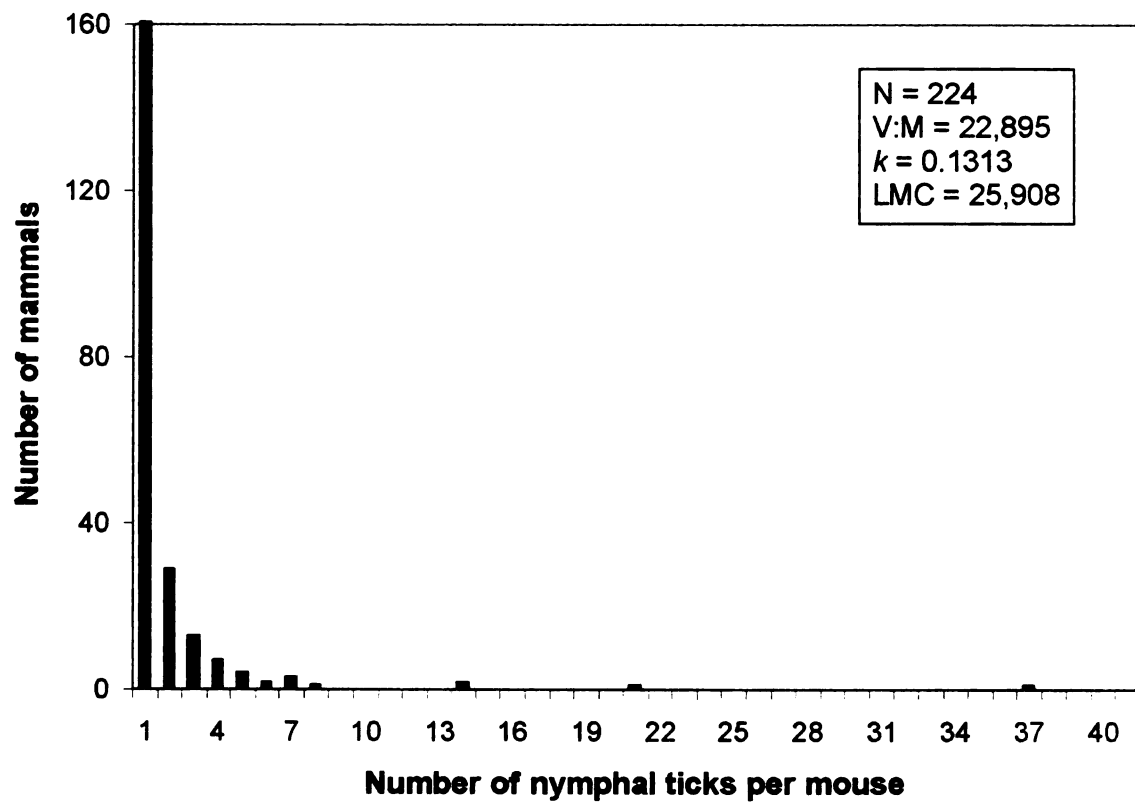
Figure 3.22. Frequency histogram for number of nymphal ticks on mice at first capture. The v: m ratio and k statistic indicate a high degree of aggregation. The LMC index indicates that the average parasite endures a high degree of crowding.
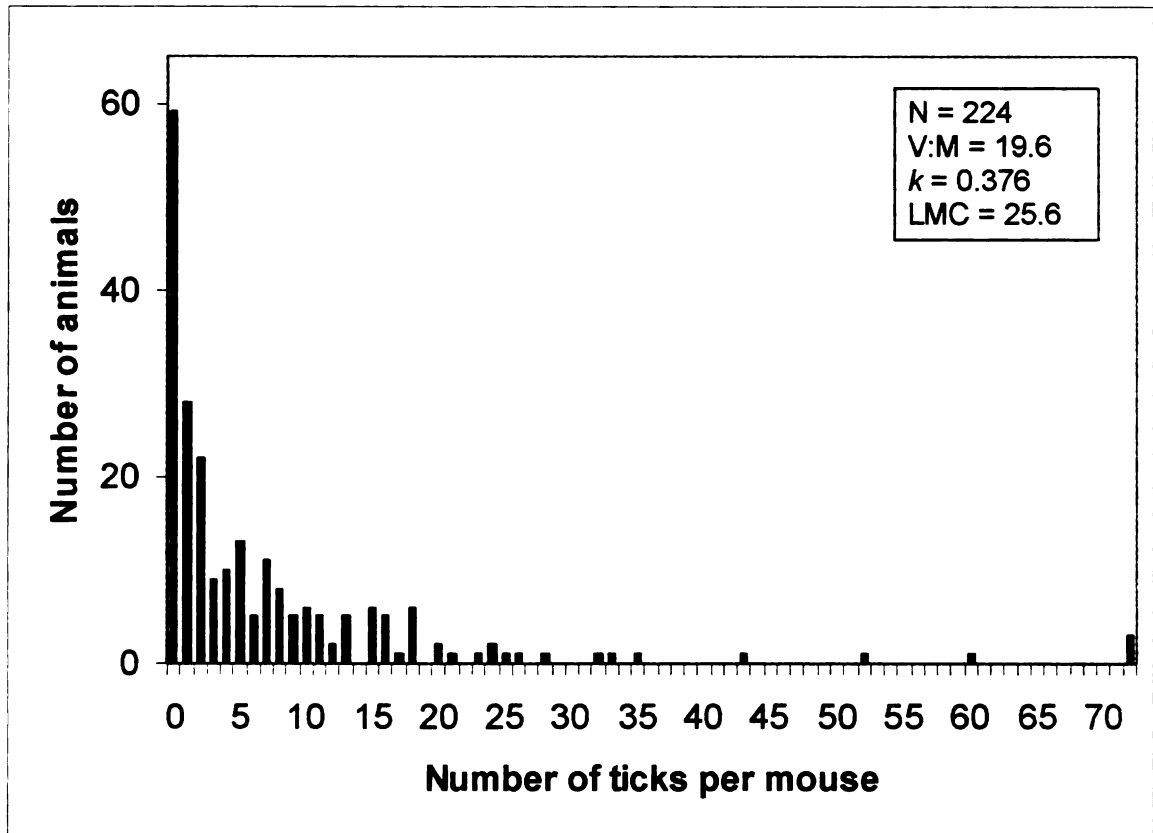
Figure 3.23. Frequency histogram for number of total ticks on mice at first capture. The v: m ratio and *k* statistic indicate a high degree of aggregation. The LMC index indicates that the average parasite endures a high degree of crowding.
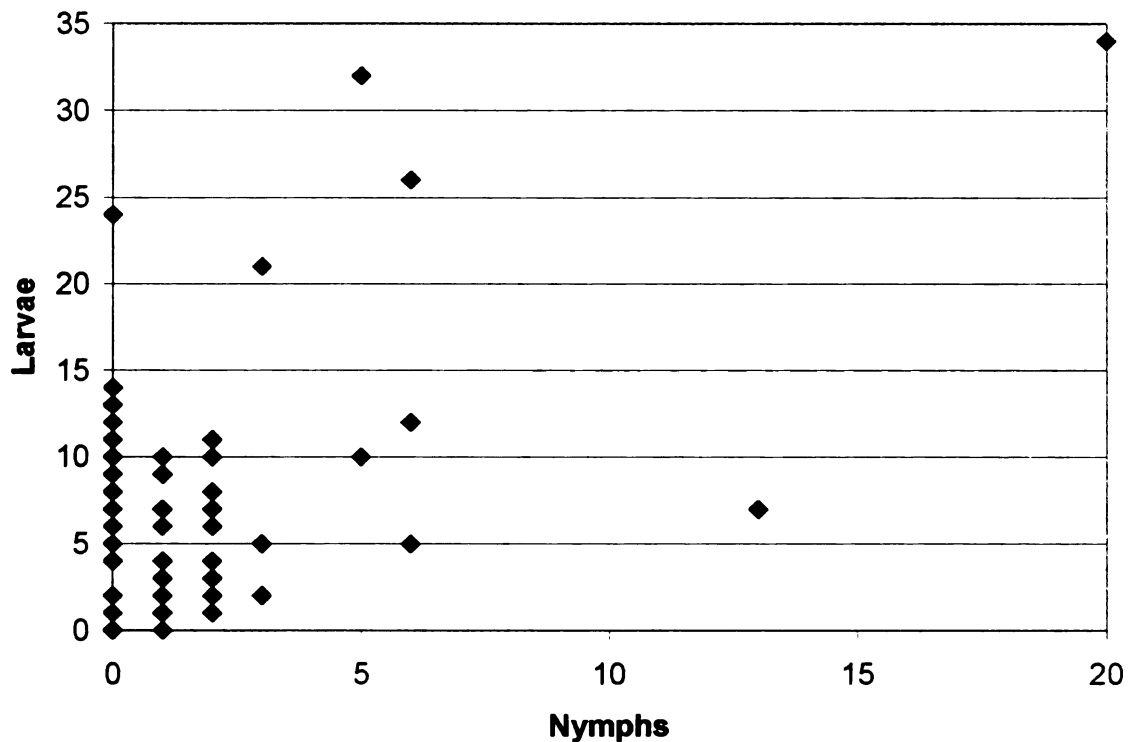
Figure 3.24. Simultaneous parasitism of larval and nymphal *I. scapularis* on individual mice. Graph shows the number of larvae and the number of nymphs that an individual mouse had at first capture. When multiple mice had the same configuration of larvae and nymphs, the graph still just displays one symbol. Overall, mice had higher larval burdens than nymphal burdens. Not all mice that had larvae had nymphs, but nearly all mice that had nymphs also had larvae feeding.

Ticks can be considered to be clustered, or aggregated in space both on and off hosts. Since we have exact location data for hosts and the data of their tick burdens at that time, we can create a map of where the ticks are, and thus, see how they aggregate in space. Tick clustering by lifestage and species was analyzed using kernel density (for a visual of where the most ticks were) and Moran's Index to get a degree of clustering. Table 3.5 and Figure 3.25 show ticks cluster spatially based on both lifestage and species. Nymphal ticks were mapped using kernel density, and demonstrate a clustered pattern by lifestage and species as well (Figure 3.26).

Table 3.5. Determining spatial autocorrelation of ticks species and lifestage, using Moran's Index.

Category	Moran's Index	p-value	Pattern
Total ticks	0	0.05	Somewhat clustered
Total larvae	0	0.05	Somewhat clustered
Total nymphs	-0.01	>0.10	Random
I. scapularis larvae	0.01	0.01	Clustered
I. scapularis nymphs	0.01	0.01	Clustered
D. variablis larvae	0	0.01	Somewhat clustered
D. variablis nymphs	0.2	0.01	Clustered
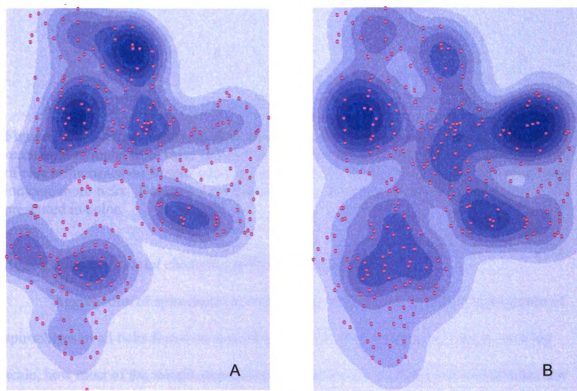
Figure 3.25. Kernel density of all species of larvae from mice (A) a somewhat clustered pattern, and of *I. scapularis* larvae from mice (B) also a clustered pattern. Descriptions of clustering based on Moran's Index analysis. Map shows all three grids together. Darker areas indicate more ticks. Dots show GPS-located trap locations. Figures in this thesis presented in color.
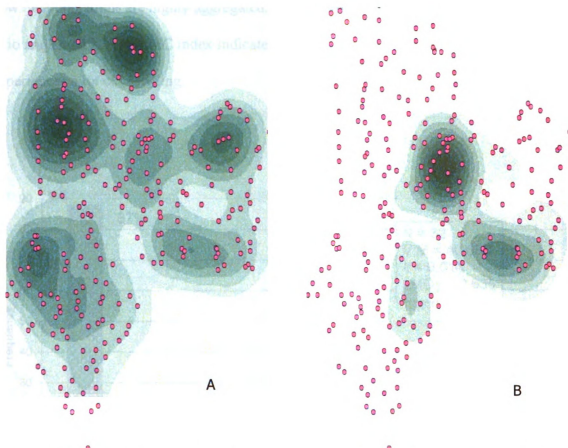
Figure 3.26. Kernel density of all nymphs from mice (A) a random pattern, and of *I. scapularis* nymphs from mice (B) a clustered pattern, centered on grid IV. Descriptions of clustering based on Moran's Index analysis. Map shows all three grids. Darker areas indicate more ticks. Dots show GPS-located trap locations. Figures in this thesis presented in color.

Aggregation and spatial clustering of Borrelia burgdorferi

Aggregation of spirochetes in mice occurs (Figure 3.27), as does aggregation of spirochetes in all ticks found on mice (Figure 3.28). These histograms show, on a log scale, how most of the sample population contained zero *B. burgdorferi* organisms, few to none in the 10-100 range, with a peak in the 1000s for both populations. Although possible, quantitative PCR was not perfectly accurate at picking up spirochete loads less than 10 and thus, this bin in nearly empty for both histograms. Both histograms show

how the populations are highly aggregated, as indicated by the large variance to mean

ratio and small k. The LMC index indicates that the average parasite in this population

experiences a lot of crowding.
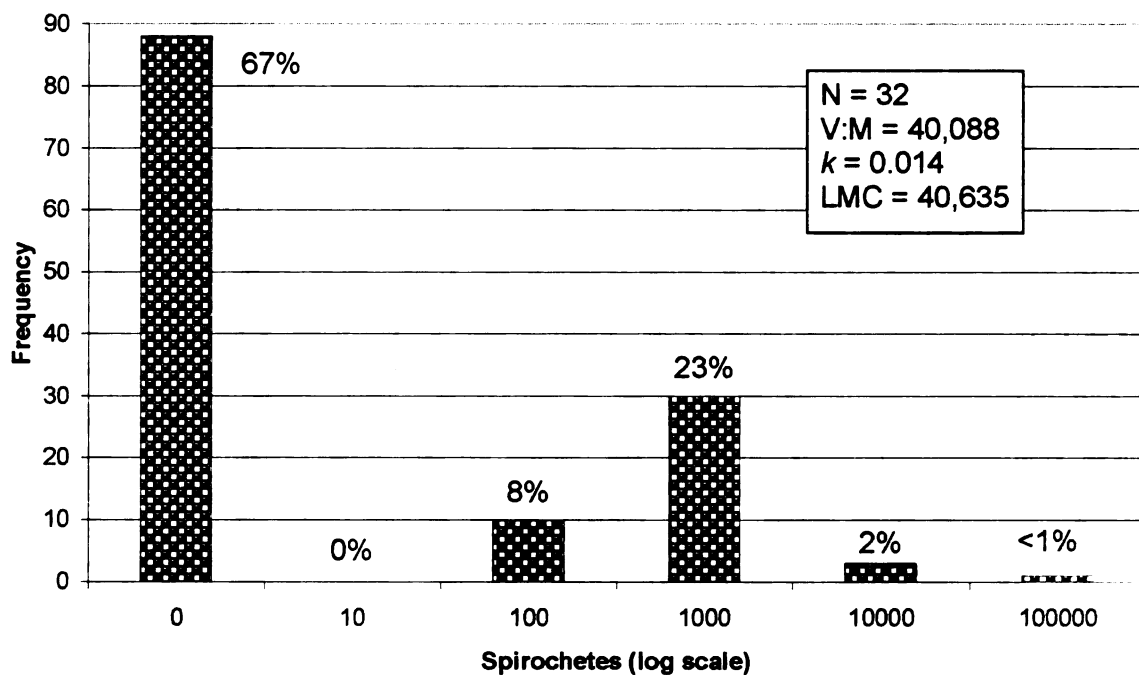
Figure 3.27. Frequency histogram of number of mice with numbers of spirochetes.
This population is highly aggregated, as indicated by the large v:m ratio, small k. LMC
index indicates that the average parasite in this population experiences a lot of crowding.
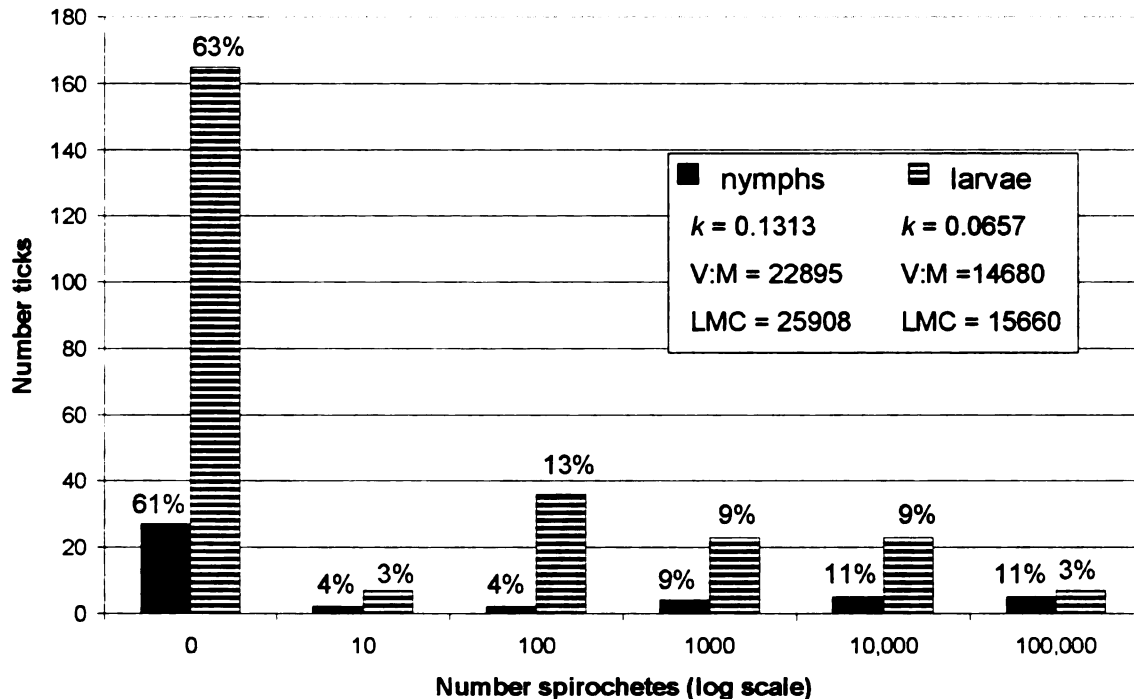
Figure 3.28. Frequency histogram for spirochete loads in all ticks recovered from hosts. The number of spirochetes is presented on a log scale. For each group, summary statistics are presented: k parameter for the negative binomial distribution, variance to mean ratio (v: m), and Lloyd's mean crowding index (LMC). The k statistic indicates that the larvae are more highly aggregated. Both sample populations have a v: m ratio to the same order of magnitude, 10^4, indicating aggregation. The LMC index for nymphs is higher, showing that that the average spirochete in a nymph on a host feels more crowded than the average spirochete in a larva feeding on a host.

Further, the method of spirochete detection in mammal tissues is not completely accurate or reliable due to the nature of where in the bacteria may be in the animal. Sometimes, even an infected animal will show up negative because the tissue sample that we have taken is the not area where the bacteria are in the skin, or the mouse was only recently infected and the spirochetes are still circulating in the blood and have not made it into the skin. Therefore, this method of detection is not the best for determining which mice have past or current *B. burgdorferi* infection. Thus, this measure, combined with the ELISA to capture antibodies to a past infection with *B. burgdorferi* gives the best

measure of infected mice. This combination of metrics was used to count 'infected' mice, which were used as a factor in the spatial analysis. If one of the metrics gave a positive result, then the mouse was counted as infected.

Maps for datasets were created at each time period. The maps were created using ArcMap software (ESRI, Redlands, CA). In these maps, the trap points are represented by dots, and the larger the dots are, the more of that particular organism was found at that particular point. Scales for each of the maps are listed in the figure legends. These maps are shown in Figures 3.29A through 3.29O. These maps are visuals displaying how the bacteria, ticks and mammals were clustered in space. Over time, the places where these organisms were picked up changed.

Figure 3.29A. Maps for trap periods 1, 2 and 3 displaying all three grids. Dots represent trap points. Size of dots represent the number of infected mice captured at those trap points. Increasing dot sizes represent 0, 1 and 2, respectively.

Figure 3.29B. Maps for trap periods 1, 2 and 3 displaying all three grids. Dots represent trap points. Size of dots represents the average adjusted OD values for the mice captured at those trap points. The smallest dots represent mice with no developed antibody response to *B. burgdorferi*, and the large dots represent those that do have antibodies against the pathogen.

Figure 3.29C. Maps for trap periods 1, 2 and 3 displaying all three grids. Dots represent trap points. Size of dots represents the number of spirochetes in the mice captured at those trap points. Increasing dot sizes represent 0, 150, 500, 1500 and 5500, respectively.
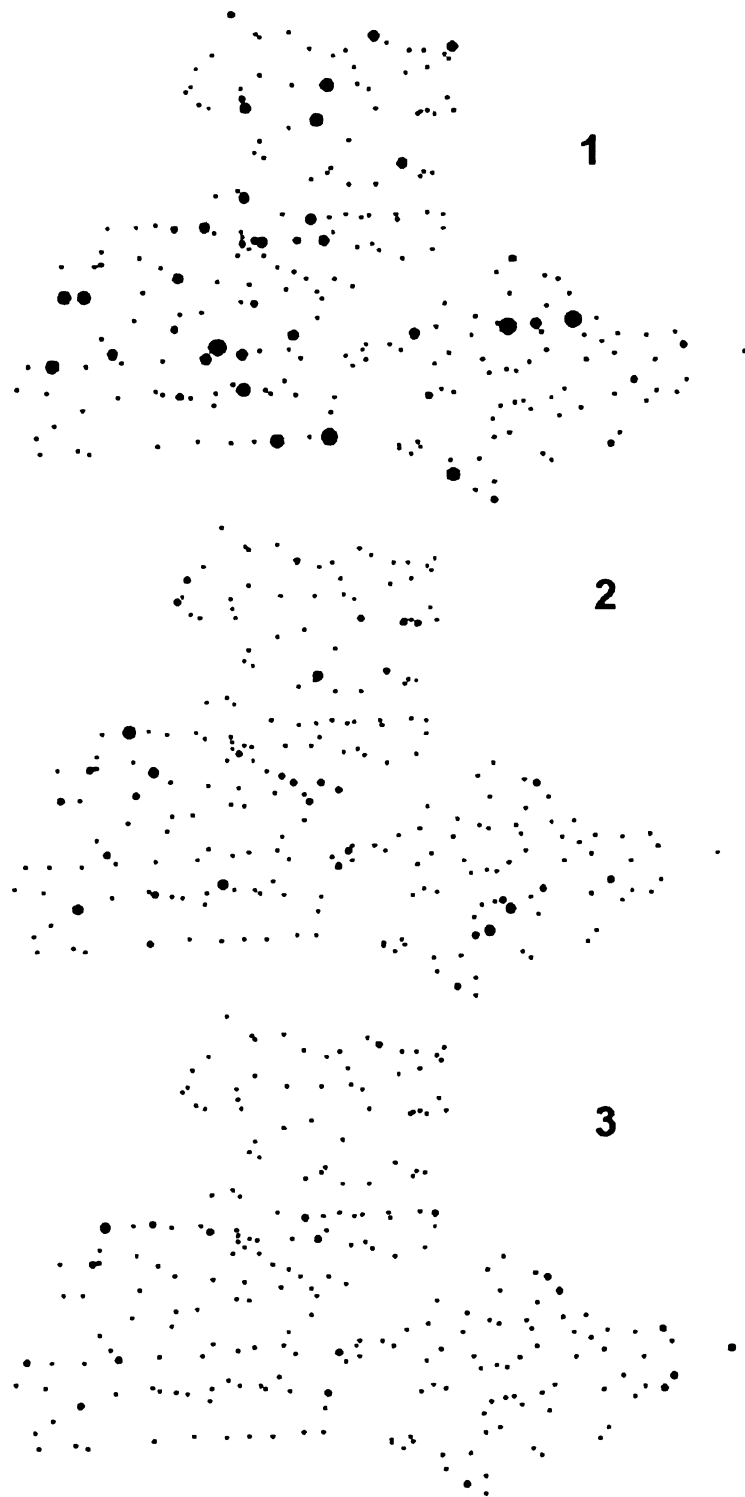
Figure 3.29D. Maps for trap periods 1, 2 and 3 displaying all three grids. Dots represent trap points. Size of dots represents the number of larvae on the mice captured at those trap points. Increasing dot sizes represent 0, 5, 10, 20 and 35, respectively.

Figure 3.29E. Maps for trap periods 1, 2 and 3 displaying all three grids. Dots represent trap points. Size of dots represents the number of infected larvae on the mice captured at those trap points. Increasing dot sizes represent 0, 1, 2 and 3, respectively.

113

Figure 3.29F. Maps for trap periods 1, 2 and 3 displaying all three grids. Dots represent trap points. Size of dots represents the number of spirochetes in larvae on the mice captured at those trap points. Increasing dot sizes represent 0, 100, 1000, 9999 and 35,000 respectively.
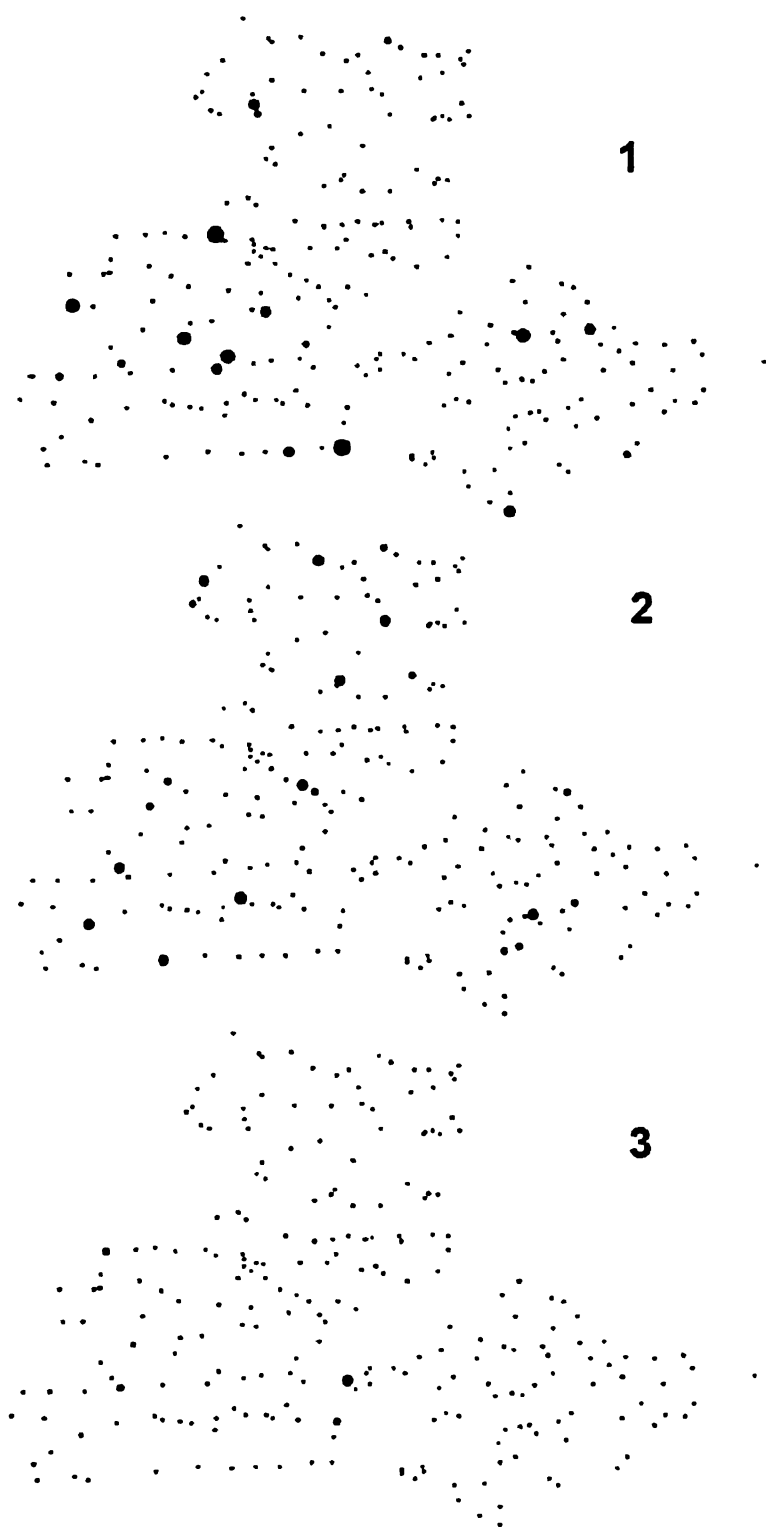
Figure 3.29G. Maps for trap periods 1, 2 and 3 displaying all three grids. Dots represent trap points. Size of dots represents the number of nymphs on the mice captured at those trap points. Increasing dot sizes represent 0, 1, 3, 6 and 20 respectively.

115

Figure 3.29H. Maps for trap periods 1, 2 and 3 displaying all three grids. Dots represent trap points. Size of dots represents the number of infected nymphs on the mice captured at those trap points. Increasing dot sizes represent 0, 1 and 2 respectively.

Figure 3.29I. Maps for trap periods 1, 2 and 3 displaying all three grids. Dots represent trap points. Size of dots represents the number of spirochetes in nymphs on the mice captured at those trap points. Increasing dot sizes represent 0, 100, 500, 1000 and 37,000 respectively.

117

Figure 3.29J. Maps for trap periods 1, 2 and 3 displaying all three grids. Dots represent trap points. Size of dots represents the total ticks on the mice captured at those trap points. Increasing dot sizes represent 0, 3, 8, 15 and 54 respectively.

Figure 3.29K. Maps for trap periods 1, 2 and 3 displaying all three grids. Dots represent trap points. Size of dots represents the questing larvae at those trap points. Increasing dot sizes represent 0, 2, 5, 16 and 79 respectively.

119
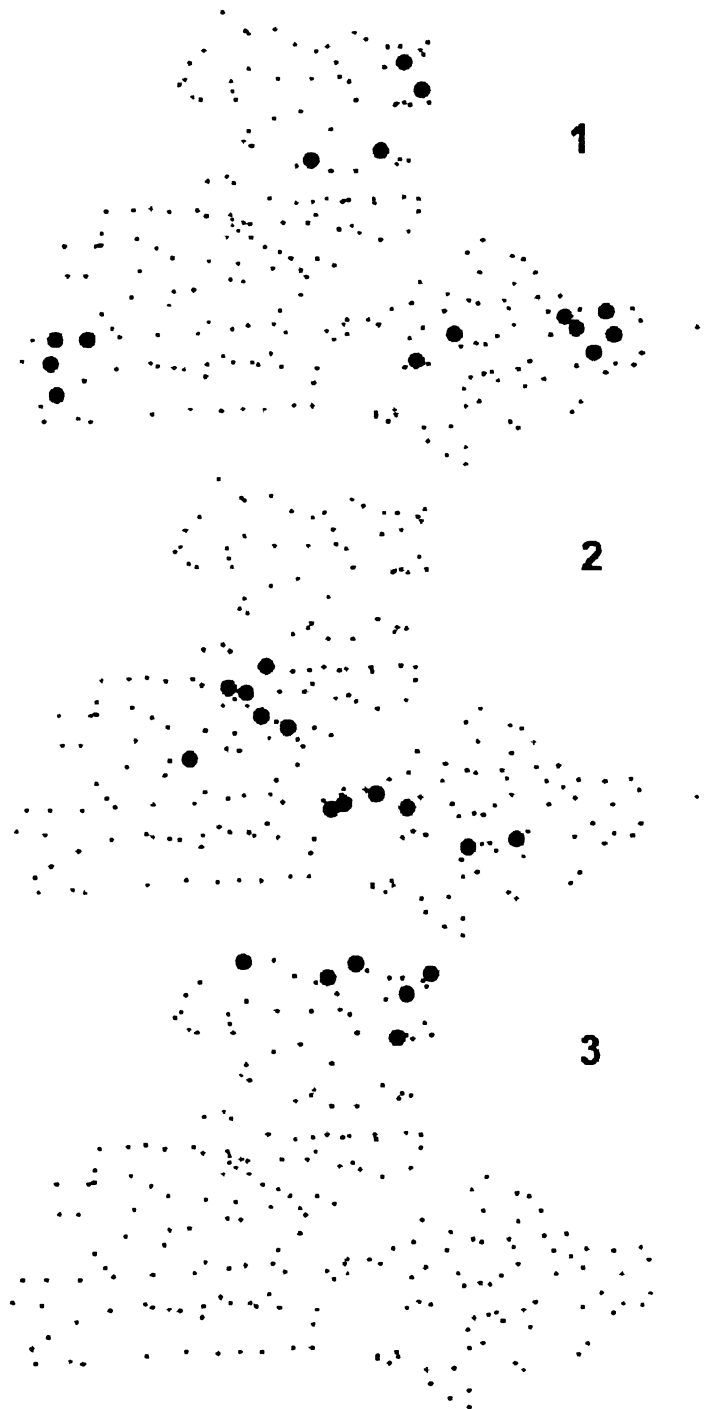
Figure 3.29L. Maps for trap periods 1, 2 and 3 displaying all three grids. Dots represent trap points. Size of dots represents the questing nymphs at those trap points. Small and large dot sizes represent 0 and 1 respectively.
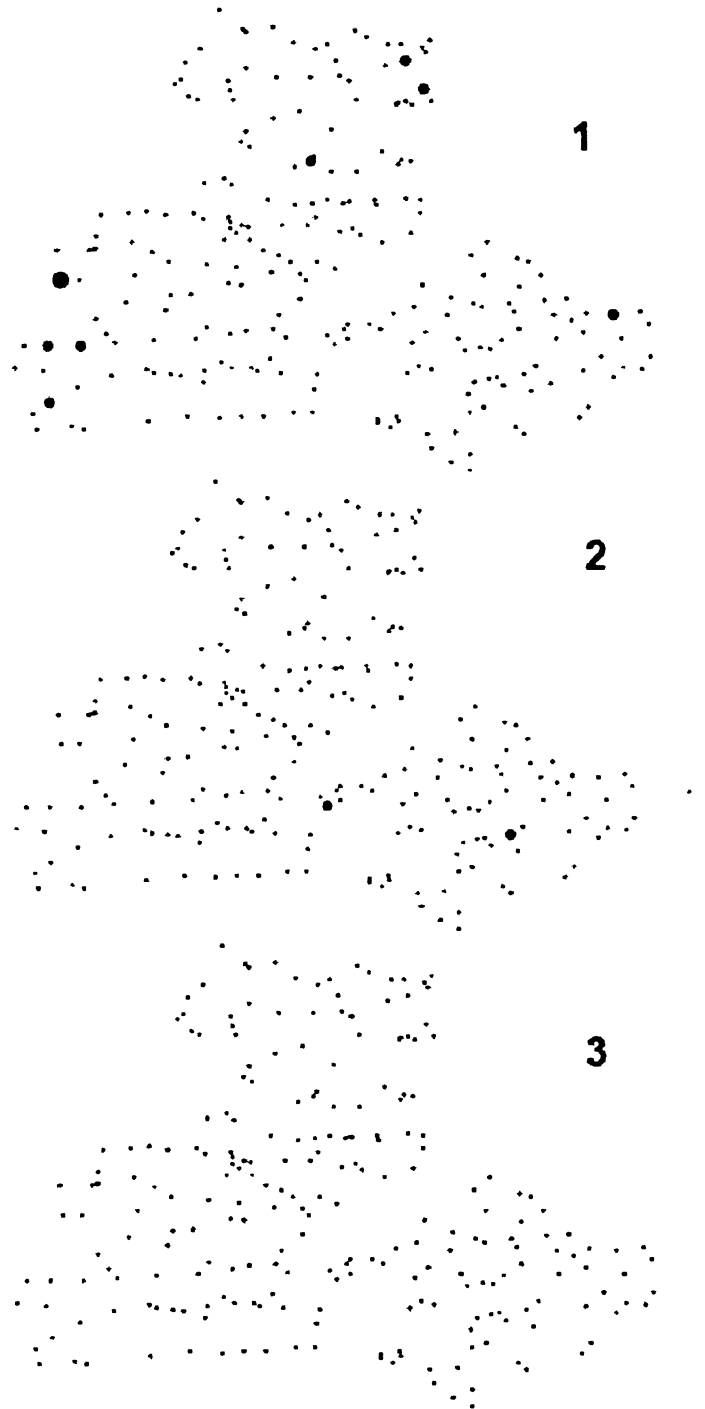
Figure 3.29M. Maps for trap periods 1, 2 and 3 displaying all three grids. Dots represent trap points. Size of dots represents the infected questing nymphs at those trap points. Increasing dot sizes represent 0, 1 and 2 respectively.

Figure 3.29N. Maps for trap periods 1, 2 and 3 displaying all three grids. Dots represent trap points. Size of dots represents the total questing ticks at those trap points. Increasing dot sizes represent 0, 5, 17 and 79 respectively.

Figure 3.29O. Maps for trap periods 1, 2 and 3 displaying all three grids. Dots represent trap points. Size of dots represents the total questing ticks at those trap points. Increasing dot sizes represent 0, 250, 1500 and 5500 respectively.

To ensure that these aggregated distributions did indeed deviate from a random, or Poisson distribution, the index of dispersion (I_D) for the datasets were compared with the Chi-square values for datasets with the same sample size. I_D values that exceed the Chi-square value are considered to deviate from the random distribution. These values all exceeded the Chi-square value for the appropriate $n - 1$ sample size, and are listed in Table 3.6.

Table 3.6. Null hypothesis testing for aggregated spirochetes in the following populations. For each listed population, the index of dispersion, $n - 1$ and Chi-square value with ($n - 1$) degrees of freedom are listed. Populations with indices of dispersion > the Chi-square value are considered to deviate from a random distribution.

Population	Index of dispersion	$n - 1$	Chi-square value
All larval ticks on mice	3816800	260	149.48
Larval ticks, trap period 1, grid III	69580	14	36.12
Larval ticks, trap period 1, grid IV	581532	43	77.42
Larval ticks, trap period 1, grid V	38016	33	63.87
Larval ticks, trap period 2, grid III	135744	28	56.89
Larval ticks, trap period 2, grid IV	627804	27	55.48
Larval ticks, trap period 2, grid V	192105	27	55.48
Larval ticks, trap period 3, grid III	211360	32	62.49
Larval ticks, trap period 3, grid IV	486127	29	58.3
Larval ticks, trap period 3, grid V	102467	19	43.82
All nymphal ticks on mice	1007380	44	78.75
Nymphal ticks, trap period 1	518000	25	52.62
Nymphal ticks, trap period 2	251037	9	27.88
Nymphal ticks, trap period 3	21344	8	26.13
Questing larvae	158.4	18	42.31
Questing nymphs	209440	35	66.62
Questing adults	136800	38	70.71
Mice, trap period 1, grid III	35503	13	34.53
Mice, trap period 1, grid IV	8060	20	45.32
Mice, trap period 1, grid V	1785	15	37.7
Mice, trap period 2, grid III	11700	20	45.32
Mice, trap period 2, grid IV	2990	13	34.53
Mice, trap period 2, grid V	3458	13	34.53
Mice, trap period 3, grid III	641544	12	32.91
Mice, trap period 3, grid IV	738	9	27.88
Mice, trap period 3, grid V	8590	10	29.59

Analysis of spatial correlation

Spatial analysis

Trap points were located with a GPS unit with an error of approximately 30m. The traps were spaced at 12 m intervals, so distances cannot be accurately measured on the map outputs. In the future, traps could be spaced further apart, although this may not be biologically meaningful, or a more accurate GPS unit is needed. As a result of this, and because drag tick sample locations were not georeferenced with a GPS unit, false coordinates were used to derive the number of drag ticks at each trap point for the spatial analysis portion of the data analysis.

The three grids were rotated through in order to serve as replicates. However, sample sizes at the individual grid level were too small for meaningful comparisons to be made. Therefore, possible associations were examined by grouping the grids by time period in order to increase the numbers of the positive responses per analysis and serving to increase power. Indeed, the trends within time periods are more similar than the trends within a single grid over time, suggesting that seasonality is one of the strongest factors influencing the activity and thus, the aggregation of the organisms in the system.

For the spatial autocorrelation procedure, I used SAS (SAS Institute, Cary, NC). Latitude and longitude coordinates were used, along with the first capture of an individual mouse at that time period. Only data related to *I. scapularis* was used. Other mammal species, repeat captures, other species of tick were not used. Measured factors were compared in a pair-wise fashion to determine which of the pairs were correlated spatially. These comparisons along with the distances at which they were spatially correlated with significant coefficient of correlation are listed in Table 3.7.

Of the 27 pair-wise comparisons made for each time period, for the purpose of 'screening' variables to see which were spatially related, a total of 17 were significant at any distance. For Figures 3.30 to 3.32, the x-axis shows the distance in decimal degrees at which the pairs are spatially correlated. The y-axis shows the r value, the coefficient of correlation. The significant $r = 0.1069$ is represented by the dashed line. See Methods for the calculation.

Cross-correlograms for significant associations for trap period 1 were number of infected mice and conifers (Figure 3.30A) and infected questing nymphs and conifers (Figure 3.30B). For trap period 2, there were significant associations between deciduous trees and questing larvae (Figure 3.31A), and conifers and questing larvae (Figure 3.31B). For trap period 3, significant associations were total ticks and conifers (Figure 3.32A), number of mice and conifers (Figure 3.32B) and questing nymphs and conifers (Figure 3.32C).

Table 3.7. Comparisons made using the cross-correlograms. The distance at which the pairs were spatially correlated is listed for each trap period. Units are in decimal degrees. Distance values listed all had an *r* value greater than the value of significance, 0.1069, although individual *r* values are not listed here. If a 0 is listed, factors were not correlated at any distance. Numbers smaller than 0.0002 (the minimum lag distance) and greater than or equal to 0.0036 (the maximum lag distance) were not considered to be significant. Variables with (*) were log-transformed for the analysis.

Factor 1	Factor 2	TP 1	TP 2	TP 3
Number of mice	Understory	0	0	0
	Deciduous trees	0	0	0
	Coniferous trees	0	0	0.0032-0.0034
Number of infected mice*	Understory	0	0	0
	Deciduous trees	0	0	0
	Coniferous trees	0.0004-0.0027	0	0
	Questing larvae	0	0	0
	Questing nymphs	0	0	0
	Infected quesitng nymphs	0	0	0
Total ticks on mice*	Understory	0	0	0
	Deciduous trees	0	0	0
	Coniferous trees	0	0	0.0028-0.0034
	Questing larvae	0	0	0
	Questing nymphs	0	0	0
	Infected quesitng nymphs	0	0	0
Questing larvae*	Understory	0	0	0
	Deciduous trees	0	0.0018-0.0020	0
	Coniferous trees	0	0.0018-0.0024	0
Questing nymphs*	Understory	0	0	0
	Deciduous trees	0	0	0
	Coniferous trees	0	0	0.0002
Infected questing nymphs*	Understory	0	0	0
	Deciduous trees	0	0	0
	Coniferous trees	0.0021-0.0025	0	0
	Infected nymphs on mice	0	0	0
Spirochetes in questing nymphs*	Infected larvae on mice	0	0	0
	Infected nymphs on mice	0	0	0
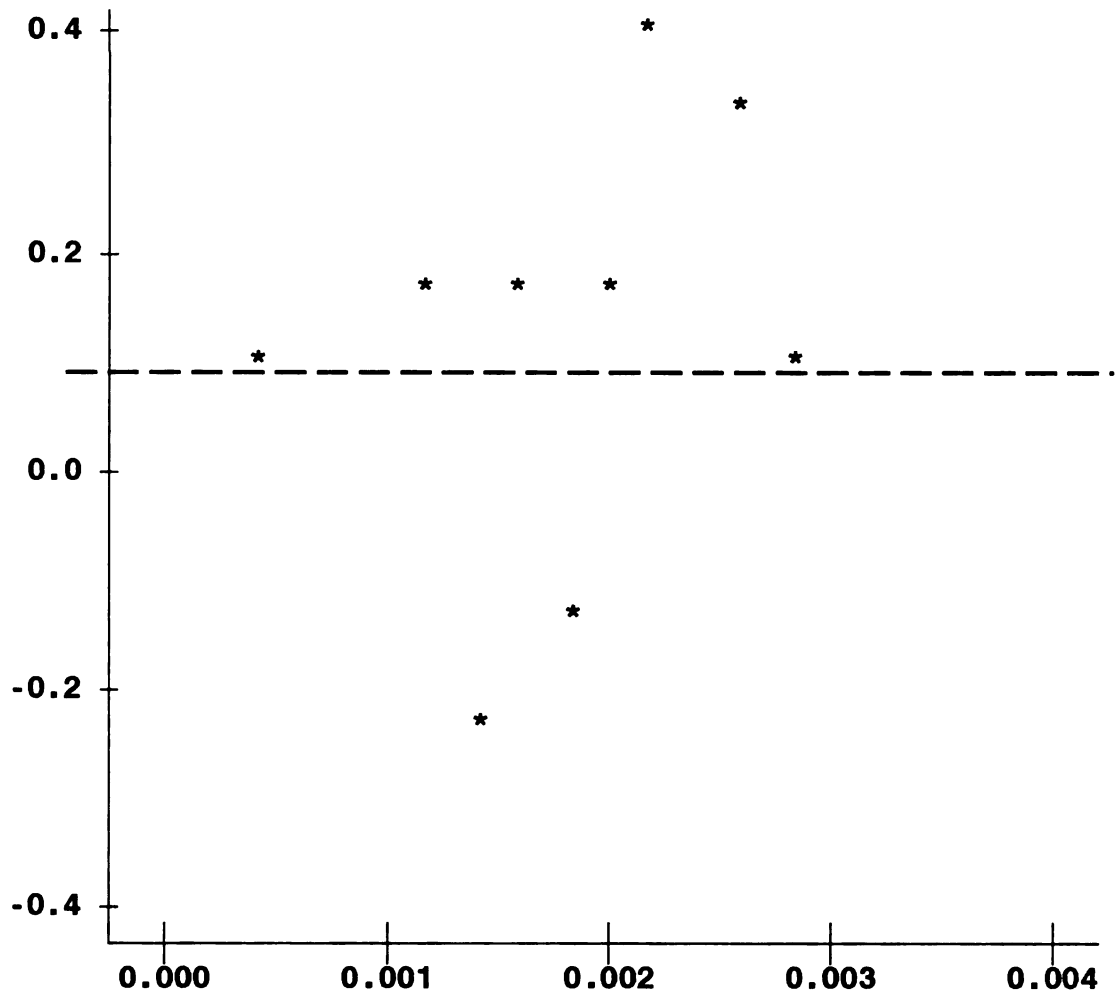
Figure 3.30A. Significant cross-correlogram for time 1. The x-axis shows the distance in decimal degrees at which the pair is spatially correlated. The y-axis shows the r value, the coefficient of correlation. The significant $r = 0.1069$ is represented by the dashed line. Graph compares the spatial correlation between the number of infected mice and conifers. They are spatially correlated between 0.0004 and 0.0027 decimal degrees.
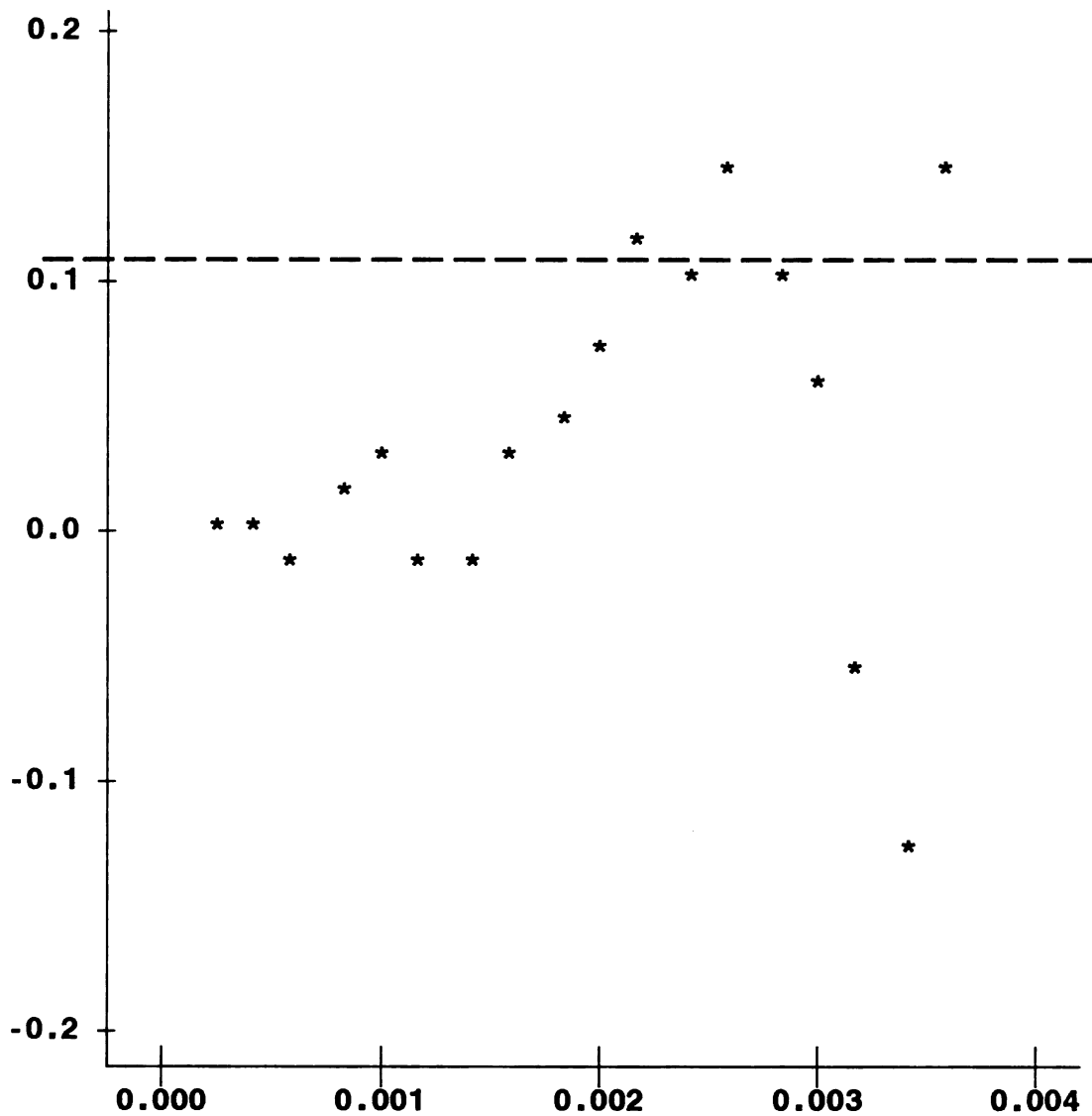
Figure 3.30B. Significant cross-correlogram for time 1. The x-axis shows the distance in decimal degrees at which the pair is spatially correlated. The y-axis shows the r value, the coefficient of correlation. The significant $r = 0.1069$ is represented by the dashed line. Graph compares the spatial correlation between the number of infected questing nymphs and conifers. They are spatially correlated between 0.0021 and 0.0025 decimal degrees.
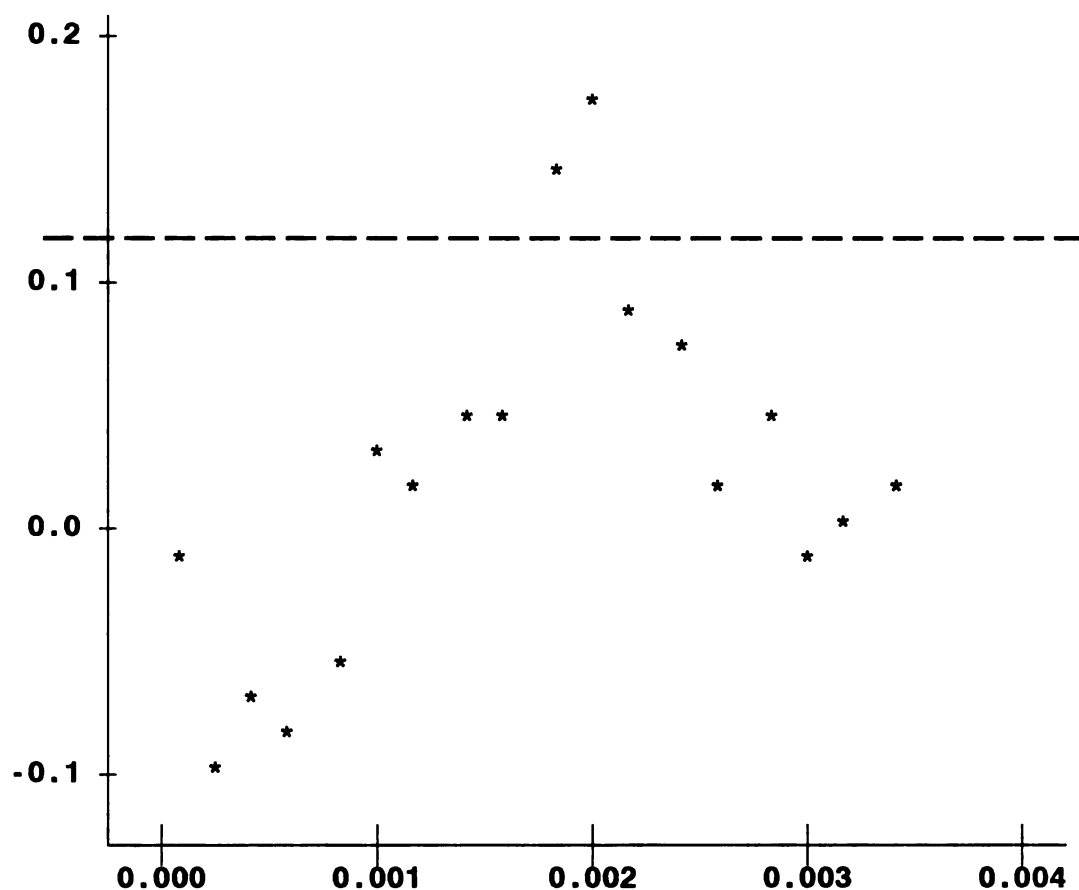
Figure 3.31A. Significant cross-correlogram for time 2. The x-axis shows the distance in decimal degrees at which the pairs are spatially correlated. The y-axis shows the *r* value, the coefficient of correlation. The significant *r* = 0.1069 is represented by the dashed line. Graph compares the spatial correlation between deciduous trees and questing larvae. They are spatially correlated between 0.0018 and 0.0020 decimal degrees.
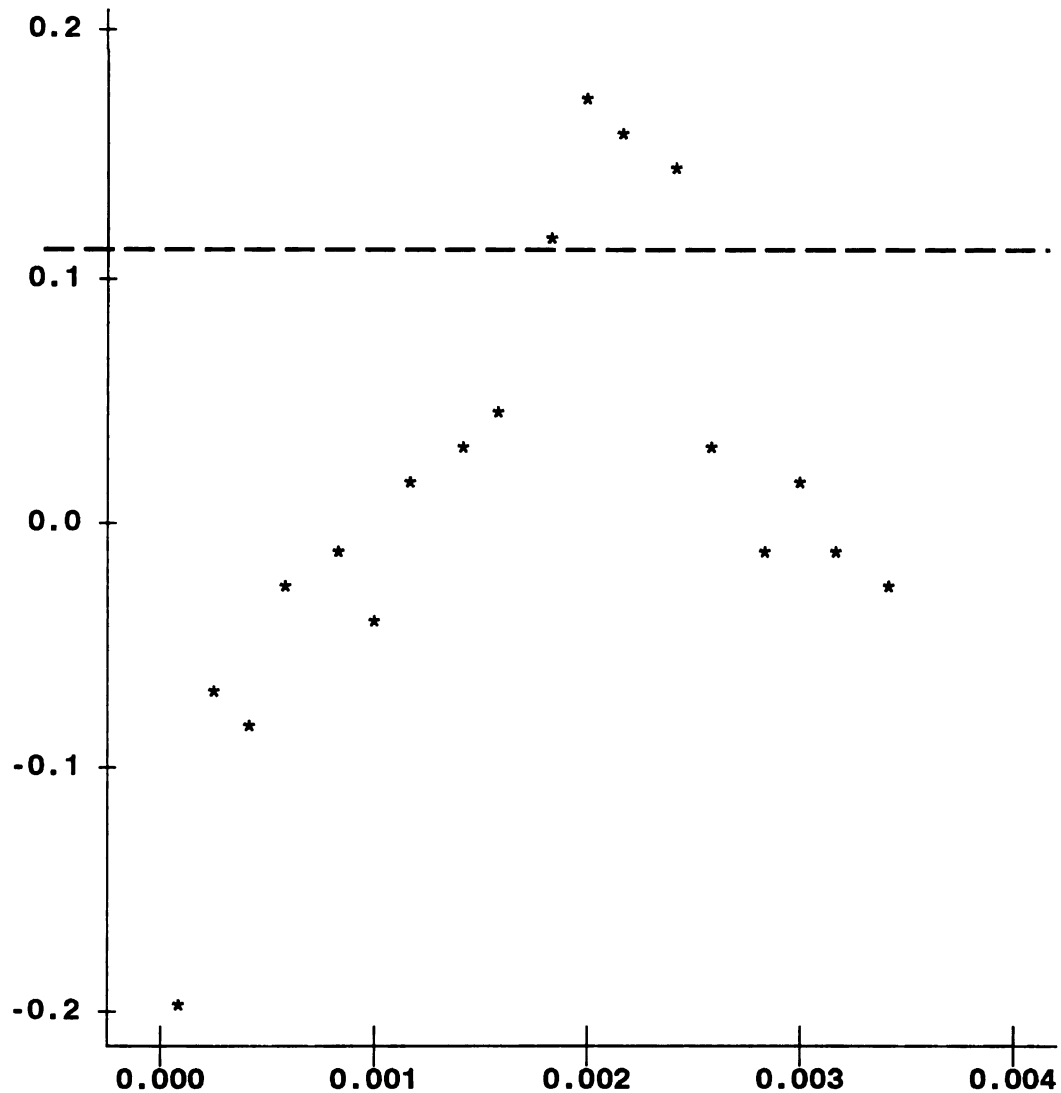
Figure 3.31B. Significant cross-correlogram for time 2. The x-axis shows the distance in decimal degrees at which the pairs are spatially correlated. The y-axis shows the *r* value, the coefficient of correlation. The significant *r* = 0.1069 is represented by the dashed line. Graph compares the spatial correlation between conifers and questing larvae. They are spatially correlated between 0.0018 and 0.0024 decimal degrees.
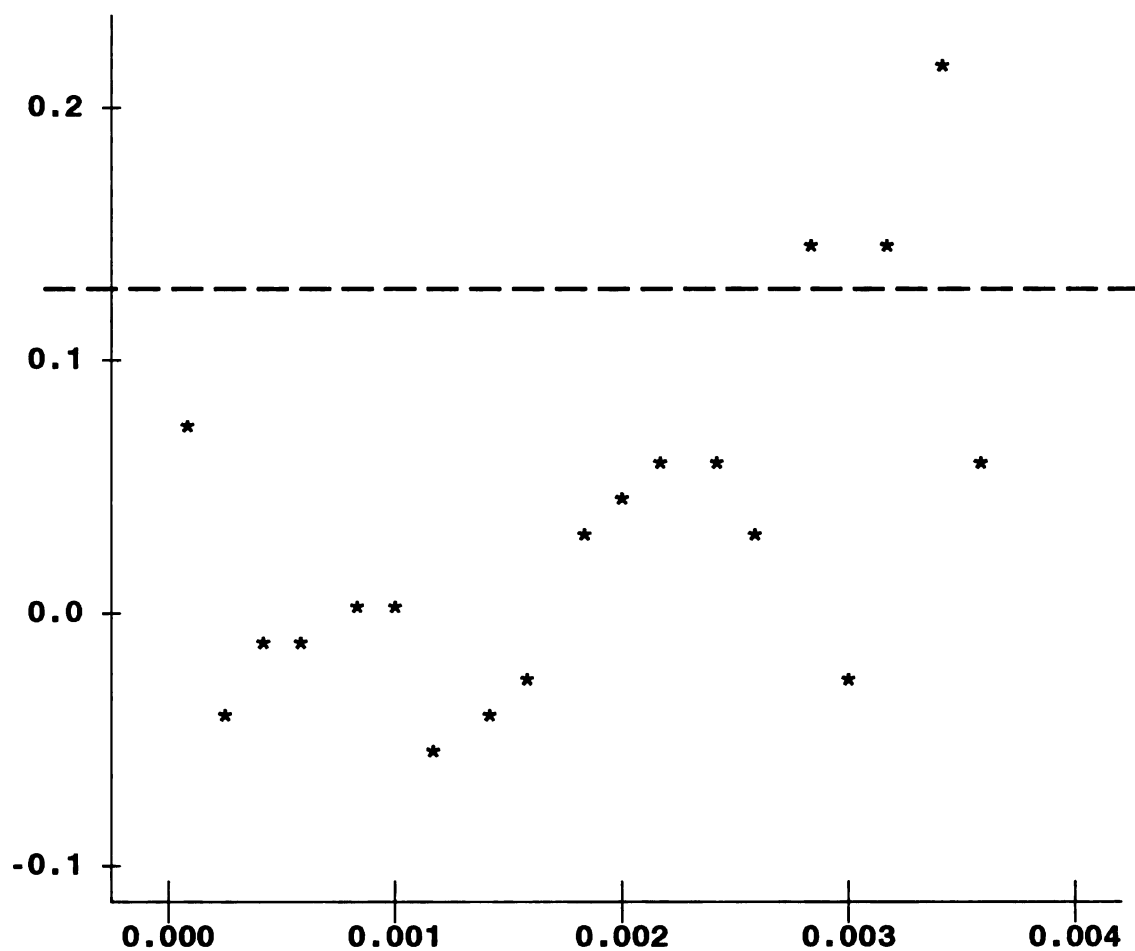
Figure 3.32A. Significant cross-correlogram for time 3. The x-axis shows the distance in decimal degrees at which the pairs are spatially correlated. The y-axis shows the r value, the coefficient of correlation. The significant $r = 0.1069$ is represented by the dashed line. Graph compares the spatial correlation between total ticks and conifers. They are spatially correlated between 0.0028 and 0.0034 decimal degrees.
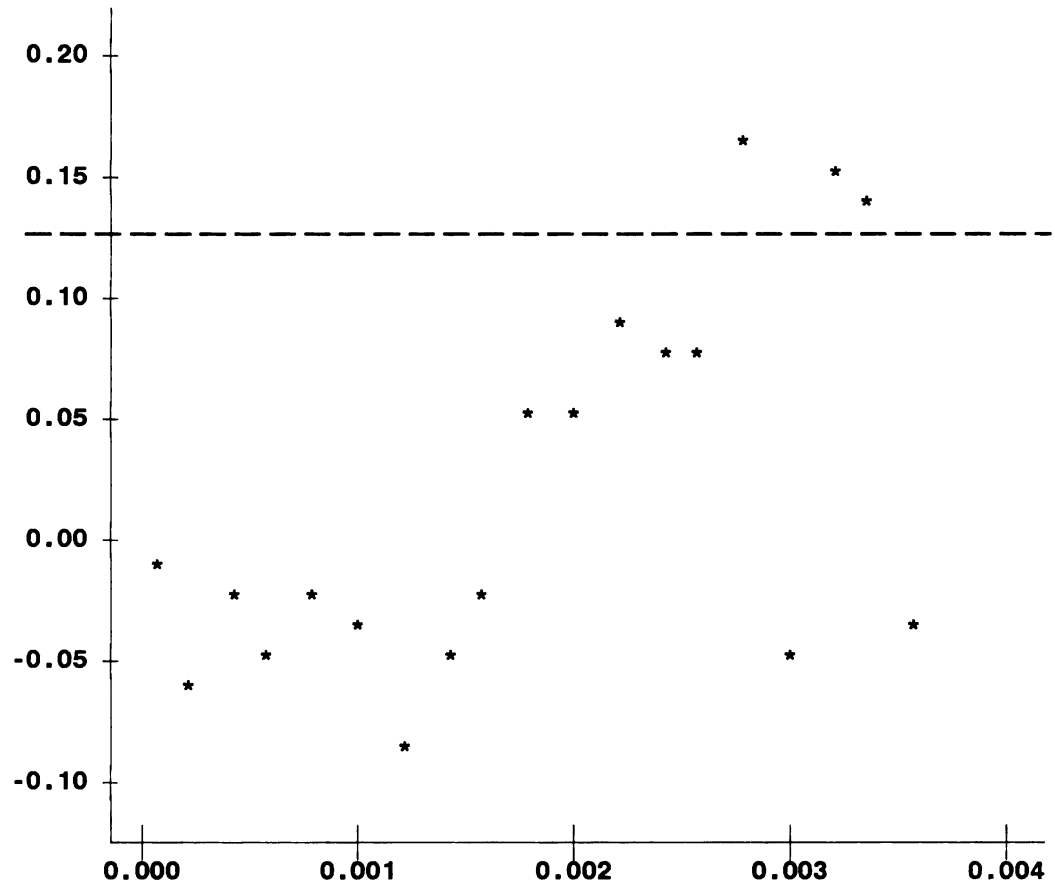
Figure 3.32B. Significant cross-correlogram for time 3. The x-axis shows the distance in decimal degrees at which the pairs are spatially correlated. The y-axis shows the r value, the coefficient of correlation. The significant $r = 0.1069$ is represented by the dashed line. Graph compares the spatial correlation between number of mice and conifers. They are spatially correlated between 0.0032 and 0.0034 decimal degrees.
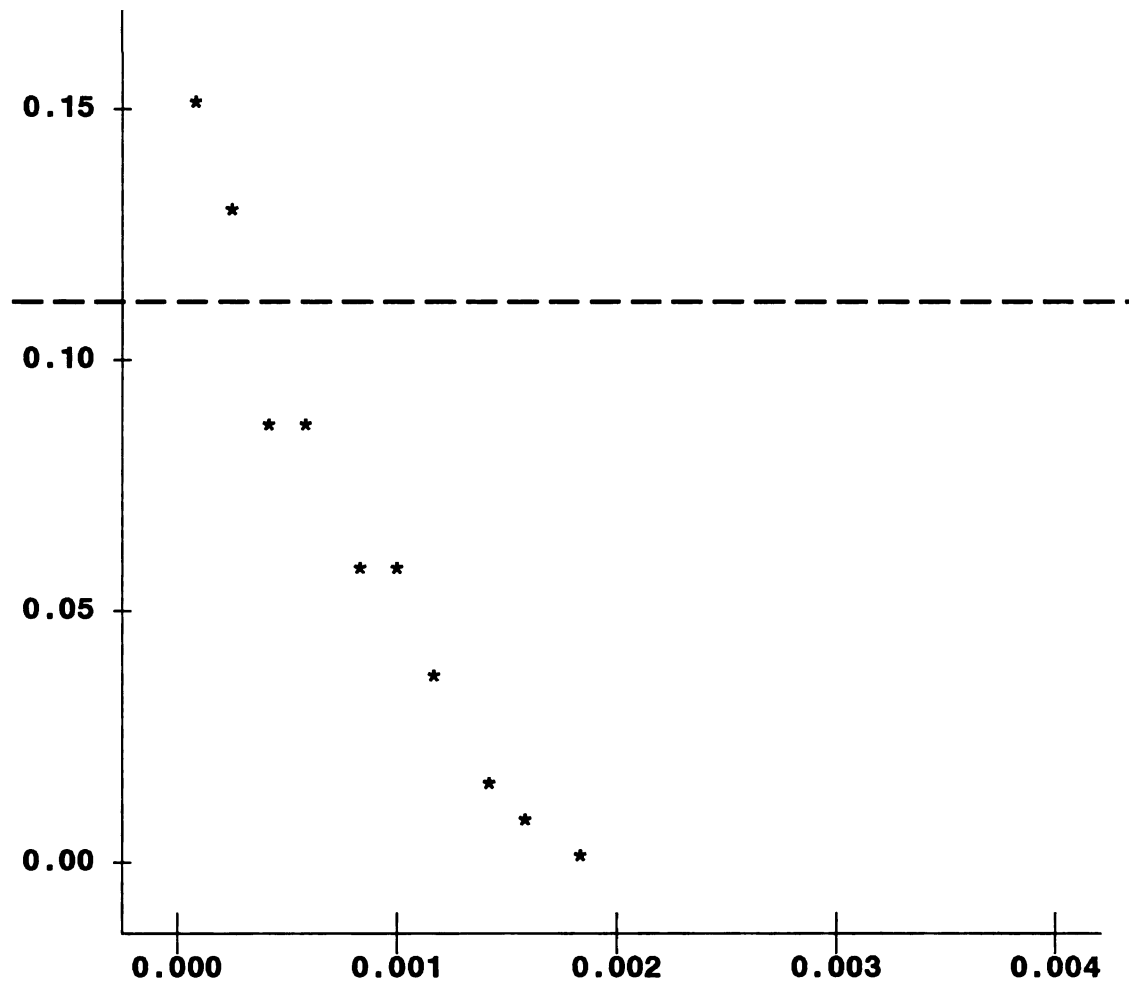
Figure 3.32C. Significant cross-correlogram for time 3. The x-axis shows the distance in decimal degrees at which the pairs are spatially correlated. The y-axis shows the r value, the coefficient of correlation. The significant $r = 0.1069$ is represented by the dashed line. Graph compares the spatial correlation between questing nymphs and conifers. They are spatially correlated at 0.0002 decimal degrees.
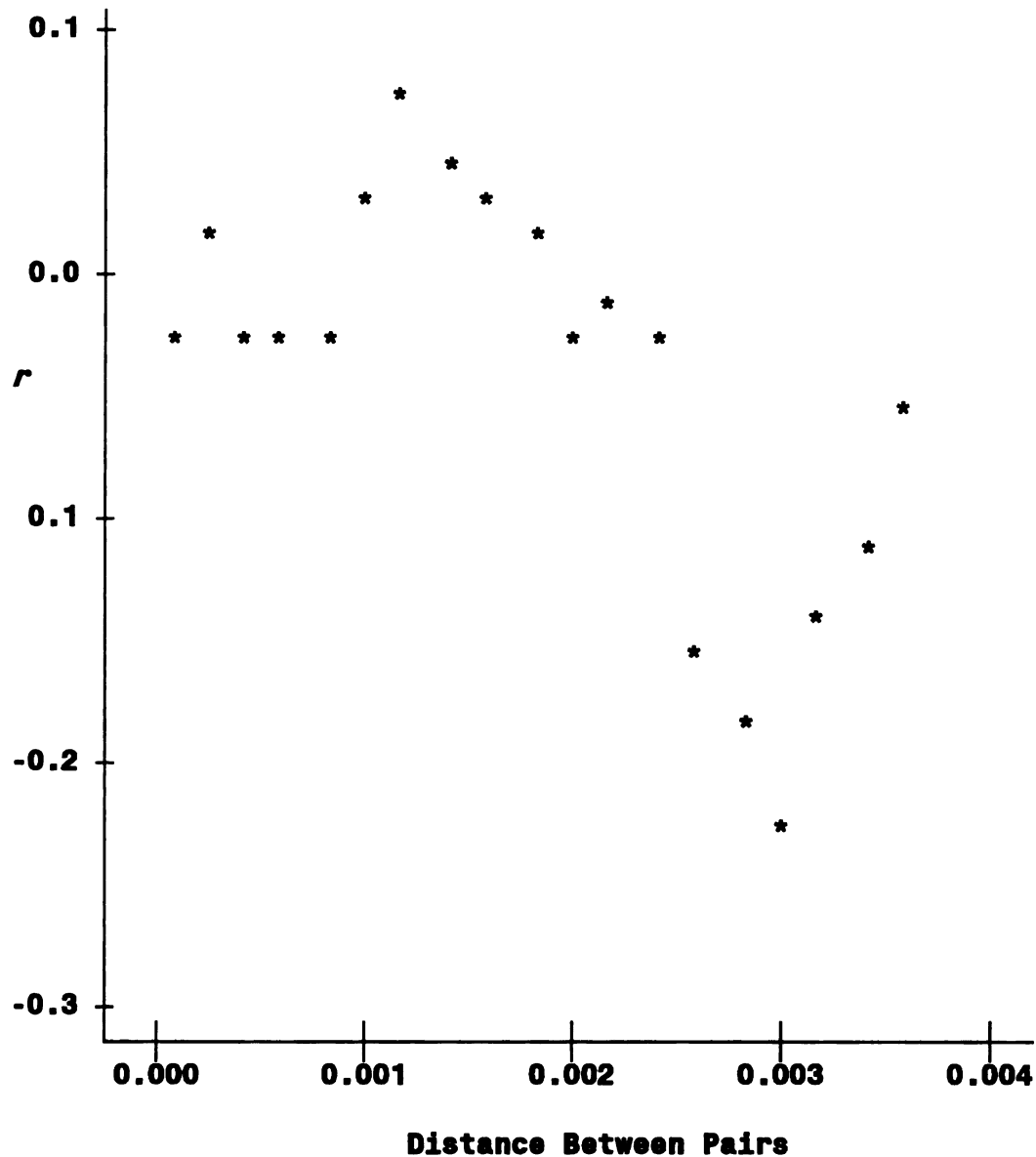
Figure 3.33. Cross-correlogram for spatial correlation between deciduous trees and total ticks on mice at time 3. Significant r = 0.1069, and all values are below that level. Thus, there is no spatial correlation at any distance.

The remaining comparisons were not spatially correlated. An example of a non-significant cross correlogram is shown in Figure 3.33, with all values below the significant r value of 0.1069. Thus, there is no spatial correlation at any distance. Non-

135

significant correlograms included those with individual values that were above the significant *r* value, but lacked a trend in the data points and demonstrated a scattered 'cloud' of points where there were points at the same distances where some were above the level of significance and some were below. Distances at which comparisons were significant are listed in meters in Table 3.8.

Table 3.8. Distances at which pairs of data were spatially correlated, for significant associations only. Units listed are meters. Figure column listed figure where cross-correlogram can be seen.

Factor 1	Factor 2	Figure	Distance (m)
Number of mice	conifers	3.32B	352 – 377
Number of infected mice	conifers	3.30A	44 – 300
Total ticks on mice	conifers	3.32A	311 – 377
Questing larvae	deciduous trees	3.31A	200 – 222
	conifers	3.31B	200 – 266
Questing nymphs	conifers	3.32C	22
Infected questing nymphs	conifers	3.30B	231 – 275

Distances at which correlations were significant ranged from 22 m to 377 m. Conifers were involved in 6 of the associations and deciduous trees in one. Questing larvae and questing nymphs were correlated to vegetation variables as were ticks on mice. Mice themselves were not spatially correlated to any other factor.

Significant associations were further examined using a cross-variogram, for the purpose of model building and the ability to make predictions of a dependent variable based on the value of another. This method will allow a model to be developed and thus, be able to get a prediction when only one variable of interest is available later on. All pairs with significant cross-correlograms (Table 3.7, Table 3.8, Figures 3.30A to 3.32C) were further examined by cross-variogram.

136

Only four of these showed significant spatial autocorrelation according to the cross-variograms. (Figure 3.33A thru 3.33D). No significant spatial regression equations were produced from the datasets.

CHAPTER 4

DISCUSSION

Summary

The aim of this project was to examine the phenomenon of aggregation in the parasites of the endemic Lyme disease system in Menominee County, and speculate how this aggregation and spread of the parasites through time and space might contribute to the maintenance of such a disease cycle. Furthermore, I was able to look at the question of aggregation in a spatially explicit manner. Through this research I have gained insights and answers to the following questions.

- Is aggregation occurring in the parasite populations of Menominee County's endemic Lyme disease system?

All parasite population datasets did indeed show aggregation. Spirochetes in ticks, ticks on mice and spirochetes in mice all handily exceed the cutoff value that indicates aggregation for each of the metrics with which they were measured.

- If aggregation is occurring, do habitat factors contribute to this aggregation?

Multiple factors were examined as potential contributors to the aggregation of the system in addition to being potentially aggregated themselves. These were deciduous trees, coniferous trees, understory coverage, the number of mice, the number of mice infected with *B. burgdorferi*, the antibody response of mice to *B. burgdorferi*, the number of spirochetes in the mice, the number of larvae on the mice, the number of infected larvae on the mice, the number of spirochetes in the infected larvae on the mice, the

number of nymphs on the mice, the number of infected nymphs on the mice, the number of spirochetes in the infected nymphs on the mice, the total number of ticks on the mice, the number of questing larvae, the number of questing nymphs, the number of infected questing nymphs, the number of spirochetes in the infected questing nymphs and the total number of questing ticks. These factors were examined spatially to determine relationships in space between these variables. However, coniferous trees were most often significantly spatially autocorrelated with other populations.

- Are any of these factors spatially correlated, and what are the possible explanations for this spatial correlation?

The examined pairs of data are listed in Table 3.7, and significant correlograms which indicate spatial correlation between variables are shown in Figure 3.30A through Figure 3.32C. In six of these seven significant associations, conifers were spatially correlated to questing larvae, questing nymphs, infected questing nymphs, total ticks on mice, number of mice and number of infected mice.

Since both larval and nymphal ticks are dispersed by their hosts, it appears as though the hosts have a preference for the coniferous trees, producing these positive associations with these other populations. It makes sense biologically, and for the transmission of the pathogen, that both the vector species and the host species frequent the same places. This data show that the infected and uninfected tick vectors and the mouse hosts are both found in association with coniferous trees.

Crucial to the Lyme disease cycle is the interaction between infected ticks and naive hosts, to create more infected hosts, and the interaction between infected hosts and

naïve vectors, to create more infected vectors. This indicates that the spatial nature of this ecological disease process is critical for its perpetuation.

Discussion

The three grids were rotated through in order to serve as replicates. Indeed, the trends within time periods are more similar than the trends within a single grid, suggesting that seasonality is one of the strongest factors influencing the activity and thus, the ecology and aggregation of the organisms in the system.

Ecological interactions are often dictated by abiotic factors. To say a system seasonally driven means that a combination of sunlight availability, temperature, air moisture, precipitation and other factors are cues to the organisms in the system to begin activity. That activity consists of different things for different classes of organism. Trees, for example, will begin to grow buds and leaf out as response to sunlight and temperature cues. Mice come out of hibernation and mate when the seasons change from winter to spring. Ticks, in response to the right temperature and moisture conditions also become active in the spring and begin to host-seek. The activities change as the seasons progress and the abiotic conditions alter.

For ticks, those levels of activity can be tracked by phenology curves. As shown with the phenology curve for questing ticks at the study site (Figure 3.1), each lifestage of the tick has a slightly different time at which its activity peaks. The measured activity in this case is host-seeking behavior. A drop in activity occurs as more and more of those ticks find hosts and take a bloodmeal or die off. This removes ticks from the cohort of

host-seekers, and eventually, as all the ticks find a bloodmeal, there are no more left to detect in the environment as the measured activity of those ticks has stopped occurring.

Each parasite dataset shows aggregation. Spirochetes in ticks, ticks on mice and spirochetes in mice all demonstrate aggregation according to the variance to mean ratios, the 'k' statistic and Lloyd's mean crowding index for those populations (Table 3.4). This holds true whether the groups are lumped by time period or separated by grid.

However, I found LMC no more useful to use than any other measure of aggregation such as the variance to mean ratio or the 'k' parameter of the NBD. In fact, it tracks fairly closely with the variance to mean ratio in value for all sample populations in this project (Table 3.4). It is perhaps important to have the 'parasite's perspective'. Looking at this measure for highly aggregated populations may eventually reveal a limit or a threshold at which the parasites no longer tolerate the crowding and at which their fitness is decreased.

I had predicted an upper asymptotic threshold for *B. burgdorferi* spirochete load in *I. scapularis*. The upper asymptotic threshold was predicted because the physical space inside the tick for these bacteria is limited. This number is hypothesized by Wang (2003) to be above 200,000 but the exact figure is not known. In this dataset, the highest spirochete burden was 103,429 spirochetes, and was found in a questing, adult male *I. scapularis*.

For most of the analyses, the dataset consisted of only *I. scapularis* species ticks. However, in order to understand what effect multi-species parasitism has on the small mammal population and whether aggregation patterns change when multiple species are examined, I looked at both *I. scapularis* and *Dermacentor variabilis* nymphs together for

a kernel density and Moran's Index analysis. When both species of nymphal tick are analyzed together, the pattern of clustering is not evident (Table 3.4, Figure 3.25, Figure 3.26).

The study was conducted as such a scale that no differences were detected between areas of the property in terms of disease risk. Further, areas of aggregation identified were just that- the areas identified. Certainly there were areas where aggregation was occurring, but not identified because those places were not sampled on that date or that particular area may have been missed. No clear area of constant tick and mouse host aggregation was identified.

The data do indicate that on a larger scale, areas that are preferred by hosts such as white-tailed deer, mice and ticks will be the areas where patterns of aggregation are seen. If an area is preferred, populations of these organisms will be higher. These data show that the higher the population size, the better the chance for aggregation (Figure 3.17 and Figure 3.18). If hosts are frequenting an area, there may be many engorged larvae there that fell off their host in that spot, contributing to next year's infected nymphs. If the area remains favorable, the hosts will visit it again the following season and then have the opportunity to pick up those infected nymphs. Aggregation effectively increases the chance of a vector infecting more vectors. If a tick with a high spirochete burden feeds on a mouse that is also feeding many larvae, or will feed many larvae, that tick has a better chance of spreading the spirochetes than one with a low load. If only a few spirochetes are passed to a host, it may be that none can survive since there are too few to override the host's immune system.

Infection appears to be additive by life stage (Figure 3.3A), where very few, if any larvae are infected, then up to a third of nymphs are infected and over half of adults are infected. The previously described aggregation scenario could contribute to this as each tick picks up more spirochetes with each bloodmeal, and since they have three chances to become infected by the time they are adults.

Perhaps this is a manifestation of parasite dilution where one species of parasite subsumes space that the other might use. If a host is located by an *I. scapularis* nymph, but is already loaded with feeding *D. variabilis* ticks, there is less space for the *I. scapularis* tick to feed, and vice versa. In this case, if *D. variabilis* ticks, (which are non-competent vectors for *B. burgdorferi* (Piesman and Happ 1997),) are taking feeding space away from potentially infected *I. scapularis* ticks, they may serve to dilute the effect of disease transmission from the competent vector. However, the effect of feeding *D. variabilis* ticks did not seem to prevent the aggregation and feeding of *I. scapularis* ticks, since that population was strongly aggregated. Since there was no control area where *D. variabilis* ticks were not present and feeding, it is not possible at this time to determine what specific effects those ticks had on the aggregation response of *I. scapularis*.

There are multiple potential effects that aggregation may have on *B. burgdorferi* transmission dynamics. First, there is the establishment of the pathogen in a foreign geographic area. It is possible that aggregation may help increase the rate of spread in a new area, whereby only a few hosts need to be highly infected in order to efficiently infect more naïve vectors. The second potential effect is the maintenance of the disease cycle in that newly established area. Although a definitive link cannot be proven, this

143

system appears to be a deeply entrenched ecologically-based disease system in tandem with multiple levels of highly aggregated parasites.

The examined factor that emerged as having the most spatial autocorrelation was the most stationary, the vegetation. Spatial spread of plants is determined by exogenous processes, such as water availability and soil type (Fortin and Dale 2005). The response of the spatial structure of trees is influenced by exogenous variables whose spatial autocorrelation is what drives the spatial structure of the tree species. Thus, trees are not considered to have an independent spatial structure, and instead it is considered that their spatial structure is a reflection of the other factors their growth relies on, such as bedrock, soil and water. These assumptions were also held for the understory vegetation. The vegetation exhibited no movement in the time frame of the project and thus the nature of these variables (understory, deciduous trees and coniferous trees) is entirely stationary. One measurement was taken for the vegetation during the first time period and then used in the analysis for that grid for the remaining time periods. Vegetation may be aggregated by type due to the exogenous factors of an area and that aggregation may exert some pressure on the spatial structure of the hosts that require a particular species or habitat type for food and shelter.

The next least mobile of the examined variables were the questing larval blacklegged ticks. Since larval ticks hatch in a clutch of eggs, and a clutch may number in the hundreds or thousands (Main et al. 1982), they begin their lives aggregated. Where the eggs are placed is a function of where the mother tick has laid them. The mother tick lays her eggs in the spot she drops off her final host- likely a white-tailed deer (*Odocoileus virginianus*), where she has blood-fed and presumably mated with a male.

Engorged with blood and now carrying fertilization for her eggs, she drops off the deer wherever the deer happens to be. Due to her engorged state, she does not have the use of her legs, and must wait to digest the meal and produce the eggs she lays in that very spot. Thus, to travel back on the chain of events, the eggs are laid where the deer come to rest. Deer, like other mammals, prefer and rely on certain habitat types and cover- and this habitat preference is largely based on vegetation (MDNR 1999).

Once the eggs hatch, the larval ticks cannot move far from that spot when they begin to host-seek, and rarely move farther than 3 m away (Daniels and Fish 1990). Any small host that encounters this clutch of newly hatched ticks will likely be parasitized by multiple ticks. Another host that does not encounter a larval clutch may escape larval parasitism altogether. This provides the set-up for a highly aggregated system. If a mouse that encounters the ticks is already infected with *B. burgdorferi* from a previous parasitism event with an infected nymph, then most of the naïve larvae that feed on that mouse will also become infected (LoGiudice et al. 2003). If the larvae feed on an uninfected host, then they will also remain uninfected, and maintain that status until they become nymphs. Since blacklegged ticks feed only once per lifestage, and only feed on our host of interest, the mouse, at most twice in a lifetime (as a larvae and then again as a nymph), if a larval tick does not pick up the *B. burgdorferi* pathogen on its first go-round, it will not be able to spread that infection at its nymphal feeding.

Even if a tick becomes infected as a nymph by feeding on a mouse, it is essentially no longer playing a role in the maintenance of Lyme disease in the environment. Since many adult ticks feed on white-tailed deer, and the deer are capable of clearing the pathogen from their system, that tick is not contributing to any more

infected hosts. However, the infected nymphs play an important role when we look at cases of Lyme disease in humans. Infected nymphs are implicated in most cases of Lyme disease, due to their small size and ability to be easily overlooked for 2 to 3 days while feeding on a human. Thus, although the infected nymphs are not contributing back into the LD cycle when they feed on a human (who are dead-end hosts for the pathogen, since infected humans will not usually be fed on by additional uninfected ticks while spirochetemic) the pathogen will cause cases of LD in the human population of the endemic area.

Nymphs are any more mobile than larvae. Nymphs of the *Ixodes ricinus* species have been documented to move only about 1 m (Gray 1985). Although they may be able to climb up on vegetation in order to obtain a better position to find a host, nymphs rarely move more than 2 m (Falco 1987). It is assumed that they do not go far from the place where they dropped off as an engorged larva after a bloodmeal. They are dispersed by hosts and less aggregated in the environment than larvae (Madhav et al. 2004).

Adult ticks do not feed on mouse hosts, and although they were picked up on drag cloths, they do not contribute to the maintenance of the cycle in the small mammal hosts, except that they are able to reproduce and then generate the next cohort of blacklegged ticks. Even if the mother tick is infected with *B. burgdorferi*, her offspring will not be, as *B. burgdorferi* is not passed transovarially.

These results support the current knowledge of how larval and nymphal *I. scapularis* ticks are clustered and dispersed. Larvae and nymphs both showed high levels of aggregation, and were both considered clustered by Moran's Index criteria (Table 3.5). Further, larvae and nymphs did have a similar spatial structure, as they were often both

associated with the same hosts (Figure 3.5). Again, this is critical for the transmission and maintenance of the disease cycle because it allows the interaction of both naïve and infected hosts and vectors.

Table 3.5 and Figure 3.25 show ticks cluster spatially based on both lifestage and species. The larval clustering may be due to mammals moving through a recently hatched clutch of eggs. Larval ticks do not have the ability to move very far on their own, and emerge together in a synchronous fashion. Nymphal ticks were mapped using kernel density, and demonstrate a clustered pattern by lifestage and species as well (Figure 3.26).

In order to determine spatial correlation between measured variables in order to infer that these variables are indeed related spatially, 27 comparisons were made for each of 3 trap periods, for a total of 81. These comparisons are listed in Table 3.7. Distances at which pairs were significantly correlated are listed in Table 3.8.

The correlograms for significant associations are shown in Figure 3.30A through Figure 3.32C. Conifers were the most associated factor, making up half of six pairs of data. Coniferous trees were spatially correlated with number of mice, number of infected mice, total ticks on mice, questing larvae, questing nymphs and infected questing nymphs. Each of these pairs were significant at only one time period.

The data show that larvae were spatially correlated with conifers upwards of dozens of meters, but typically only travel a maximum of 3 m (Daniels and Fish 1990). This suggests that the larvae are where they are not because of their own preference, but because of where the mother tick laid the eggs where the tick dropped off the deer. Deer do prefer habitat with plentiful edible cedar browse and cover, and prefer to bed down for

the night in areas where cover is thickest (MDNR 1999). Thus, their preferences may belie where the larval ticks end up questing.

The closest association was between questing nymphs and conifers; these are spatially correlated at 22 m, at time 3. Questing larvae were also associated with conifers; this may not be surprising given the preference of white-tailed deer in Michigan to prefer swampy and coniferous habitat (MDNR 1999). This makes sense in light of the earlier assumption that white-tailed deer are actually responsible for the dispersal of larvae, and larvae quest from the same spot they hatch.

Deciduous trees were spatially correlated in only one of the pairs, in this case, with questing larvae. Since the cover of deciduous trees was fairly even, and most points had at least one deciduous tree, it is reasonable that there was no 'effect' detected. The 'variable' of deciduous trees was almost a 'constant' in this study because of its ubiquity. Of 240 trap points, only 19, or only 7.9% of trap points did not have a deciduous tree within 6 m of the point. In other words, 92.1% of trap points had at least 1 deciduous tree with 6 m.

The study system is an endemic Lyme disease system in Menominee County in Michigan's Upper Peninsula. There is thought to have been an established transmission cycle and blacklegged tick population there since the 1980's, the evidence for which was the number of Lyme disease cases in humans reported from the area at that time. The first confirmed case in Michigan was from Menominee County in 1985 (MG Stobierski, personal communication). Studies confirmed the presence of the vector population later on (Strand et al. 1992).

In Menominee County, the density of infected nymphs (epidemiologically the most important life stage of the tick) is about 6 per 1000 m^2 (county-wide average), similar to other endemic areas in the Northeast, such as Westchester County, where the density of infected nymphs is approximately 8 infected nymphs per 1000 m^2 (Diuk-Wasser et al. 2006). The LD case rate of Menominee County, about 50 people per 100,000 per year, is similar to Westchester County New York which also has about 50 cases per 100,000 per year (New York State Department of Health 2005).

Although much of what we have learned about this disease cycle agrees with what is understood about the cycle in other endemic areas of the US, there are still some notable differences. First, the habitat structure in Menominee County is different. In the northeast, the preferred habitat type for the hosts of *I. scapularis* is oak or maple-dominated forest with sandy soil (Ostfeld et al. 1996) and this habitat type is widespread in that area. Furthermore, in the northeast, increased understory has been associated with the small mammal hosts of *I. scapularis* (Prusinski 2006).

In Menominee County, we primarily observed lowland cedar swamp, interspersed by farmland. The study site was most similar to the northeast sites in that it was maple and oak dominated with no standing water and sandy soil. However, the majority of the county is either cedar swamp or farmland. Since *I. scapularis* cannot survive in standing water, which is common in swampy lowland areas, these areas do not seem to be suitable habitat. However, drag-sampling to assess the presence of blacklegged ticks in this habitat type was still successful and *I. scapularis* specimens of all life stages were recovered.

Secondly, the phenology of the tick's life stage in Menominee is different from what is observed in the northeastern US. In the northeast, the adults have a peak of host-seeking activity in the spring and again in the fall, but the fall peak tends to be larger. Further, the nymphs are out feeding in spring and early summer, followed by the larvae throughout the summer (Fish 1995). This set up seems to be ideal for allowing infected nymphs to transmit the pathogen to as many hosts as possible before the naïve larvae come out to feed, increasing a larva's chances of picking up *B. burgdorferi*.

Conifers were the factor most frequently positively associated with other populations. The distances at which these pairs were correlated are listed in Table 3.8. Presumably, nymphal ticks are dispersed on the landscape by vertebrate hosts (Madhav et al. 2004). Nymphal ticks are not constrained by hatch site as are the larvae, and hence their clustering may have more to do with their fitness and host factors such as habitat preference.

Even though conifers were positively associated with the presence of the tick and its mouse hosts, this statement cannot be applied to all areas of Menominee County. Given that Menominee County is largely swampy, it is surprising to see that these ticks thrive here. Typically associated with higher and drier areas in the Midwest (Guerra et al. 2002), the ticks are clearly surviving and having an impact in Menominee. So, what is it about this place that makes it so ideal for this tick and pathogen? Perhaps it is the interspersion of farmland and forest creating forest fragments where deer and mice thrive without the presence of many of their predators. This is one of the reasons posited for the thriving populations of *I. scapularis* and *B. burgdorferi* in northeastern US habitats (Allen et al. 2000, Ostfeld and Keesing 2000). These forest fragments may be too small

for the predators of these animals to live, so the populations of white-tailed deer and white-footed mice are allowed to grow relatively unchecked. These hosts are ideal for the survival of *I. scapularis* ticks and *B. burgdorferi*, so the disease cycle is maintained.

The study site was a mix of hardwood and conifers, and is located near a river but with sandy soil. It may be the mix of oak and maple in the drier areas combined with hemlocks and cedar in the wetter areas to provide both the habitat that the deer prefer with plenty of cedar browse, with the habitat the ticks prefer, with dry, sandy soils.

In Menominee, the lowland cedar swamps certainly do house ticks, but because of the frequent standing water in these areas, they are not ideal habitat for *I. scapularis*. These areas may actually be limiting where the ticks can survive, and perhaps help explain why Lyme disease has not spread far beyond Menominee County's borders in the past 30 years.

Closer examination of the data reveals additional deviations from Lyme disease cycle patterns in the northeastern US. In Michigan, a different pattern in the phenology of the life stages has been observed in this data and others (Walker and Hamer, personal communications). First, the bi-modal adult peak does exist, but the spring peak seems larger than the fall peak. Additionally, the nymphs and larvae are out feeding at around the same time; there is not a large nymphal peak preceding the larval peak (Figure 3.1).

The data were analyzed to see if it fit the 20/80 distribution described in the literature (Woolhouse et al. 1997) (i.e., if 20% of the ticks account for 80% of the infections). In order to see if this could hold true for this dataset, the number of questing ticks in the upper 20% of spirochete burden was calculated. Ticks off hosts were not used because of the confounding factor that we are unable to know if a tick was infected

on this host or a previous host. The number that comprised 80% of infected mouse hosts was also calculated. In this scenario, we only use nymphs, since they are the only life stage capable of infecting a mouse host.

Our drag-sample size of nymphs from the 3 grids was low, only 36 individuals, and the upper 20% infected was only 7 nymphs. It is not then possible for that small number of nymphs to infect 80% of our mouse population, which are approximately 121 animals if each tick takes only one bloodmeal. Therefore, these data do not support the 20/80 hypothesis for ticks and infected mouse hosts. However, 22% of the nymphs do have spirochetes and spirochetes are aggregated in questing nymphs. Even though the data do not necessarily support this theory, it is important to note that we certainly did not detect all the questing nymphs. However, we can use this data to make a prediction. Based on the rate of infectivity of questing nymphs (22%), if a mouse had 5 nymphs feeding on it, we could predict that at least one of those ticks was positive and thus, the mouse would also become infected with *B. burgdorferi*.

Other studies documenting aggregation of *B. burgdorferi* and *I. scapularis* have not measured aggregation of *B. burgdorferi* in the vertebrate host. To our knowledge, this is the first study that does. That said, it is important to acknowledge that that particular quantification aspect poses potential problems. Since quantification was done on an ear tissue biopsy sample from the animal, it represents only a small portion of the total animal, but is not a representation of the total spirochete load in the animal.

Secondly, spirochete loads may not be evenly distributed throughout the vertebrate body; it is assumed that since most ticks will feed around the head and neck area where the blood vessels are close to the surface of the skin that taking a

representative sample from that area would be most appropriate; however, no 'control' samples were taken from other areas of the body and quantified by spirochete load. Further, if a mouse is newly infected, the spirochetes will still be circulating in the bloodstream and may not yet have had time to migrate to the skin (Hanincová 2008).

Additionally, it may be that the ELISA test was not the most sensitive or specific test that could have been run. The antigen used was sonicated whole-cell B31 *Borrelia burgdorferi*, specifically, a strain that produces a lot of OspC. The strain in circulates in all Lyme endemic areas, however, it may not be the prevalent circulating strain here in the Midwest. It may be that the antibodies produced by the mice here are not as specific to the OspC in this strain as they are to the strain or strains that infected them. This calls the sensitivity of the ELISA test into question, and it should be acknowledged that the positive antibody response prevalence could have been underestimated as a result.

In order to get around these limitations, mouse infection status was determined based on a combination of infected larvae pulled off of them, the number of spirochetes measured in their tissues and their antibody response to prior infection with *B. burgdorferi*.

Not all potential factors were examined with respect to the aggregated populations in the system. There may be some factors not examined in this study, such as immunological variables or grooming behavior, which may play a role in either promoting or deterring tick presence. Including these factors in future studies may provide more insight to this disease system's dynamics.

Conclusion

There is a delicate balance for parasites between aggregating and evenly dispersing. If they are too evenly dispersed, and each host gets only a few parasitic organisms, chances of survival of that parasite are not good if that number of parasites is overwhelmed by the host immune system. On the other extreme, if the parasites are highly overdispersed, they will be crowded into only a few hosts; that parasite burden may be too much for those hosts and the hosts instead may succumb to the infection. If the host is killed off too quickly to allow transmission of the parasite to a new host, the parasite has also lost out on an opportunity to propagate. However, this may not be the case for the LD system. Since the wildlife reservoirs never show evidence of disease even though they are infected, morbidity may not play a role. Instead, it could be the parasites that suffer, and too many in one host may limit their fitness and ability to find their way into a new tick vector.

It is assumed that the parasites in this system have achieved a balance. All of the parasite populations are aggregated, but not so aggregated that they have killed off their hosts before they can be passed on to other hosts. Further, the evidence for a balanced system is in the case rates of human disease which have stayed fairly constant in the past 20 years.

Several clear conclusions have come of this research. First, Menominee County has a unique, isolated endemic Lyme disease system. Aggregations of ticks and spirochetes are spatially associated and driven by habitat, especially proximity to coniferous trees. Some of these associations are surprising based on what we know about

154

other endemic LD systems, where oak-dominated habitats are the most suitable *I. scapularis* habitat (Glass et al. 1994).

Spatial work like this may allow predictions based on habitat type and aggregations of spirochetes, ticks and reservoir hosts to help predict risk. Ability to predict disease risk can lead to an increase in prevention and thus be used to target public health messages. For many emerging diseases, as well as invasive species, rarely are there baseline data against which to measure rates of spread. These data represent a current snapshot of Lyme disease cycle dynamics in Menominee County and provide data for future comparisons.

In order to target public health messages, it is important to be able to identify areas and populations of highest risk and then focus the efforts there. The predictions here that conifers positively predict the presence of infected questing nymphs in Menominee County could be an important one. Nymphs are the most epidemiologically important lifestage (Barbour and Fish 1993), and the habitat heterogeneity of the endemic county indicates that not all of the area is high-risk. Even infected mouse hosts are positively associated with these conifers, putting people at risk by exposing more naïve vectors to the pathogen. Therefore, the predictions made from the data may be information that can be used by agencies and citizens in the state to measure risk to companion animals, domestic animals and humans.

This research sheds light on areas of Menominee County where people should be especially vigilant about tick prophylaxis. Wooded areas of mixed oak-dominated sandy upland and low cedar swamp are perhaps the most dangerous for encountering an infected questing *I. scapularis* nymph. Aggregation, in combination with the spatial

distribution of the pathogen, vector and host organisms is the driver of this disease cycle in Menominee County. The ecological factors contributing to this system provide a deeply entrenched disease cycle that allows for its perpetuation. Avoidance of these high-risk habitats and other prophylactic behaviors such as tucking pants into socks, the use of acaricides and checking oneself for ticks regularly are the norm among Menominee County citizens. Without drastic changes to the ecosystem, it will not be possible to disrupt the disease cycle. Until our understanding of Lyme disease system dynamics increases even further, we should continue to emphasize vigilance in high-risk areas.
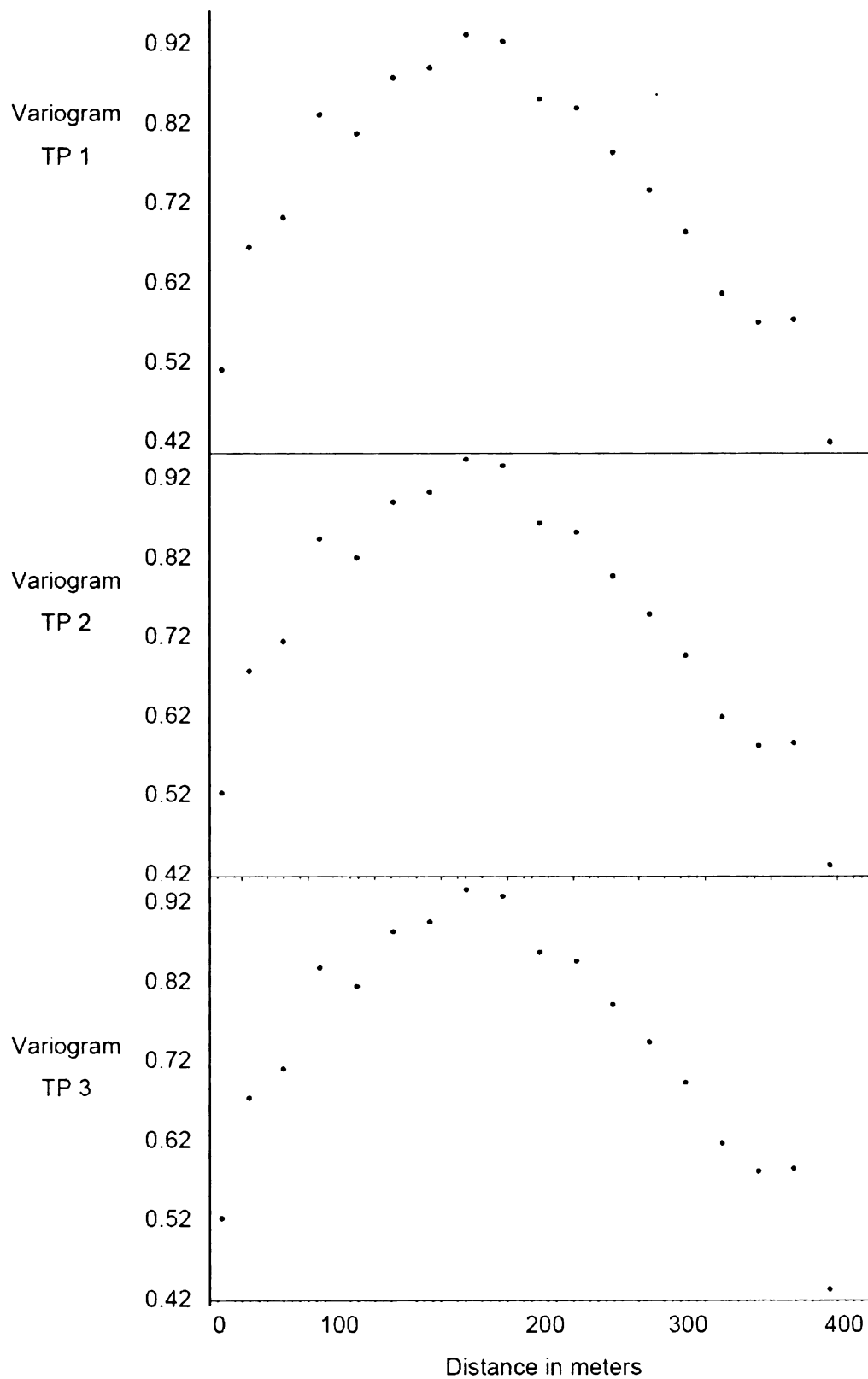
Figure A.1. Variograms for deciduous tree data for all trap periods. The variograms are the same because data was taken once and used for all 3 trap periods.
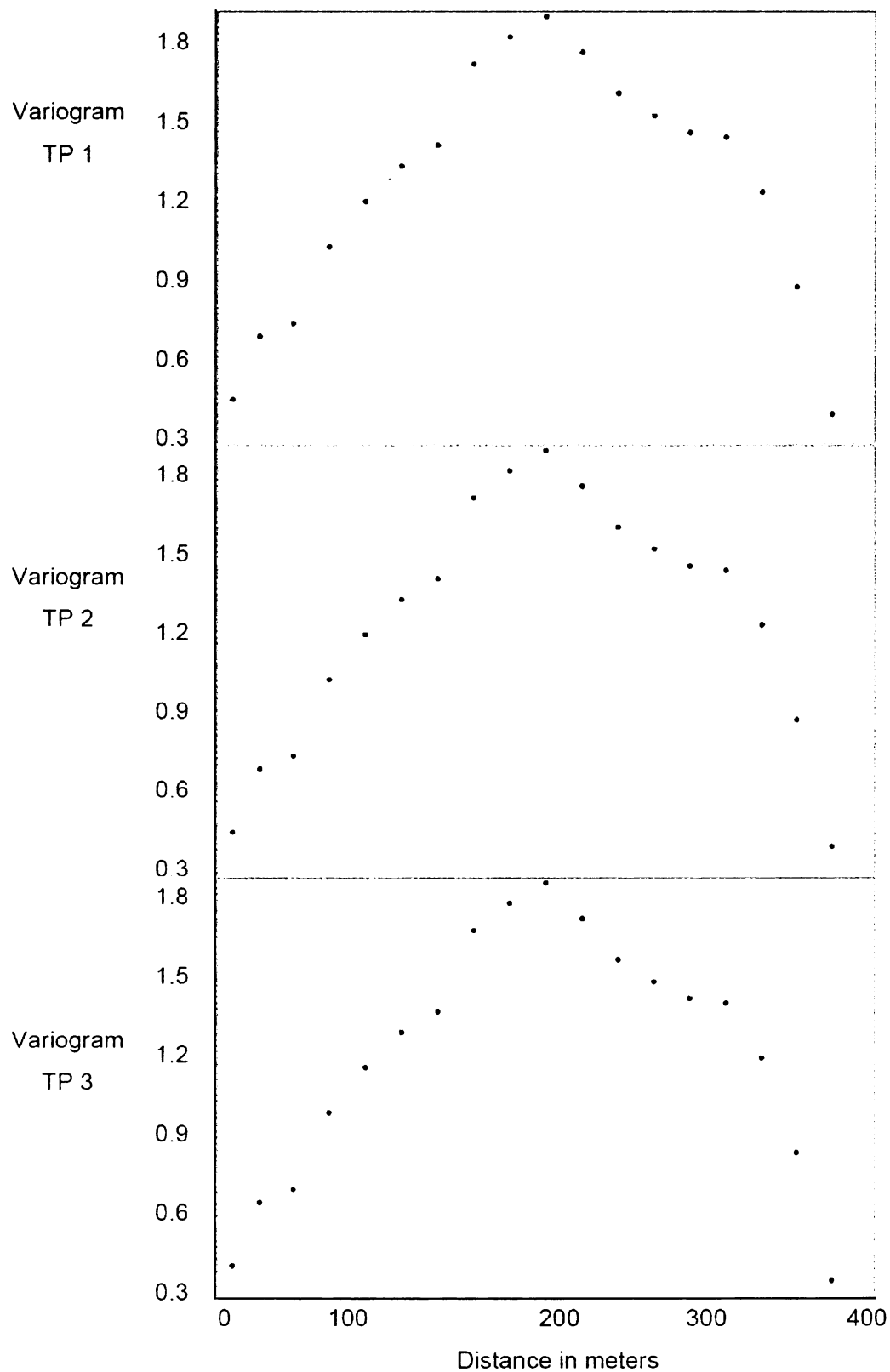
Figure A.2. Variograms for coniferous tree data for all trap periods. The variograms are the same because data was taken once and used for all 3 trap periods.
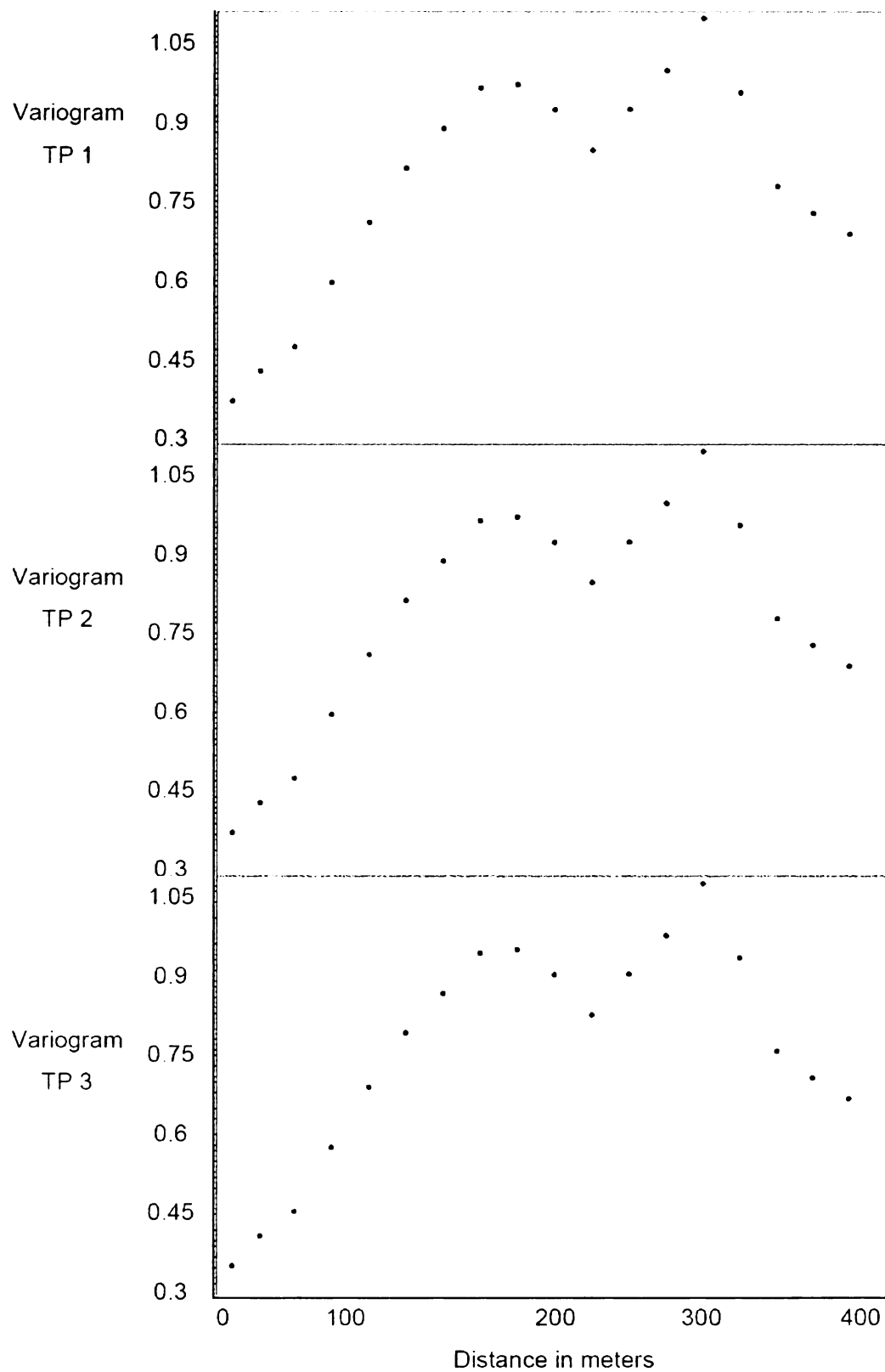
Figure A.3. Variograms for understory data for all trap periods. The variograms are the same because data was taken once and used for all 3 trap periods.
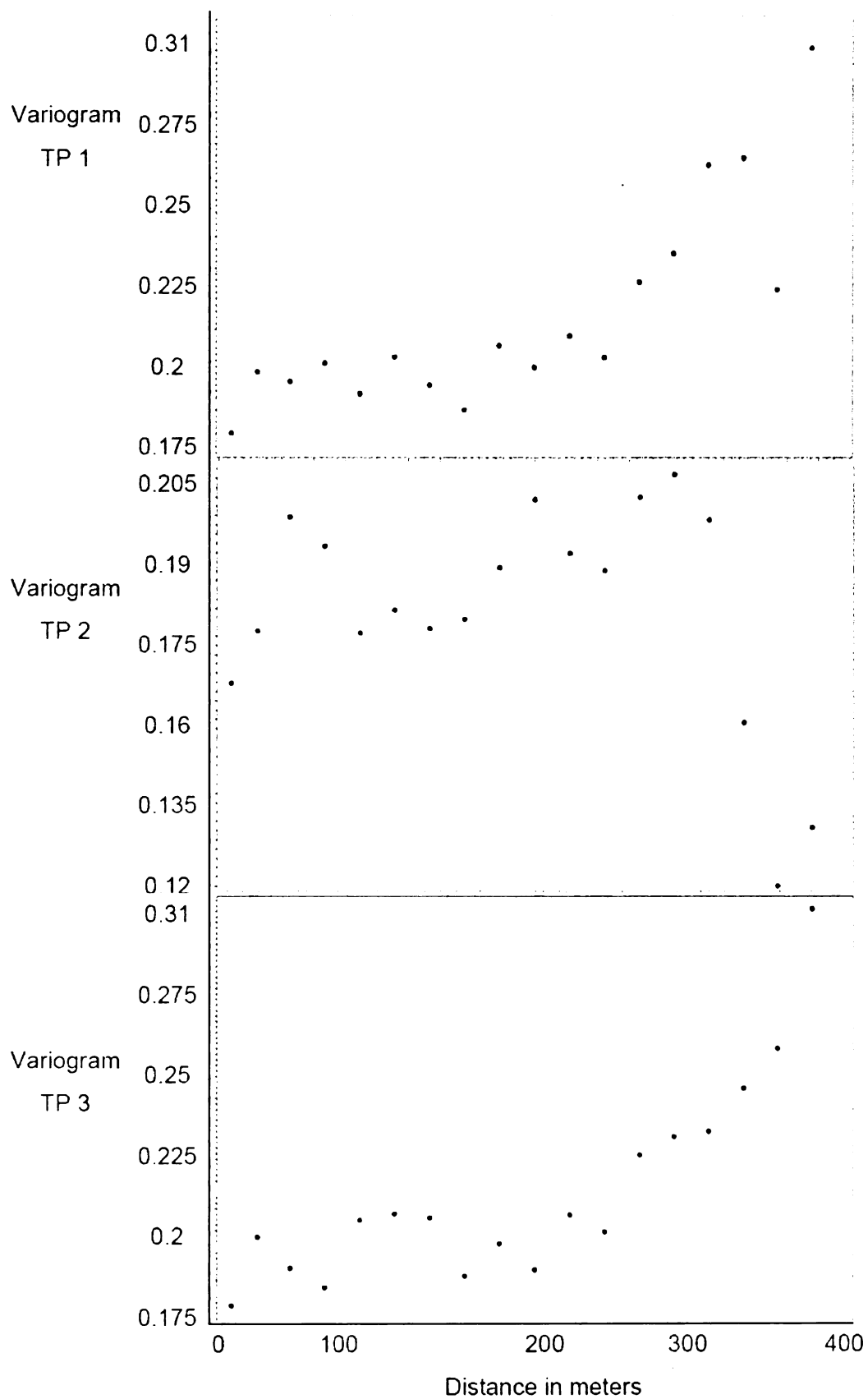
159

Figure A.4. Variograms for number of mice data for all trap periods.
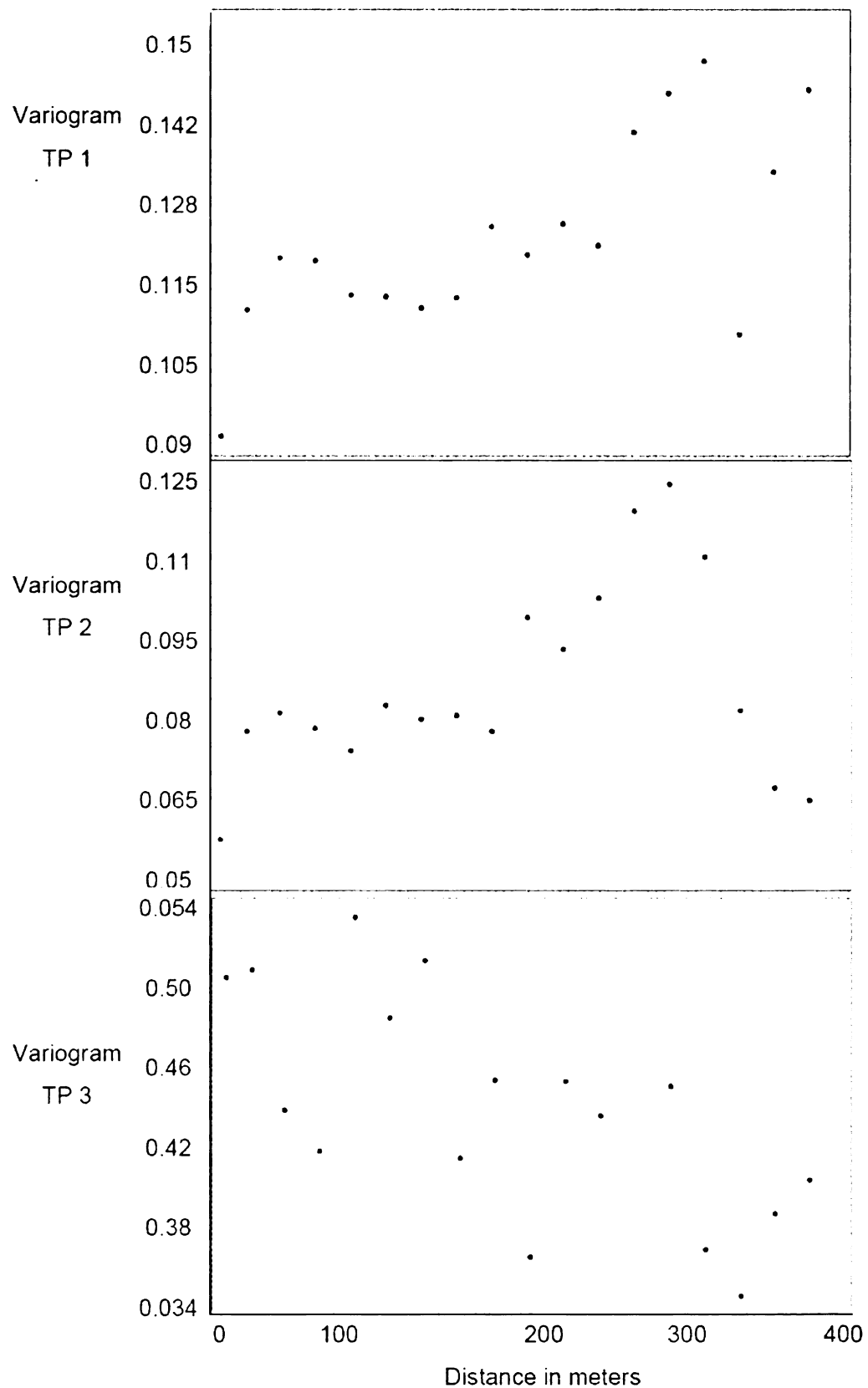
Figure A.5. Variograms for number of infected mice data for all trap periods.

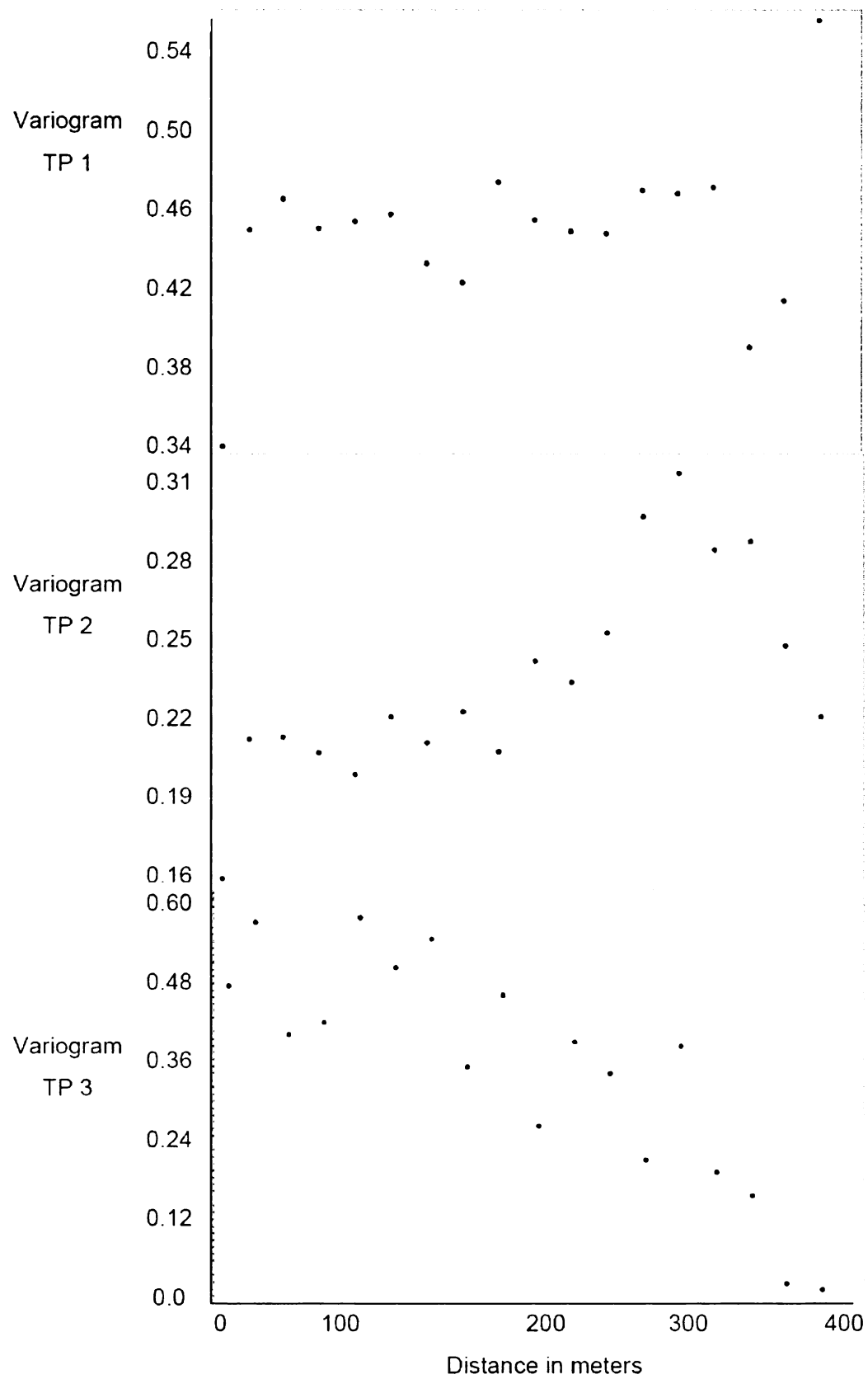**Figure A.6. Variograms for average adjusted OD values for all trap periods.**

162
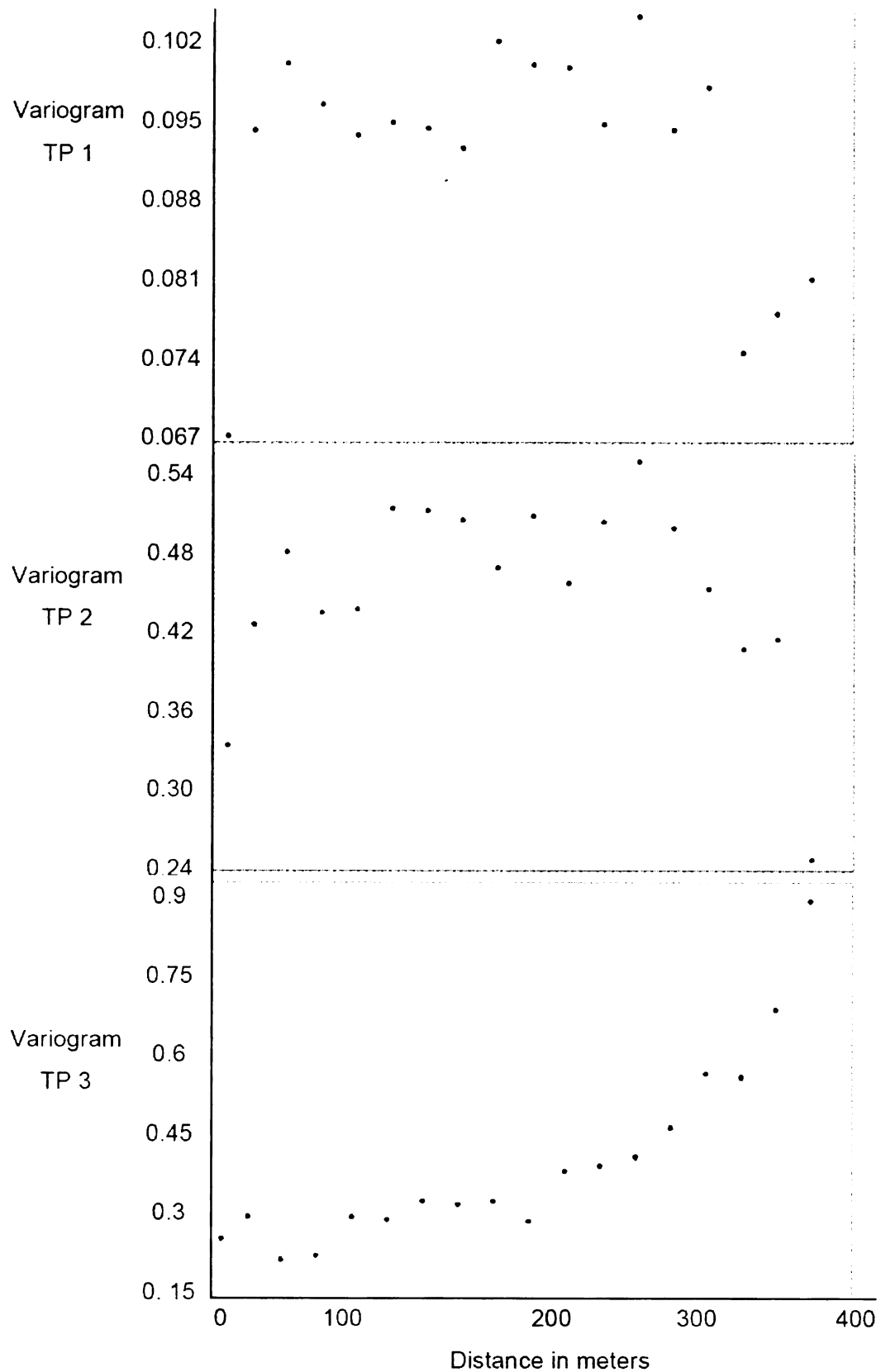
Figure A.7. Variograms for spirochetes in mice for all trap periods.

163
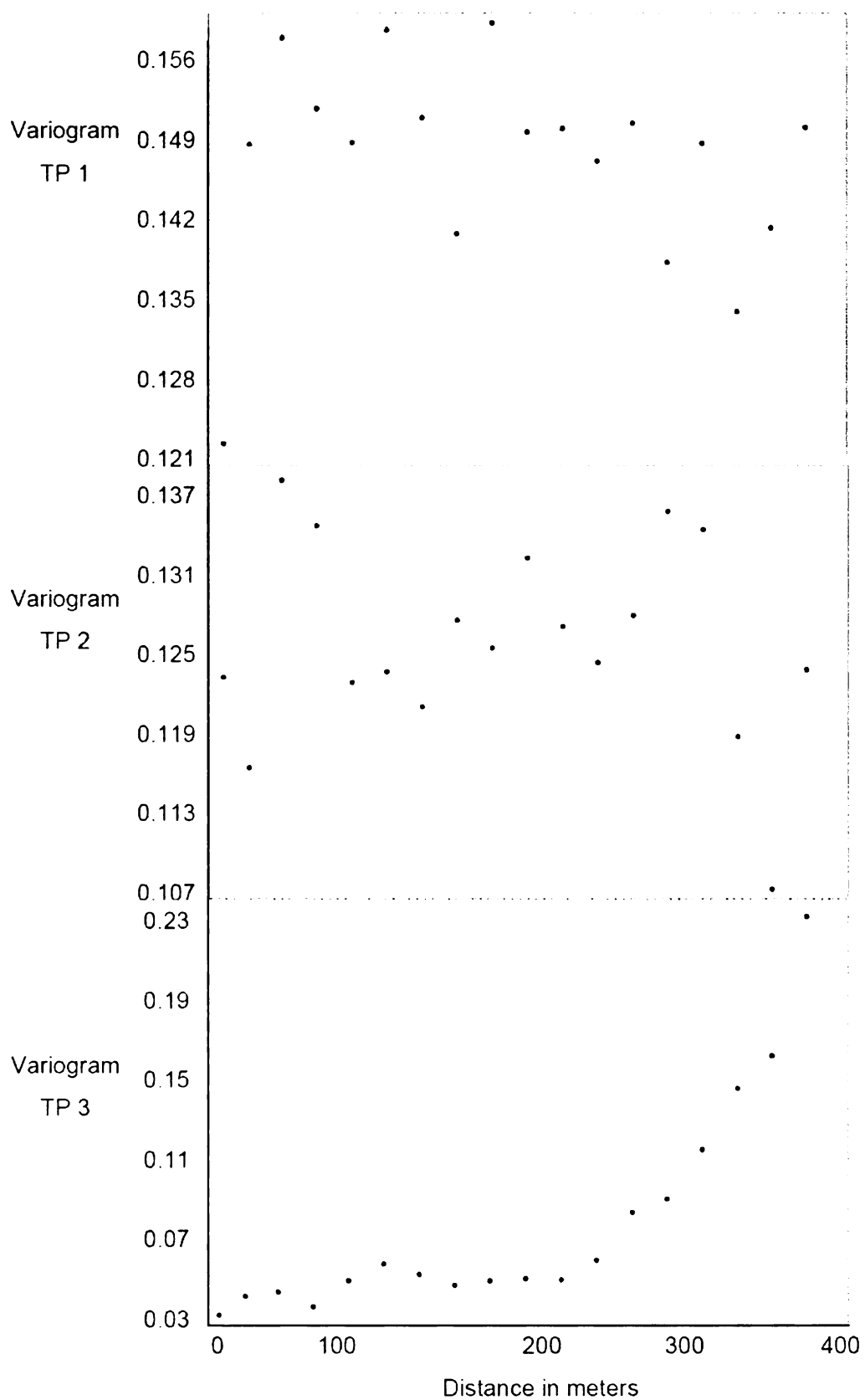
Figure A.8. Variograms for larvae on mice for all trap periods.

164
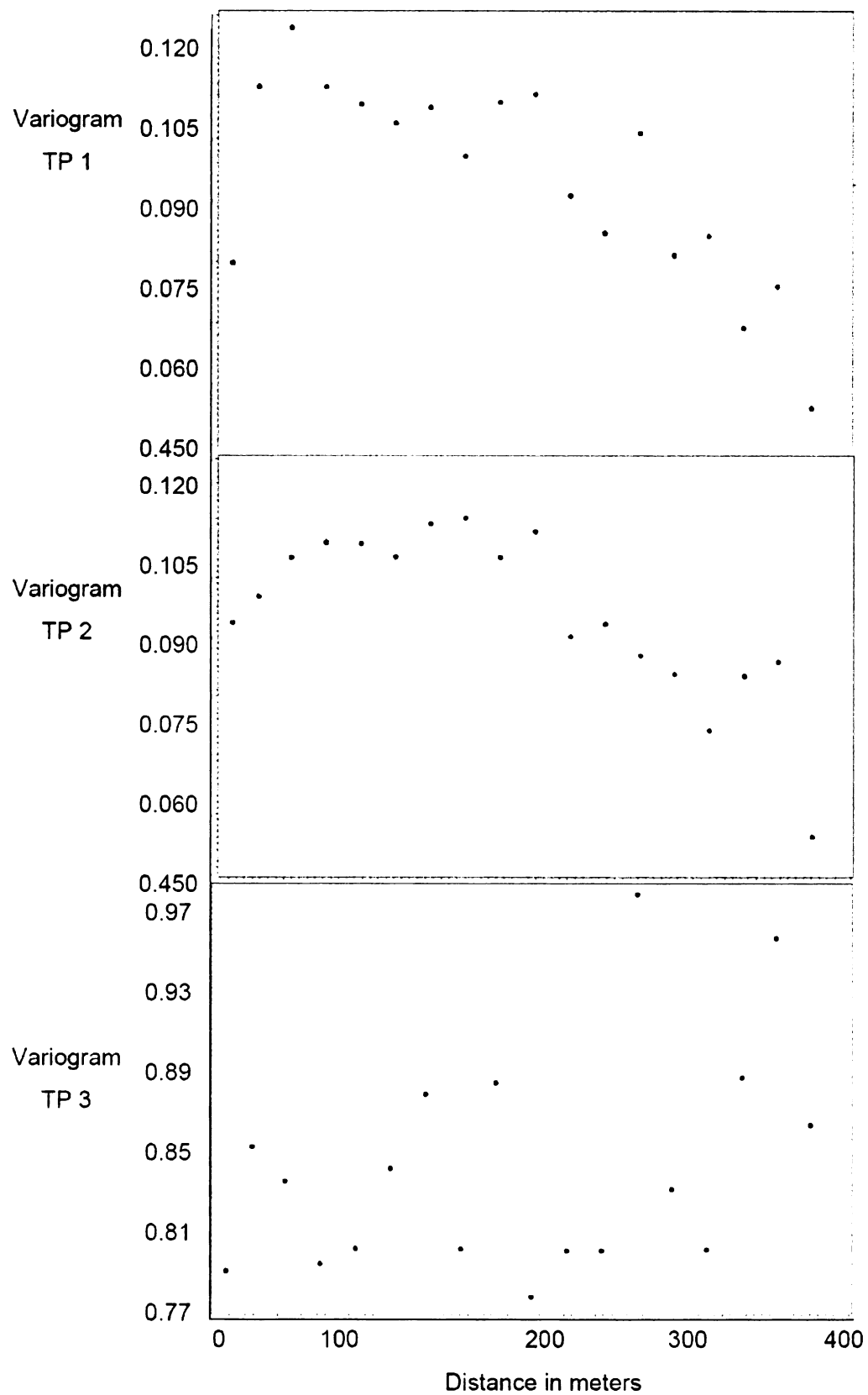
Figure A.9. Variograms for infected larvae on mice for all trap periods.
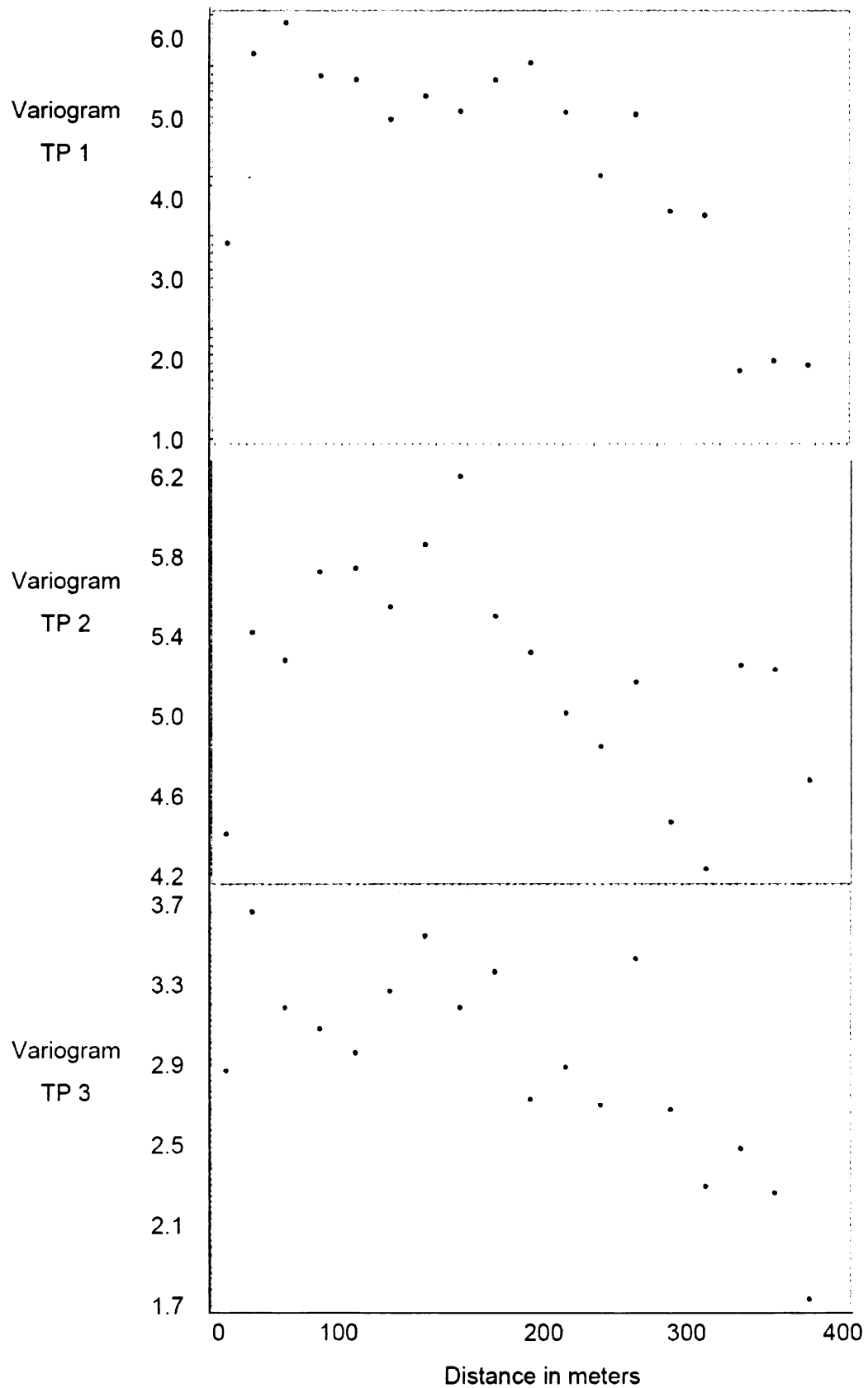
Figure A.10. Variograms for spirochetes in larvae on mice for all trap periods.
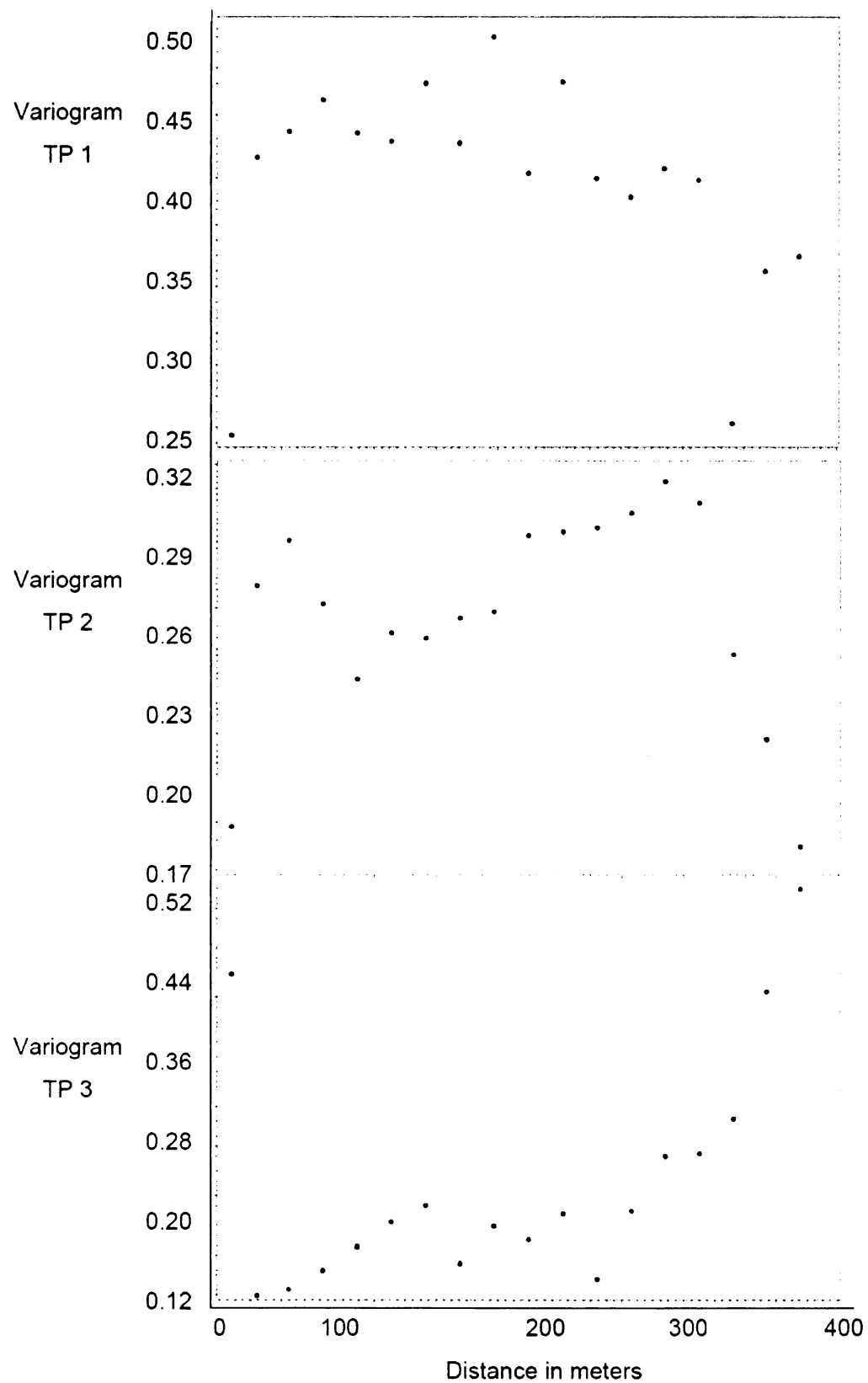
Figure A.11. Variograms for nymphs on mice for all trap periods.
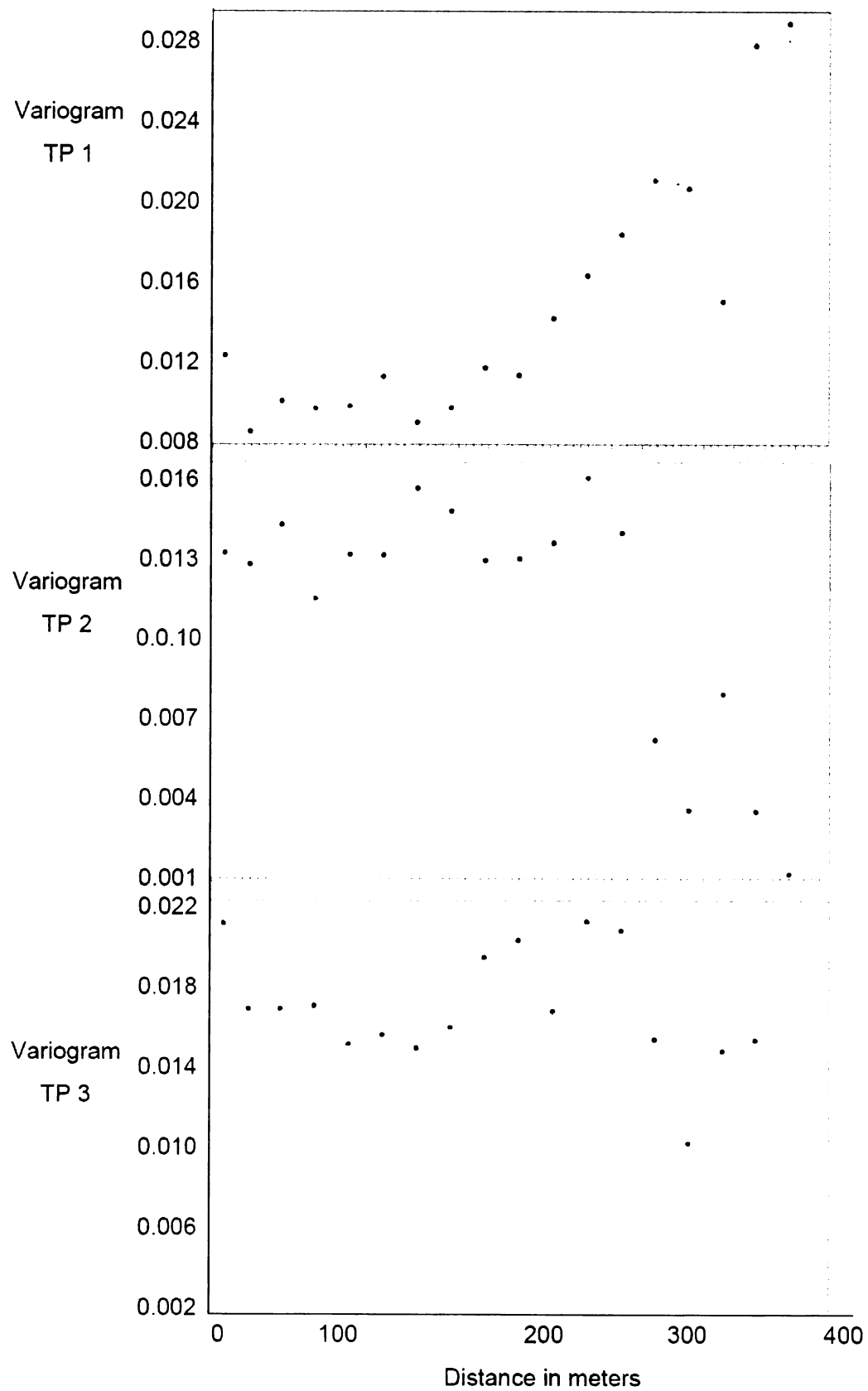
Figure A.12. Variograms for infected nymphs on mice for all trap periods.
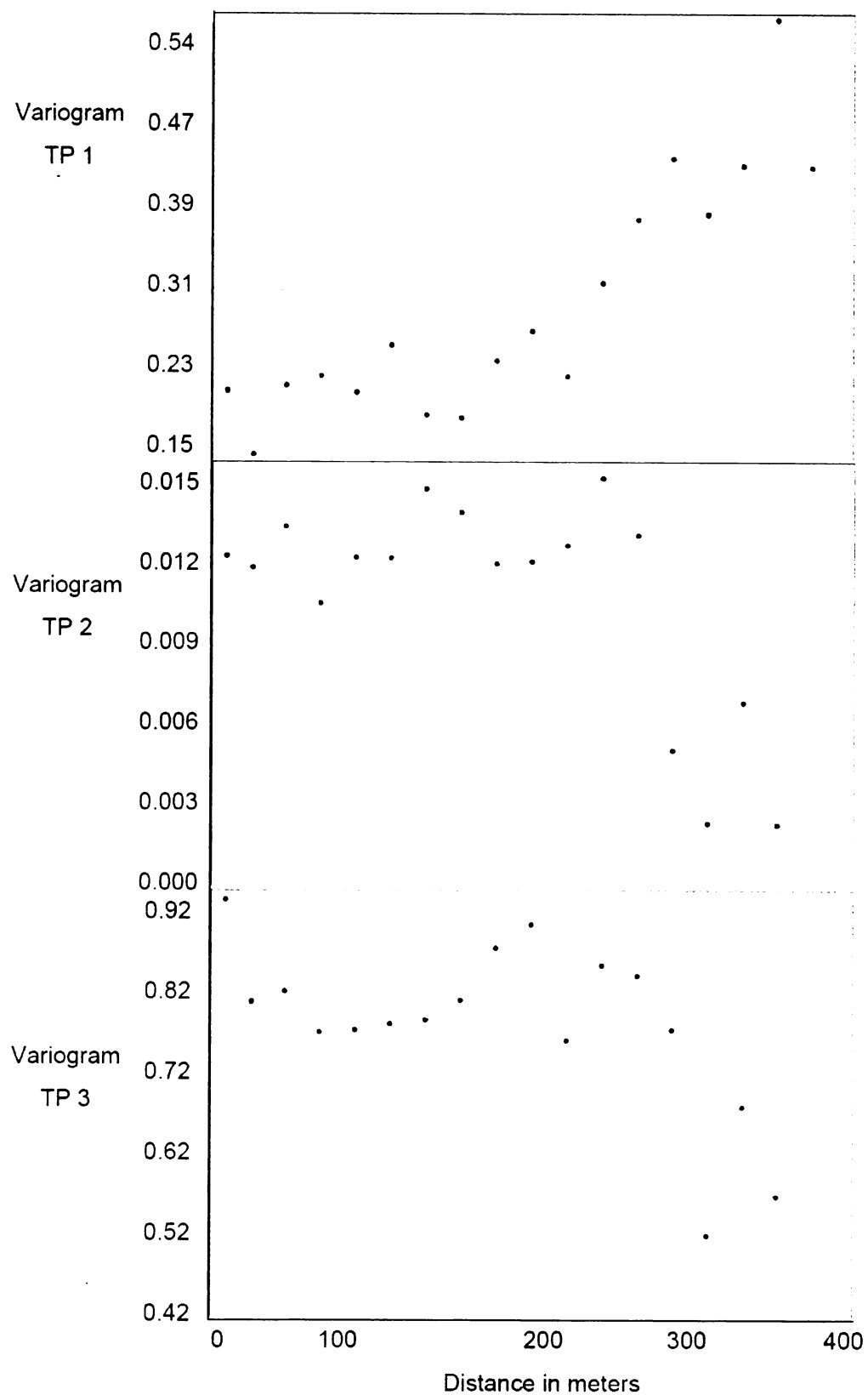
Figure A.13. Variograms for spirochetes in nymphs on mice for all trap periods.
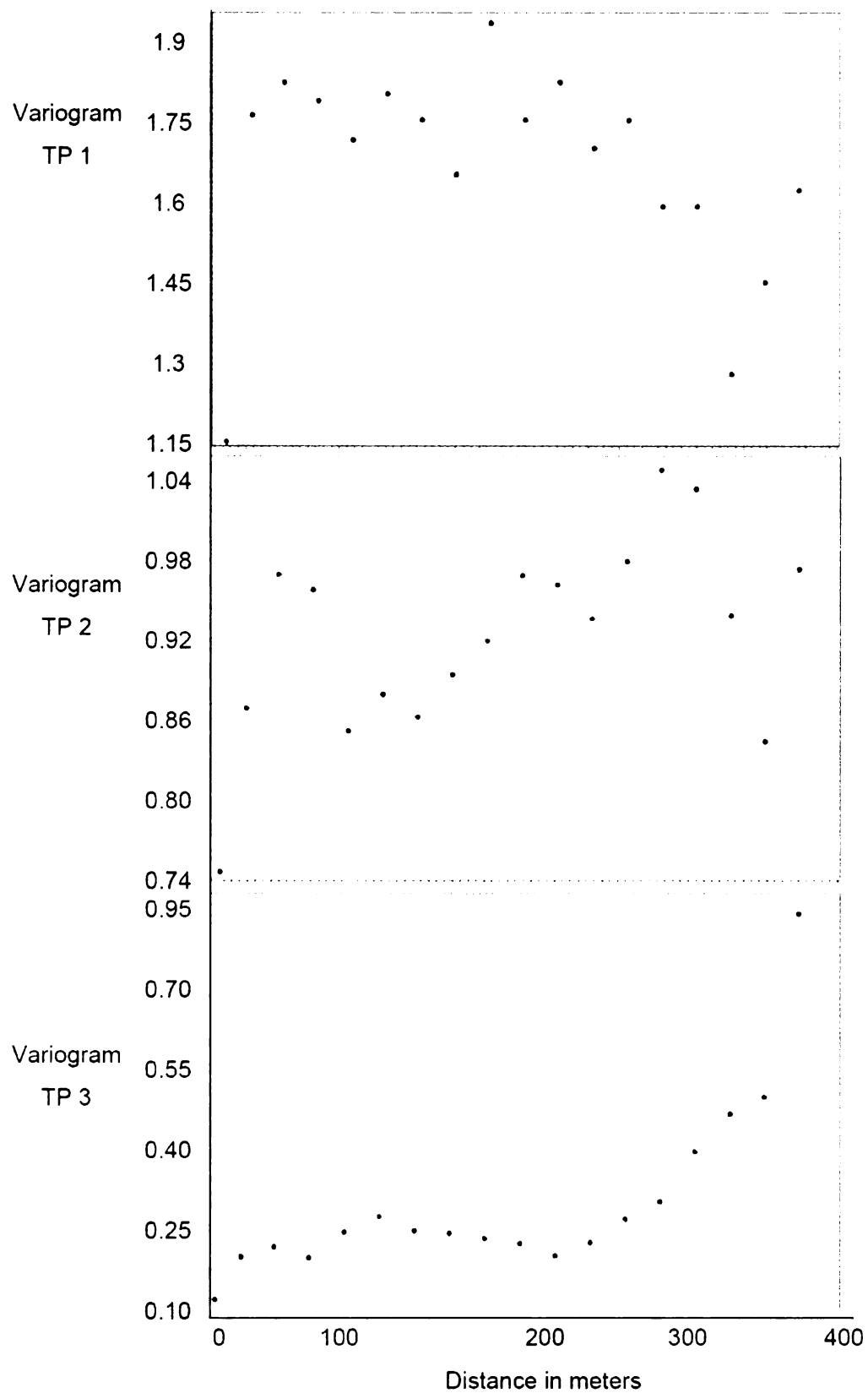
Figure A.14. Variograms for total ticks on mice for all trap periods.

Figure A.15. Variograms for questing larvae for all trap periods.

Figure A.16. Variograms for questing nymphs for all trap periods.

Figure A.17. Variograms for infected questing nymphs for all trap periods.
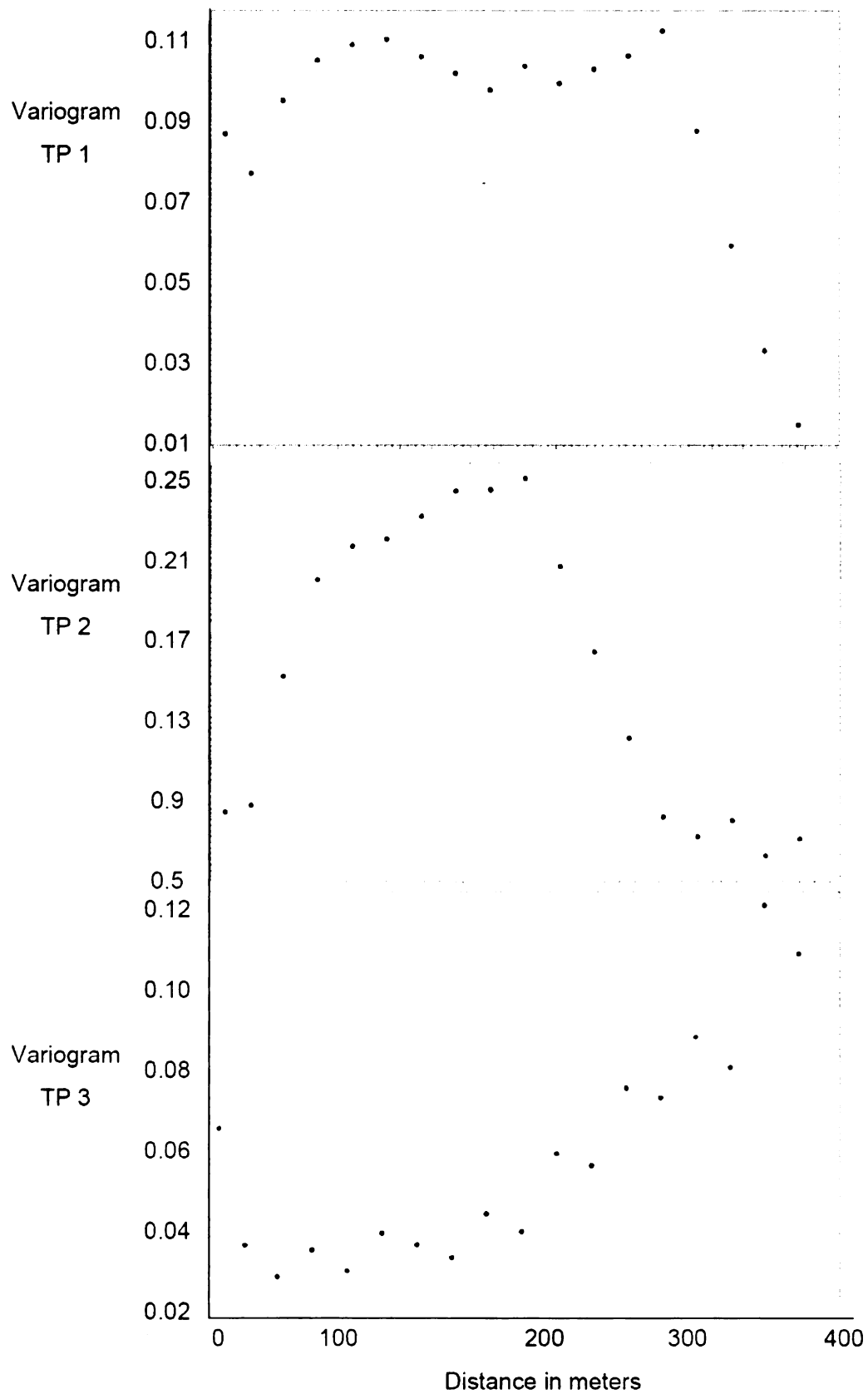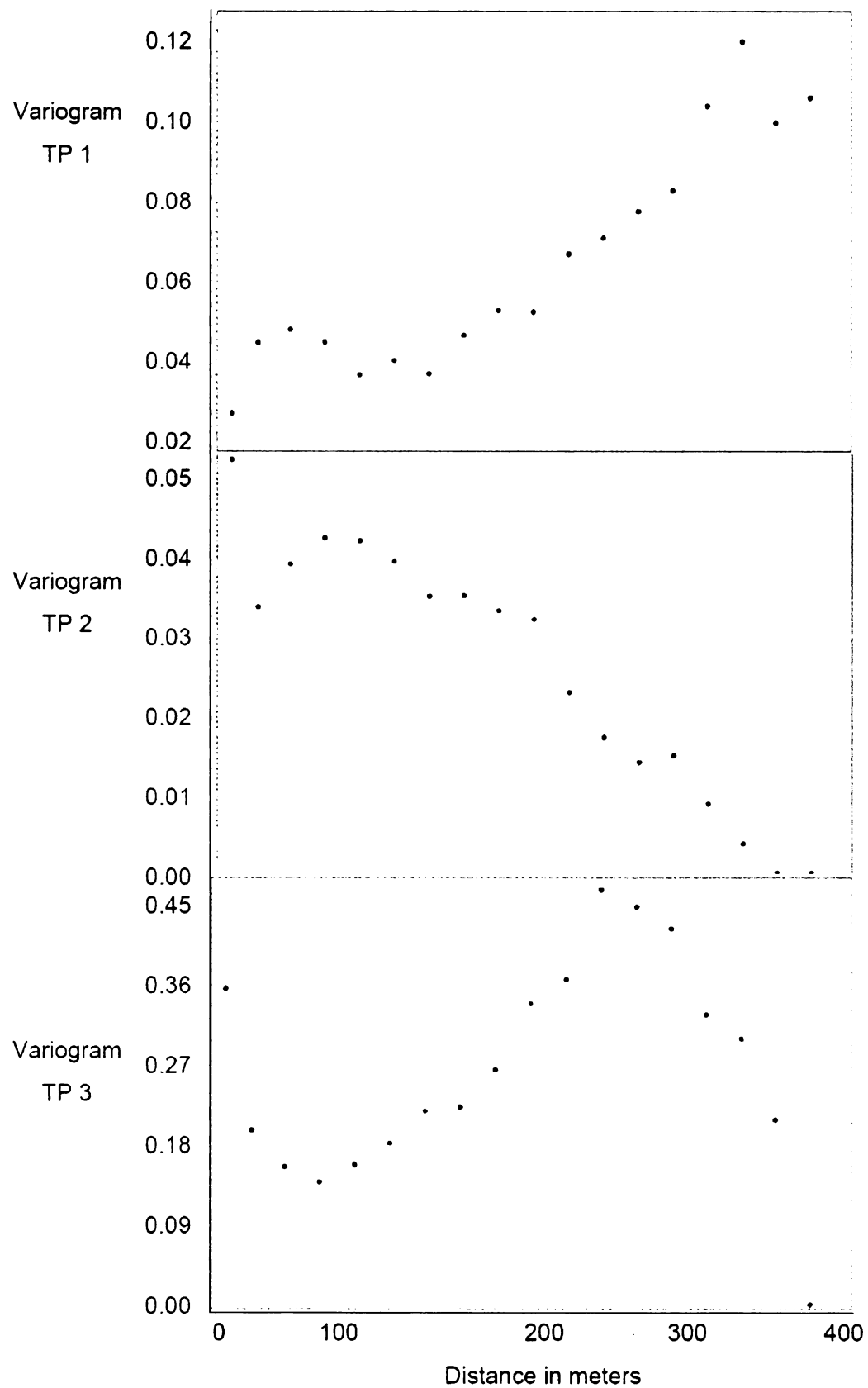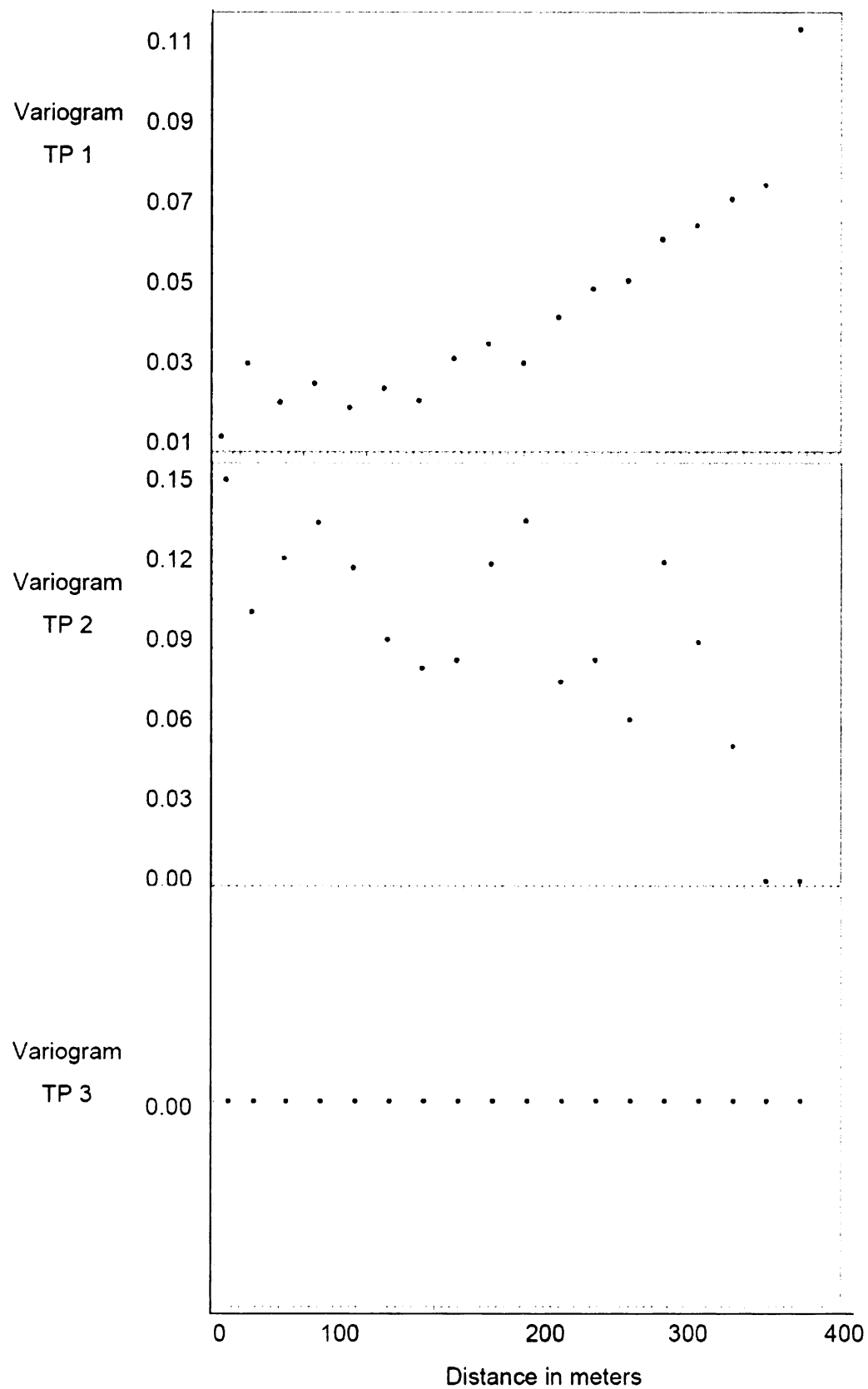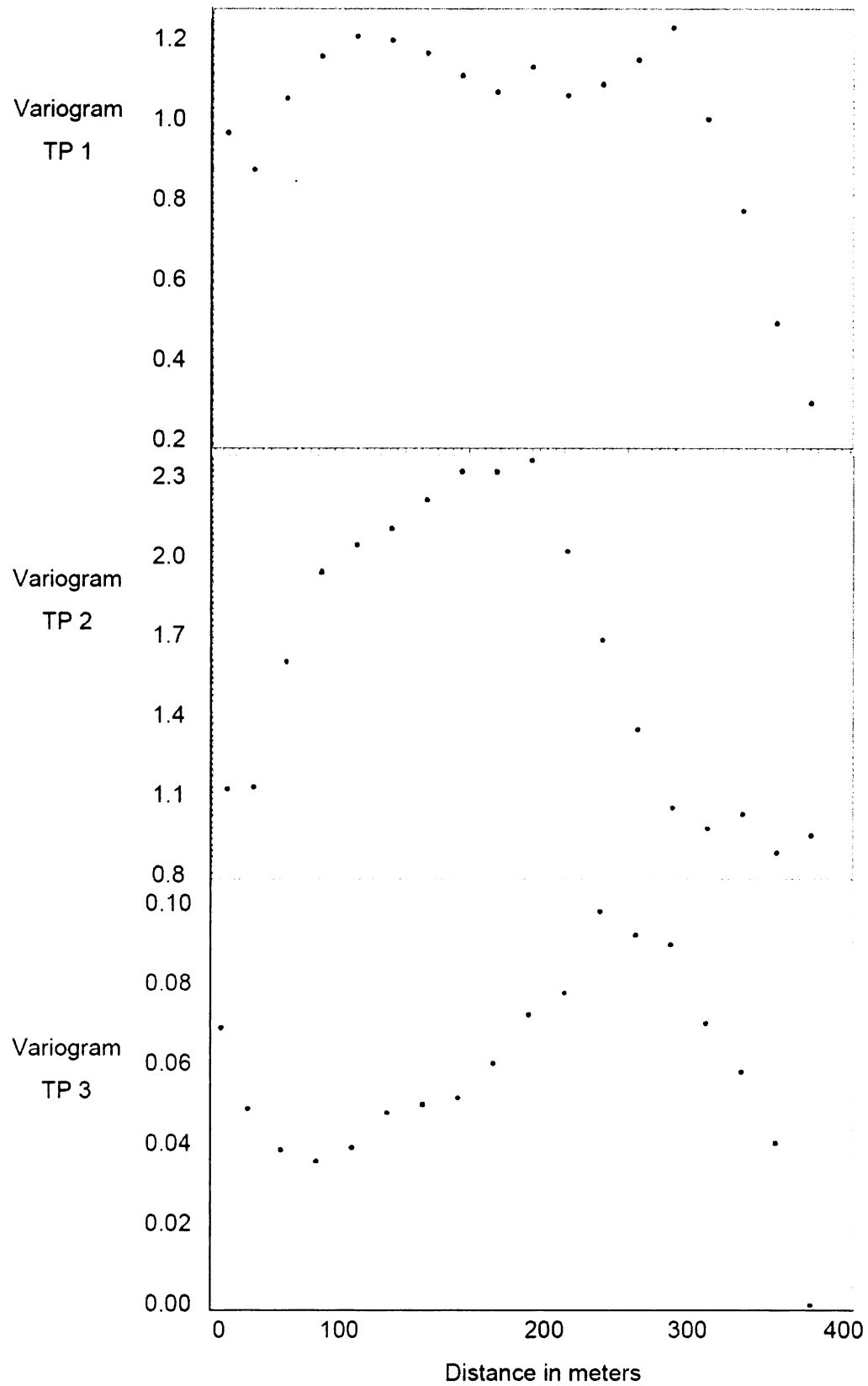
173

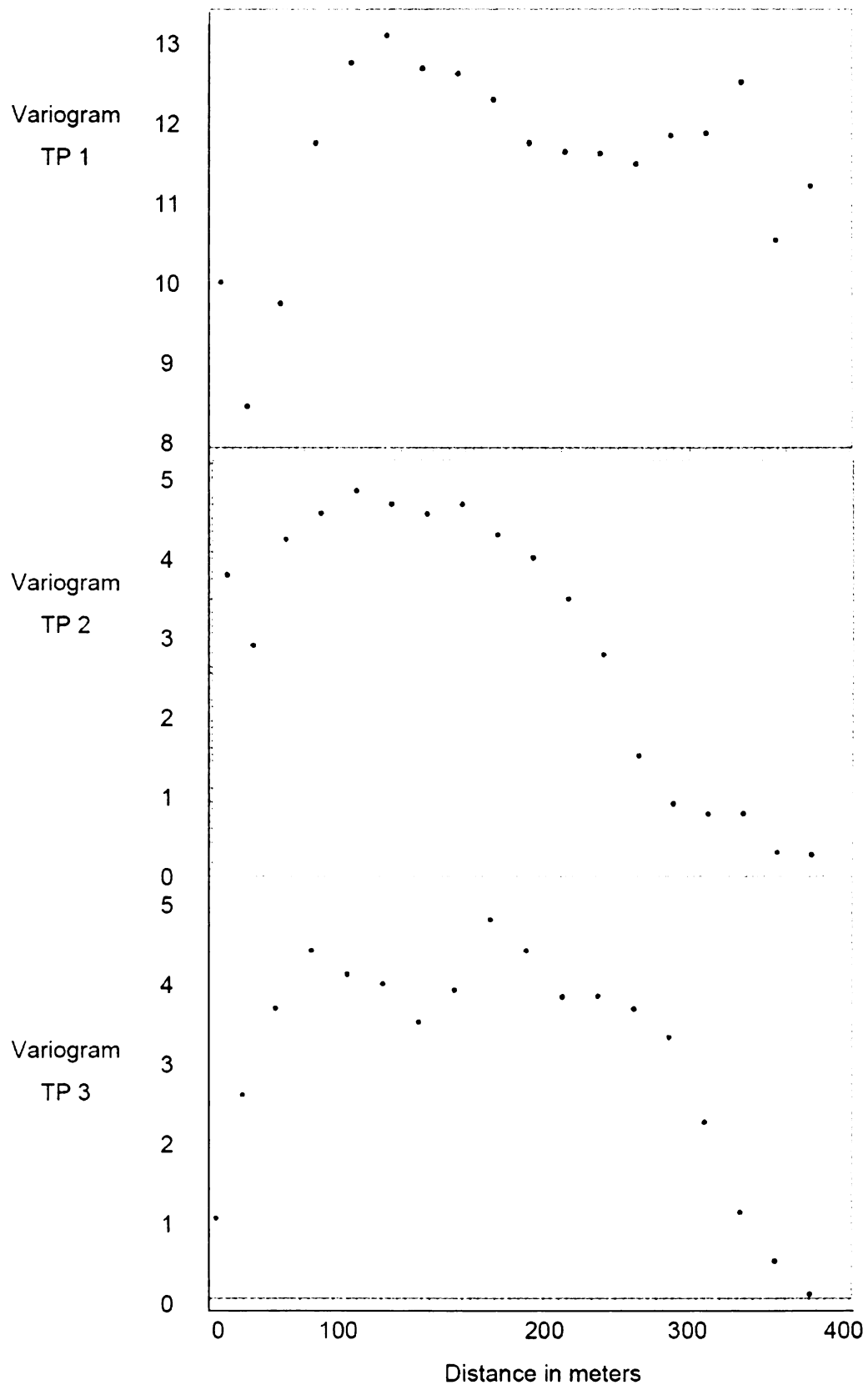**Figure A.18. Variograms for all questing ticks for all trap periods.**

Figure A.19. Variograms for spirochetes in questing ticks for all trap periods.

175

REFERENCES

Anderson JF, Duray PH, et al. 1987. Prevalence of *Borrelia burgdorferi* in white-footed mice and *Ixodes dammini* at Fort McCoy, Wisconsin. Journal of Clinical Microbiology 25(8): 1495-1497.

Anderson RM and May RM. 1978. Regulation and stability of host-parasite population interactions: I. Regulatory processes. Journal of Animal Ecology 47: 219-247.

Barbour AG and Fish D. 1993. The biological and social phenomenon of Lyme disease. Science. 260: 1610-1616.

Begon M, Bennett M, et al. 2002. A clarification of transmission terms in host-microparasite models: numbers, densities and areas. Epidemiology of Infections 129: 147-153.

Bliss CI and Fisher RA. 1953. Fitting the negative binomial distribution to biological data. Biometrics 9: 176-199.

Bunikis J, Tsao J, et al. 2004. Population of *Peromyscus leucopus* mice: a longitudinal study in an area where Lyme borreliosis is highly endemic. Journal of Infectious Diseases 189: 1515-1523.

Bunikis J, Garpmo U, et al. 2004. Sequence typing reveals extensive strain diversity of the Lyme borreliosis agents *Borrelia burgdorferi* in North America and *Borrelia afzelii* in Europe. Microbiology 150: 1741 – 1755.

Cattadori IM, Boag B, et al. 2005. Peak shift and epidemiology in a seasonal host-nematode system. Proceedings of the Royal Society B-Biological Sciences 272(1568): 1163-1169.

Centers for Disease Control. www.cdc.gov. 2005.

Churcher TS, Ferguson NM, et al. 2005. Density dependence and overdispersion in the transmission of helminth parasites. Parasitology 131: 121-132.

Crofton HD. 1971. A model of host-parasite relationships. Parasitology 63: 343-364.

Diehl RH, Larkin RP, et al. 2003. Radar observations of bird migration over the Great Lakes. Auk 120(2): 278-290.

Diuk-Wasser MA, Gatewood AG, et al. 2006. Spatiotemporal patterns of host-seeking *Ixodes scapularis* nymphs (Acari : Ixodidae) in the United States. Journal of Medical Entomology 43(2): 166-176.

Drew ML, Loken KI, et al. 1988. *Ixodes dammini* occurrence and prevalence of infection with *Borrelia spp* in Minnesota. Journal of Wildlife Diseases 24(4): 708-710.

Duerr HP, Dietz K, et al. 2003. On the interpretation of age-intensity profiles and dispersion patterns in parasitological surveys. Parasitology 126:87-101.

Dye C. 1992. The analysis of parasite transmission by bloodsucking insects. Annual Review of Entomology 37: 1-19.

Elliot JM. 1977. Statistical analysis of samples of benthic invertebrates. Ambleside, Freshwater Biological Association.

Elston DA, Moss R, et al. 2001. Analysis of aggregation, a worked example: numbers of ticks on red grouse chicks. Parasitology 122: 563-569.

Falco RC. 1987. Abundance of the deer tick, *Ixodes dammini* (Acari: Ixodidae), in a Lyme endemic area of southeastern New York state. PhD dissertation, Fordham University.

Falco RC and Fish D. 1988. Ticks parasitizing humans in a Lyme disease endemic area of southern New York State. American Journal of Epidemiology 128(5): 1146-1152.

Falco RC and Fish D. 1992. A comparison of methods for sampling the deer tick, *Ixodes dammini*, in a Lyme disease endemic area. Experimental & Applied Acarology 14(2): 165-173.

Fish D. 1995. Environmental risk and prevention of Lyme disease. American Journal of Medicine 98: S2-S9.

Foster E. 2004. *Ixodes scapularis* (Acari: Ixodidae) and *Borrelia burgdorferi* in southwest Michigan: population ecology and verification of a geographic risk model. Entomology. East Lansing, MI, Michigan State University: 87.

Friedrich T. 2003. Ecology of sympatric species of *Peromyscus* as hosts for *Ixodes scapularis* and *Borrelia burgdorferi* in northern Michigan forests. Ecology and Evolutionary Biology. Ann Arbor, MI, University of Michigan: 123.

Gaba S, Ginot V, et al. 2005. Modelling macroparasite aggregation using a nematode-sheep system: the Weibull distribution as an alternative to the negative binomial distribution? Parasitology 131: 393-401.

Glass GE, Amerasinghe FP, et al. 1994. Predicting *Ixodes scapularis* abundance on white-tailed deer using geographic information systems. American Journal of Tropical Medicine and Hygiene 51: 538-544.

Gordis L. 1996. Epidemiology. Philadelphia, W.B. Saunders Company.

Gray JS. 1985. A carbon dioxide trap for prolonged sampling of *Ixodes ricinus* populations. Experimental Applied Acarology 1: 35-44.

Gregory RD and Woolhouse MEJ. 1993. Quantification of parasite aggregation: a simulation study. Acta Tropica 54: 131-139.

Guerra M, Walker E, et al. 2002. Predicting the risk of Lyme disease: habitat suitability for *Ixodes scapularis* in the North Central United States. Emerging Infectious Diseases 8(3): 289 - 297.

Guyatt HL, Smith T, et al. 1994. Aggregation in schistosomiasis - comparison of the relationships between prevalence and intensity in different endemic areas. Parasitology 109: 45-55.

Hamer SA, Roy PL, et al. 2007. Zoonotic Pathogens in *Ixodes scapularis*, Michigan. Emerging Infectious Diseases 13(7): 1131-1133.

Hamer S. 2008. Invasion of blacklegged ticks in Michigan. [Dissertation- in progress].

Hanincová K, Kurtenbach K, et al. 2006. Epidemic spread of Lyme borreliosis, northeastern United States. Emerging Infectious Diseases 12(4): 604-611.

Hanincová K, Ogden NH, et al. 2008. Fitness variation of *Borrelia burgdorferi* sensu stricto strains in mice. Applied and Environmental Microbiology 74(1): 153-157.

Hudson PJ, editor. 2002. The Ecology of Wildlife Diseases. 1st ed. New York, NY: Oxford University Press. 197p.

Jackson JO and Defoliart GR. 1970. *Ixodes scapularis* Say in northern Wisconsin. Journal of Medical Entomology 7(1): 124-125.

Kirby AD, Smith AA, et al. 2004. Rising burden of immature sheep ticks (*Ixodes ricinus*) on red grouse (*Lagopus lagopus scoticus*) chicks in the Scottish uplands. Medical and Veterinary Entomology 18(1): 67-70.

Kurtenbach K, Hanincová K et al. 2006. Fundamental processes in one evolutionary ecology of Lyme borreliosis. Nature Reviews in Microbiology 4(9): 660-669.

Lane RS and Loye JE. (1989). Lyme disease in California: Interrelationship of *Ixodes pacificus* (Acari: Ixodidae), the western fence lizard (*Sceloporus occidentalis*), and *Borrelia burgdorferi*. Journal of Medical Entomology 26(4): 272-278.

Leung B. 1998. Aggregated parasite distributions on hosts in a homogeneous environment: examining the Poisson null model. International Journal for Parasitology 28(11): 1709-1712.

Levin M, Papero M, et al. 1997. Feeding density influences acquisition of *Borrelia burgdorferi* in larval *Ixodes scapularis* (Acari: Ixodidae). Journal of Medical Entomology 34(5): 569-572.

Levin ML and Fish D. 1998. Density-dependent factors regulating feeding success of *Ixodes scapularis* larvae (Acari : Ixodidae). Journal of Parasitology 84(1): 36-43.

Levin ML and Fish D. 2000. Acquisition and coinfection and simultaneous transmission of *Borrelia burgdorferi* and *Ehrlichia phagocytophila* by *Ixodes scapularis* ticks. Infection and Immunity. 68(4): 2183-2186.

Levine J, Wilson ML, Spielman A. 1985. Mice as reservoirs of the Lyme disease spirochete. American Journal of Tropical Medicine and Hygiene 34: 355-360.

Liveris D, Gazumyan A, et al. 1995. Molecular typing of *Borrelia burgdorferi* sensu lato by PCR-restriction fragment length polymorphism analysis. Journal of Clinical Microbiology 33(3): 589-595.

Lloyd M. 1967. Mean crowding. Journal of Animal Ecology 36(1): 1-30.

LoGiudice K, Ostfeld R, et al. 2003. The ecology of infectious disease: effects of host diversity and community composition on Lyme disease risk. Proceedings of the National Academy of Science USA 100(2): 567-571.

Lord CC, Barnard B, et al. 1999. Aggregation and distribution of strains in microparasites. Philosophical Transactions of the Royal Society of London Series B-Biological Sciences 354(1384): 799-807.

Madhav N, Brownstein JS, et al. 2004. A dispersal model for the range expansion of blacklegged tick (Acari: Ixodidae). Journal of Medical Entomology 41(5): 842-852.

Main AJ, Carey AB, et al. 1982. Immature *Ixodes dammini* (Acari: Ixodidae) on small mammals in Connecticut, USA. Journal of Medical Entomology 19: 655-664.

Mather TN. 1993. The dynamics of spirochete transmission between ticks and vertebrates. Pages 43-60 in HS Ginsberg, editor. Ecology and environmental management of Lyme disease. Rutgers University Press, Piscataway, NJ.

Mather TN, Nicholson MC, et al. 1996. Entomological correlates of *Babesia micronoti* prevalence in an area where *Ixodes scapularis* (Acari: Ixodidae) is endemic. Journal of Medical Entomology 33(5):866-870.

179

May RM and Anderson RM. 1978. Regulation and stability of host-parasite population interactions: II. Destabilizing processes. Journal of Animal Ecology 47: 249-267.

Michigan Department of Natural Resources (MDNR). 1999. White-tailed deer: species management. http://www.michigandnr.com/publications/pdfs/huntingwildlifehabitat/Landowners_Guide/Species_Mgmt/Deer.htm.

Morrison TB, Ma Y, et al. 1999. Rapid and sensitive quantification of *Borrelia burgdorferi*-infected mouse tissues by continuous fluorescent monitoring of PCR. Journal of Clinical Microbiology 37(4): 987-992.

New York State Department of Health. 2005. http://www.health.state.ny.us/statistics/chac/general/lyme.htm.

Owen J, Moore F, et al. 2006. Migrating birds as dispersal vehicles for West Nile virus. Ecohealth 3(2): 79-85.

Ostfeld RS, Jones CG, et al. 1996. Of mice and mast: ecological connections in eastern deciduous forests. Bioscience 46: 323-330.

Ostfeld RS and Keesing F. 2000. Biodiversity and disease risk: the case of Lyme disease. Conservation Biology 14(3): 722-728.

Pacala SW and Dobson AP. 1988. The relationship between the number of parsites/host and host age: population dynamic causes and maximum likelihood estimation. Parasitology 96: 197-210.

Pal P and Lewis JW. 2004. Parasite aggregations in host populations using a reformulated negative binomial model. Journal of Helminthology 78(1): 57-61.

Paterson S and Lello J. 2003. Mixed models: getting the best use of parasitological data. Trends in Parasitology 19(8): 370-375.

Patrican L. 1997. Absence of Lyme disease spirochetes in larval progeny of naturally infected *Ixodes scapularis* (Acari: Ixodidae) fed on dogs. Journal of Medical Entomology 34(1): 52-55.

Piesman J and Spielman A. 1979. Host association and seasonal abundance of immature *Ixodes dammini* in southeastern Massachusetts. Annals of the Entomological Society of America 72: 829-832.

Piesman J, Donahue JG et al. 1986. Transovarially acquired Lyme disease spirochetes (*Borrelia burgdorferi*) in field-collected larval *Ixodes dammini* (Acari: Ixodidae). Journal of Medical Entomology 23(2): 219.

Piesman J and Happ CM. 1997. Ability of the Lyme disease spirochete *Borrelia burgdorferi* to infect rodents and three species of human-biting ticks (blacklegged tick, American dog tick, lone star tick) (Acari: Ixodidae). Journal of Medical Entomology 34(4): 451-456.

Pinger R, Timmons RL, et al. 1996. Spread of *Ixodes scapularis* (Acari: Ixodidae) in Indiana: Collections of adults in 1991-1994 and description of a *Borrelia burgdorferi*-infected population. Journal of Medical Entomology 33(5): 852-855.

Prusinski MA, Chen HY, et al. 2006. Habitat structure associated with *Borrelia burgdorferi* prevalence in small mammals in New York State. Environmental Entomology 35(2): 308-319.

Pugliese A, Rosa R, et al. 1998. Analysis of a model for macroparasitic infection with variable aggregation and clumped infections. Journal of Mathematical Biology 36(5): 419-447.

Randolph SE, Gern L, et al. 1996. Co-feeding ticks: Epidemiological significance for tick-borne pathogen transmission. Parasitology Today 12(12): 472-479.

Randolph SE. 1999a. Epidemiological uses of a population model for the tick *Rhipicephalus appendiculatus*. Tropical Medicine & International Health 4(9): A34-A42.

Randolph SE, Miklisova D, et al. 1999b. Incidence from coincidence: patterns of tick infestations on rodents facilitate transmission of tick-borne encephalitis virus. Parasitology 118: 177-186.

Reed KD, Meece JK, et al. 2003. Birds, migration, and emerging zoonoses: West Nile virus, Lyme disease, influenza A and enteropathogens. Clinical Medicine & Research 1(1): 5-12.

Rosa R and Pugliese A. 2002. Aggregation, stability, and oscillations in different models for host-macroparasite interactions. Theoretical Population Biology 61(3): 319-334.

Schauber EM and Ostfeld RS. 2002. Modeling the effects of reservoir competence decay and demographic turnover in Lyme disease ecology. Ecological Applications 12(4): 1142-1162.

Schauber EM, Ostfeld RS, Evans AS. 2005. What is the best predictor of annual Lyme disease incidence: Weather, mice, or acorns? Ecological Applications 15(2): 575-586.

Scrimenti R. 1970. Erythema chronicum migrans. Archives of Dermatology 102(1): 104-105.

Shaw DJ and Dobson AP. 1995. Patterns of macroparasite abundance and aggregation in wildlife populations: a quantitative review. Parasitology 111: S111-133.

Shaw DJ, Grenfell BT, Dobson AP. 1998. Patterns of macroparasite aggregation in wildlife host populations. Parasitology 117: 597-609.

Sonenshine DE. 1979. Ticks of Virginia (Acari: Metastigmata). Insects of Virginia No. 13. Research Division Bulletin 139, Virginia Polytechnic Institute and State University, Blacksburg VA.

Steere AC, Coburn J, et al. 2004. The emergence of Lyme disease. Journal of Clinical Investigation 113(8): 1093-1101.

Strand RM, Walker ED, et al. 1992. Field studies on *Ixodes dammini* in the Upper Peninsula of Michigan. Vector Control Bulletin of the North Central States 1: 111-118.

Telford SR, TN Mather, et al. 1988. Incompetence of deer as reservoirs of the Lyme-disease spirochete. American Journal of Tropical Medicine and Hygiene 39(1): 105-109.

Van Buskirk J and Ostfeld RS. 1995. Controlling Lyme-disease by modifying the density and species composition of tick hosts. Ecological Applications 5(4): 1133-1140.

Van Buskirk J and Ostfeld RS. 1998. Habitat heterogeneity, dispersal, and local risk of exposure to Lyme disease. Ecological Applications 8(2): 365-378.

Walker ED, Smith TW, et al. 1994. Prevalence of *Borrelia burgdorferi* in host-seeking ticks (Acari: Ixodidae) from a Lyme disease endemic area in Northern Michigan. Journal of Medical Entomology 31(4): 524-528.

Walker ED, Stobierski MG, et al. 1998. Geographic distribution of ticks (Acari:Ixodidae) in Michigan, with emphasis on *Ixodes scapularis* and *Borrelia burgdorferi*. Journal of Medical Entomology 35(5): 872-882.

Wang G, Ojaimi C, et al. Impact of genotypic variation of *Borrelia burgdorferi* sensu stricto on kinetics of dissemination and severity of disease in C3H/HeJ mice. Infection and Immunity 69(7): 4303-4312.

Wang G, Liveris D, et al. 2003. Real-time PCR for simultaneous detection and quantification of *Borrelia burgdorferi* in field-collected *Ixodes scapularis* ticks from the northeastern United States. Applied and Environmental Microbiology 69(8): 4561-4565.

Wilson K, Grenfell BT, et al. 1996. Analysis of aggregated parasite distributions: A comparison of methods. Functional Ecology 10(5): 592-601.

Wilson, ML and Spielman A. 1983. Seasonal activity of immature *Ixodes dammini* (Acari: Ixodidae). Journal of Medical Entomology 22: 408-414.

Woolhouse MEJ, Dye C, et al. 1997. Heterogeneities in the transmission of infectious agents: implications for the design of control programs. Population Biology 94(1): 338-342.

Woolhouse MEJ, Etard JF, et al. 1998. Heterogeneities in schistosome transmission dynamics and control. Parasitology 117: 475-482.